LBL-10125

Lawrence Berkeley Laboratory
UNIVERSITY OF CALIFORNIA

ENERGY & ENVIRONMENT
DIVISION

DETERMINATION OF LOW-Z ELEMENTS IN ATMOSPHERIC AEROSOLS BY CHARGED-PARTICLE-INDUCED NUCLEAR REACTIONS

Mark Steven Clemenson
(Ph.D. thesis)

November 1979

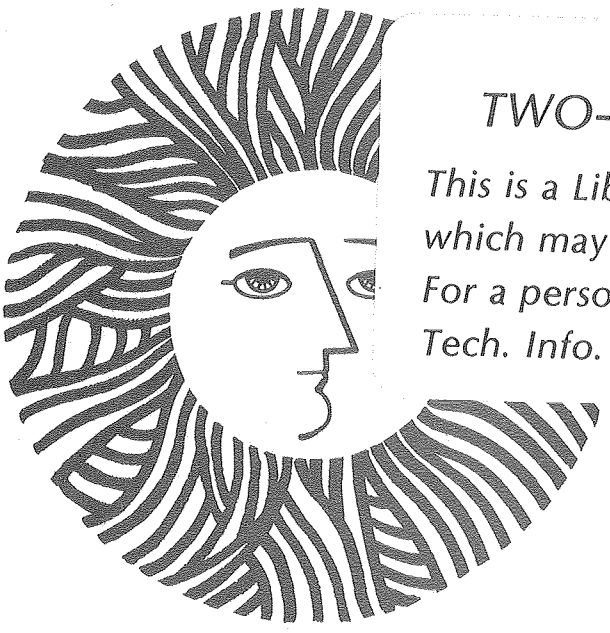

Prepared with the support of the National Science Foundation and for the U. S. Department of Energy under Contract W-7405-ENG-48

DISCLAIMER

DETERMINATION OF LOW-Z ELEMENTS IN ATMOSPHERIC AEROSOLS BY CHARGED-PARTICLE-INDUCED NUCLEAR REACTIONS

Mark Steven Clemenson

Energy and Environment Division
Lawrence Berkeley Laboratory
University of California
Berkeley, California 94720

ABSTRACT

Nuclear reactions induced by charged particles are used to determine total carbon, nitrogen, and oxygen in atmospheric aerosols. The methods are nondestructive of the sample, permitting the same sample to be studied by other experiments such as x-ray photoelectron spectroscopy. These simple activation methods are quite sensitive and require only a short amount of beam time (one minute in most cases) for each sample analysis.

The method for determination of nitrogen in aerosols uses a proton beam to induce the $^{14}N(p,\alpha)^{11}C$ reaction. Radioactive ^{11}C, a 20.4-minute positron emitter, is detected via its 0.511-MeV annihilation radiation.

The detection system consists of a Ge(Li) gamma-ray spectrometer. A comparison of nitrogen found by the proton activation method with that found by an independent but destructive combustion method gave an average percent difference of 14% for 17 samples analyzed over a concentration range that spans two orders of magnitude. The sensitivity for detection of nitrogen is approximately 0.1 $\mu g/cm^2$.

The method for determination of carbon in aerosols uses a deuteron beam to induce the $^{12}C(d,n)^{13}N$ reaction. The 10.0-minute ^{13}N was followed by its 0.511 MeV annihilation radiation. The results of the deuteron activation analysis of 15 samples were compared to the results of an independent combustion method. The comparison shows an average percent difference of 10%. The sensitivity for detection of carbon is approximately 0.5 $\mu g/cm^2$.

Two methods were developed for determination of oxygen in atmospheric aerosols. One method uses a ^{3}He beam to induce the $^{16}O(^{3}He,p)^{18}F$ reaction. The 109.8-minute ^{18}F was followed by its 0.511 MeV annihilation radiation. The second method uses a proton beam to induce the $^{16}O(p,\alpha)^{13}N$ reaction. The two methods were used to check one another. A comparison of the oxygen found in ten samples by ^{3}He activation analysis with that found by proton activation analysis shows an average percent difference of 18%. The sensitivity for detection of oxygen is approximately 5 $\mu g/cm^2$ and is primarily limited by the rather large oxygen blank in the silver filter.

CONTENTS

I. INTRODUCTION

A. History of Air Pollution 1

B. Definition of Air Pollution 2

C. Effects of Air Pollution 3

D. Photochemical Air Pollution 4

E. Atmospheric Aerosols 7

F. Analytical Methods for Elemental Analysis of Atmospheric Aerosols 9

G. Principles of Activation Analysis 15

II. EXPERIMENTAL

A. The 88-Inch Cyclotron 32

B. Irradiation Apparatus 34

C. Detectors and Counting Equipment 38

D. Data Analysis 45

III. RESULTS

A. Nitrogen Determinations 51

B. Carbon Determinations 66

C. Oxygen Determinations 82

IV. DISCUSSION 107

V. SUMMARY AND CONCLUSIONS 113

Acknowledgments 116

Appendix A: TI 960 Data Collection Program and Sample Data Output 117

Appendix B: Abstracts of Papers Presented at Meetings of the American Chemical Society 121

References 124

I. INTRODUCTION

A. History of Air Pollution

Man has always polluted the air that he breathes. In ancient communities man primarily burned wood for his domestic and industrial needs. The communities were small compared to modern standards and it is unlikely that anthropogenic activity in these communities resulted in serious air pollution problems. As man progressed, however, he found that wood was not enough to fill his increasing needs. Around the beginning of the fourteenth century coal was discovered to be an important energy source and soon replaced wood as the primary energy source. Soon thereafter the pollution of the air as a result of large-scale coal burning was found to present a public health problem. In England some attempts were made to control the use of coal, but coal use grew for the most part at an unrestricted rate. The advent of the industrial revolution brought coal use and related public health problems to a new high. The discovery of oil and natural gas as convenient large-scale energy sources in the latter nineteenth century helped to abate the problem of coal burning, but also led to new problems. The internal-combustion engine soon appeared and the tremendous rise of these vehicles in all forms of transportation began.

The first scientific studies into the causes of air pollution in major U.S. cities were mandated as the result of a series of events. In 1948, a serious air pollution episode in Donora, Pennsylvania, killed 20 people and made several hundred others ill. In London in 1952, over 4000 people were killed as smoke built up under stagnant air conditions.

In several major U.S. cities industrial effluents of smoke and malodorous gases led to public protest. The wartime industrialization in the Los Angeles basin and the increased use of petroleum products resulted in the appearance of a new type of highly irritating air pollution and presented new public health problems. This new kind of smog became a chronic condition in the Los Angeles basin and soon appeared in other U.S. cities.

The first attempt to understand the intrinsic interaction of pollutants in the urban atmosphere was carried out by A. J. Haagen-Smit and his colleagues at the California Institute of Technology in the early 1950's and stands as a milestone in the scientific investigation of urban air pollution. They demonstrated that the Los Angeles type of air pollution could be reproduced in the laboratory by the ultraviolet irradiation of a mixture of hydrocarbon vapors and nitrogen oxides. This work and subsequent work proved that much of the Los Angeles-type air pollution can be attributed to reactions of olefins and other reactive hydrocarbons with the oxides of nitrogen in the presence of sunlight. This led to the term "photochemical smog" to denote the smog formed under these conditions. This was only the beginning of the investigation of the chemistry of the polluted troposphere; since then many different types of smog conditions have been studied and characterized.

B. Definition of Air Pollution

The precise definition of air pollution is still a matter of debate and current definitions are as much a matter of personal preference as they are of science. A broad definition is that air pollution is any

circumstance that adds to or detracts from the normal constituents of the air in sufficient concentration to be measurable.[1] Under this definition any material added to the atmosphere (whether natural or man-made) can be considered "a pollutant." The pollutants can occur in any of the three physical states.

Pollutants are divided into two general groups according to their origin. The first group is represented by those pollutants which are emitted directly into the atmosphere from identifiable sources and are termed "primary pollutants." The second group is represented by those pollutants which result from the reactions of primary pollutants with themselves or with normal atmospheric conditions and are termed "secondary pollutants." It is important in any control strategy to determine whether an identified pollutant is of primary or secondary origin since it is the harmful primary pollutants that must be controlled. A current list of primary pollutants would include the following: aerosols, carbon dioxide, carbon monoxide, sulfur oxides, nitrogen oxides, and hydrocarbons. Secondary pollutants vary greatly in different locations depending on the conditions and the major primary pollutants, but a list of important secondary pollutants includes the following: sulfuric acid, nitric acid, and the salts resulting from the reactions of these acids with bases such as ammonia. There are also the well known products of photochemical activity such as ozone, aldehydes, organic peroxides, and PAN (peroxyacetyl nitrate).

C. Effects of Air Pollution

There are many effects which air pollution has on man and his environment. Although the incidences of "killer smogs" are few, they are still a reminder that the primary concern over air pollution is the physiological effect that it has on man. The primary physiological concern is the effects of long-term exposure at relatively low levels. These effects are being investigated, but much is still not known about the risks. Among the potential risks are increased cancers, bronchitis, and eye and skin irritations.

Another important effect of air pollution is the damage it causes to plant life. There are large numbers of plants which are sensitive to smog-related pollutants. Damage to materials such as buildings and fabrics by pollutants is also a major problem. Annual loss attributable to air pollution is thought to run into the billions of dollars.

The most noticeable effect of air pollution and the effect that reminds us every day of its presence is visibility reduction. This is the earliest noted effect of air pollution. It is caused primarily by particles in the 0.1 μm to 1 μm range. There are also the possible climatological effects associated with the particles changing the albedo of the earth and hence the amount of solar radiation that is received at the surface.

D. Photochemical Air Pollution

The first twenty years of scientific research into air pollution chemistry dealt almost exclusively with gas-phase photochemical studies. Although the details are not well understood, the broad mechanisms of

photochemical reactions are fairly well known. Nitrogen oxides, primarily NO, are formed during combustion at high temperatures. The primary sources of nitrogen oxides are internal combustion engines and combustion of fossil fuels in stationary sources such as power plants. At high temperatures the atmospheric nitrogen is fixed according to the reaction

$$N_2 + O_2 = 2NO$$

Even though this reaction is endothermic, the high-temperature equilibrium tends to increase the amount of NO. When the reaction gases are cooled rapidly following combustion, the time is inadequate for the ambient-temperature equilibrium to develop and some NO persists. The NO is not very harmful to man, but reacts to form harmful products. One important reaction that NO undergoes is the oxidation to NO_2, a corrosive and highly oxidizing gas. The accepted oxidation mechanism is

$$NO + O_2 = NO_3$$

$$NO_3 + NO = 2NO_2$$

The formation of NO_2 from NO in the atmosphere is normally very slow at ambient NO concentrations, almost always less than 0.5 ppm.

It is the presence of other pollutants in the atmosphere that speed up the rate of NO oxidation and result in photochemical smog formation. In the presence of hydrocarbons and sunlight the NO is quickly converted to NO_2. The solar spectrum between 300 nm and 400 nm dissociates NO_2 and gives rise to the following three reactions known as the NO_2 photolytic cycle:

$$NO_2 + h\nu \longrightarrow NO + O$$

$$O + O_2 \xrightarrow{M} O_3$$

$$O_3 + NO \longrightarrow NO_2 + O_2$$

This cycle explains the initial formation of ozone, but is not sufficient to explain the rapid build-up of ozone and NO_2 that is observed in the atmosphere. It is the presence of hydrocarbons that allows the ozone and NO_2 levels to build up. The hydrocarbons react with oxygen atoms produced in the NO_2 photolytic cycle to form oxidized hydrocarbons and free radicals. These compounds further react with NO to form more NO_2 while depleting NO levels. The steady state ozone concentration of the photolytic cycle is disrupted and the ozone level builds up. Some of the major photochemical reactions involving hydrocarbons are:[2]

$$\cdot O + R \longrightarrow \cdot RO$$

$$\cdot RO + O_2 \longrightarrow \cdot RO_3$$

$$\cdot RO_3 + R \longrightarrow RC\begin{matrix}=O\\ \diagdown H\end{matrix} \text{ (aldehydes)} + R\overset{\overset{O}{\|}}{C}R \text{ (ketones)} + \cdot RO$$

$$\cdot RO_3 + NO \longrightarrow \cdot RO_2 + NO_2$$

$$\cdot RO_3 + O_2 \longrightarrow RO_2 + O_3$$

$$\cdot RO_3 + NO_2 \longrightarrow RC\begin{matrix}=O\\ \diagdown O-O-NO_2\end{matrix} \quad \text{(PAN)}$$

Many other reactions can be suggested and new mechanisms are still being discovered. There are still many things that are not understood about smog reactions such as reaction rates, relative importance of specific

reactions, important intermediates, and the role of aerosols as catalysts in the oxidation of certain species.

E. Atmospheric Aerosols

The study of the role of aerosols in atmospheric chemistry has only begun in earnest in the past ten years. In that time it has become increasingly apparent that they play a major role in air pollution chemistry. It has long been understood that aerosols are the major cause of visibility reduction. What is not understood are the reactions primary particles undergo in the atmosphere with gases and other particles and what role aerosols play in the oxidation of species such as NO_2 and SO_2. Even such questions as the chemical and elemental composition of aerosols are not well understood.

Aerosols are particles, solid or liquid, which are suspended in the atmosphere. They are divided into two main groups: a) coarse particles of size greater than 1 μm in diameter and b) fine particles of size less than 1 μm in diameter. The size of aerosols which almost always have irregular shapes is a matter of definition. One way to define aerosol size is to say that all particles which have a certain physical property in common all have the same diameter. One example of this is the aerodynamic diameter which is the diameter of a sphere of unit density having the same falling speed in air as the aerosol particle. This is a commonly used definition since many size-segregating instruments measure this diameter and it is also involved in the mechanisms of particle deposition in the lungs. Other important diameters are those defined in terms of the surface area, mass or volume. It has been shown

that particles of size less than 1 μm are primarily combustion related and particles of size greater than this are primarily generated by mechanical means such as grinding.[3] The fine particles have a trimodal distribution of sizes. A mode centered around 0.01 μm is called the first Aitkin mode, a mode centered at 0.05 μm is called the second Aitkin mode, and a mode centered around 0.5 μm is called the accumulation mode. It has been shown that aerosols in the smaller two modes will coagulate and enter the larger mode.[4]

Aerosols are also catalogued by their origin as either primary or secondary aerosols. Primary aerosols are those emitted directly into the atmosphere from identifiable sources and secondary aerosols are those formed in the atmosphere from reactions of gases with gases, gases with particles, and particles with particles. There is currently a debate in atmospheric aerosol science as to whether the observed aerosol is mainly primary or mainly secondary in origin. The former group maintains that the main contribution to the atmospheric particulate burden is from primary particulate species from sources such as automobiles and furnaces, while the latter group maintains that the main contribution to the observed particulate burden is from secondary photochemical reactions involving gases that form products which coagulate to form aerosols. The clear resolution of the controversy involving the mechanisms for formation of secondary pollutants is of critical importance if the correct control strategies are to be chosen. One theory would suggest the control of primary particulate emissions is important while the other theory would suggest the control of primary gaseous effluents which contribute to secondary particulate formation is important.

The emphasis in the past has been placed on gas-phase photochemical reactions to explain the formation of secondary pollutants. Much less work has been devoted to the studies involving non-photochemical, heterogeneous gas-particle reactions. These reactions occur at the surface of particles which serve as the catalyst for these reactions. These heterogeneous reactions seem to play an important role in many situations. There are many instances of heavy particulate pollution that occur under non-photochemical conditions. The absence of photochemical conditions are indicated by a low ozone concentration. If the ozone concentration is low then photochemical activity is low, since ozone is an abundant product of photochemical activity. The observed particulate concentration must then be explained using a non-photochemical mechanism. The common occurrence of heavy particulate pollution during the winter in the San Francisco Bay Area under conditions of very low ozone concentration has led our research group to investigate the importance of non-photochemical reactions.

F. Analytical Methods for Elemental Analysis of Atmospheric Aerosols

An important step in assessing the relative importance of the proposed secondary pollutant formation mechanisms is the determination of the exact chemical composition of the atmospheric particulate matter. For example, it is important to know the concentration of carbon in the graphitic form in atmospheric aerosols since there are no known atmospheric mechanisms for the formation of graphitic carbon and, as such, graphitic carbon must be of primary origin. Following the amount of graphitic carbon present in an aerosol can be an important key to the determination

of the primary input to the aerosol burden. This is only one example, but it demonstrates the importance of analytical methods in air pollution studies. There are currently no methods for the *in situ* chemical analysis of aerosols and, as such, the particles must first be collected on filters, then subjected to a variety of analytical methods so that the chemical composition of the particulates can be determined.

The field of aerosol research has placed new demands of sensitivity and accuracy on existing analytical methods. A current need in the analysis of aerosols is in the area of low-Z element determinations. Aerosol research has shown that the majority of the mass of aerosols is made up of low-Z elements such as carbon, nitrogen, and oxygen.[5] The development of new methods that are capable of the rapid and nondestructive determination of these elements in atmospheric aerosols on a routine basis is an important short-term goal. Such methods are important if the mass balance of aerosols is to be obtained.

There are, of course, methods available for the analysis of low-Z elements. In one way or another, however, these methods do not meet the needs imposed on them for the determination of low-Z elements in atmospheric aerosols. The requirements for an analytical method to be useful in the analysis of aerosols would include the following points:

1) It needs to be very sensitive. The useful range of sensitivity should extend down to the order of 1 $\mu g/cm^2$.
2) The method must be able to analyze very small sample sizes. A typical aerosol sample has a loading of approximately 100 $\mu g/cm^2$, but can range well below this number. It is difficult to increase the amount of sample collected by increasing the

collection time since the filters usually clog. Long collection times also reduce the time resolution of the collection system.

3) The methods should be nondestructive of the sample. This allows other analyses to be performed on the same sample. This means that unambiguous comparisons of other aerosol characteristics can be performed on the same sample.

Combustion is the most commonly used method of low-Z element determination. This method has two undesirable features. The first is that it is destructive of the sample. As stated above, one would like the sample to remain intact after the analysis so that subsequent different analyses could be performed on the same sample. The second shortcoming is that combustion methods generally lack the necessary sensitivity. Most combustion methods are sensitive only to 50 μg to 100 μg, although some specially designed apparatus may extend down to the 1 μg range. Combustion methods also have the flaw that they generally cannot determine oxygen. This is the case since almost all combustion apparatus burn the sample in an oxygen atmosphere. It is possible to determine oxygen by heating the sample in a helium atmosphere over a bed of graphite and measuring the CO_2 that evolves. This is called the Unterzaucher method and it has many problems.[6] There is one company that makes oxygen determinations using this method, but they could not determine oxygen at the concentrations found in aerosols.[7]

The x-ray fluorescence method is an important nondestructive method of elemental analysis and is commonly used in aerosol analysis. The x-ray fluorescence method is not useful, however, for the determination of low-Z

elements. The lightest element that is routinely determined in aerosol analyses by this method is sulfur. For elements below sulfur several effects occur that prevent their determination. The first is that the fluorescence yield for the important low-Z elements is of the order of a few percent. This is to say that the dominant mode of atomic de-excitation is the emission of an Auger electron and not an x-ray. The second effect is that the characteristic x-ray energies of carbon, nitrogen, and oxygen are 0.28 keV, 0.40 keV, and 0.53 keV, respectively. These are very low-energy x-rays. Even if special windowless Si(Li) detectors were used to detect the x-rays, there would be a serious problem with self-absorption of the x-rays in the sample. There would be similar problems with trying to detect the Auger electrons. There are systems commercially available for the quantitative analysis of elements as light as carbon by α-induced x-ray analysis using the α-emitter ^{241}Am.[8] These systems are designed to be used for the analysis of thin films and surface layers and their useful extension to aerosol analysis is questionable.

Another useful tool for the nondestructive analysis of aerosol samples for low-Z elements is neutron activation analysis. This method has found widespread use for the sensitive multi-element analysis of a variety of samples. There are, however, several reasons why neutron activation analysis cannot be used for the determination of the important low-Z elements. One reason is the fact that the neutron absorption cross sections for carbon, nitrogen, and oxygen are small. The thermal neutron absorption cross section[9] is 0.0010 barns for ^{13}C, 2.4×10^{-5} barns for ^{15}N, and 2.1×10^{-4} barns for ^{18}O. Another important reason that neutron activation analysis cannot be used for low-Z element determinations is

that the product nuclides of the (n,γ) reaction on carbon, oxygen and nitrogen are either stable nuclides or are radionuclides that are not suited to counting. The products of all the (n,γ) reactions on the high abundance isotopes are stable. These are the $^{12}C(n,\gamma)^{13}C$, $^{14}N(n,\gamma)^{15}N$ and $^{16}O(n,\gamma)^{17}O$ reactions. The fact that these products are all stable means that a thermal neutron activation analysis must use the low abundance isotopes for production of a radioactive product. This means that the sensitivity is greatly reduced over that which could be achieved using reactions of the high abundance isotopes. In addition, the $^{13}C(n,\gamma)^{14}C$ reaction produces a 5730-year half-life β-activity which cannot accurately be assayed in a reasonable time. The $^{18}O(n,\gamma)^{19}O$ ($t_{1/2}$ = 26.8 seconds) and the $^{15}N(n,\gamma)^{16}N$ ($t_{1/2}$ = 7.1 seconds) reactions would require a special apparatus and counting facility at the reactor to measure the short-lived product radiations. It is possible to determine oxygen using a fast neutron activation method. The fast neutrons are generated by the reaction of 0.5-MeV deuterons on tritium. The energy of the neutrons is approximately 14 MeV. An alternate source of fast neutrons is a reactor flux. The fast neutron method measures oxygen using the $^{16}O(n,p)^{16}N$ reaction. The ^{16}N is assayed by its characteristic high-energy gamma rays using a NaI detector. There is a company that will analyze samples for oxygen using this method, but again, their method is neither sensitive nor accurate enough for the analysis of oxygen in aerosols.[10]

The inability of accepted methods to analyze aerosol samples for low-Z elements has resulted in several efforts to develop new methods for the determination of these elements. The work of Macias and coworkers

in this area is an important contribution. Their method of light-element determination (carbon, nitrogen and sulfur) involves the "in-beam" measurement of gamma rays following the inelastic scattering of protons.[11] The aerosol samples are collected on quartz filters. The light-element concentrations are determined by irradiating the samples with 7-MeV protons and analyzing the gamma rays using a high-resolution Ge(Li) detector. The samples are nondestructively irradiated in a helium atmosphere for 1000 seconds. The detection limit is in the 10 $\mu g/cm^2$ range. The method takes advantage of the large cross sections of many light elements for excitation to a low-lying excited nuclear state. The resultant gamma-ray emission is, in general, specific for a particular nuclide and thus can be used as a signature for that element. This method and similar methods, however, require lengthy use of accelerator time and an elaborate apparatus set-up at the accelerator. These can be important practical considerations because it means that the experimenters doing light-element determinations must compete with nuclear-physics experimenters for long accelerator runs. These pragmatic considerations can be alleviated if a small "chemists' cyclotron" would be built for chemical analyses and isotope production.[12]

The requirements and problems described in the previous pages have led this author and coworkers to develop a new method for the determination of light-element concentrations in atmospheric aerosols. It is a simple activation method that requires only a short amount of beam time (one minute in most cases) for each sample analysis. It is also relatively rapid and is nondestructive. This charged-particle activation method has been developed for the determination of nitrogen, carbon and oxygen in atmospheric aerosol samples. Nitrogen is determined using 7.5-MeV protons

to induce the $^{14}N(p,\alpha)^{11}C$ reaction. Carbon is determined using 7.6-MeV deuterons to induce the $^{12}C(d,n)^{13}N$ reaction. Oxygen is determined by two methods: one method uses 8.1 MeV protons to induce the $^{16}O(p,\alpha)^{13}N$ reaction and the other method uses 7.9-MeV ^{3}He ions[12] to induce the $^{16}O(^{3}He,p)^{18}F$ reaction. The activities produced are the neutron-deficient nuclides ^{11}C, ^{13}N, and ^{18}F, which have half-lives of 20.4 minutes, 10.0 minutes, and 109.8 minutes, respectively. They all decay by β^+ emission and have no nuclear gamma rays. The decay of these nuclides is followed via the 0.511-MeV β^+ annihilation radiation with a Ge(Li) counting system away from the accelerator. The method offers a simple approach to the problem of light-element analysis in atmospheric aerosols and is applicable to the routine analysis of these samples.

G. Principles of Activation Analysis

In 1933 Curie and Joliet discovered that radioactivity could be induced in boron and aluminum by bombardment with alpha rays from polonium.[13] The utility of induced radiation to the solution of analytical problems was soon recognized. The first use of charged particles for activation analysis was reported by Seaborg and Livingood in 1938.[14] They used deuterons accelerated by a cyclotron to determine minute traces of gallium in iron, copper in nickel, and iron in cobalt. In the years since then, general activation analysis has grown at a rapid rate and is now used in almost every field where sensitive elemental analyses are required. There are several texts to which one is referred for detailed derivations of the important equations and a recent article[15,16] reviews the current advances in the field.

Once the charged-particle activation method has been chosen as the most appropriate tool for the analytical problem at hand, the experimenter must follow a series of steps:

1) An optimum nuclear reaction must be chosen based on chemical and nuclear properties of the element, the matrix and the activation products. These properties determine the type of counting that can be used, whether or not a chemical separation is required, the possibility of interfering reactions, and the ultimate sensitivity.
2) The samples must be prepared in a suitable form for irradiation.
3) The samples must be irradiated in a manner that does not compromise the result. For example, samples which contain volatile compounds must not be exposed to the cyclotron vacuum during the irradiation.
4) The sample must be counted after the irradiation in order to determine the end-of-bombardment activity, A_0, of the radionuclide of interest.
5) The data must be analyzed and the final result obtained.

During an irradiation the dynamic processes occurring are governed by the laws of radioactive growth and decay. The rate of formation of a particular activation product at constant beam intensity, I, is given by the following equation,

$$D_0 = n I \sigma (1 - e^{-\lambda \tau})$$

where D_0 = the disintegration rate at the end of bombardment, in disintegrations/minute

n = the number of target atoms per square centimeter of the nuclide being determined

I = the average beam intensity, in ions/minute

σ = cross section for the nuclear reaction, in square centimeters

τ = the length of time of the bombardment, in minutes

λ = the decay constant of the product activity, in minutes^{-1}.

This equation can be viewed as having two separate parts. There is the production part of the equation, which is the product of $nI\sigma$, and the saturation factor, $(1 - e^{-\lambda\tau})$. This view illustrates the dynamics of the process. The product nuclides are produced at a constant rate which depends only on the beam intensity, the number of target atoms, and the cross section. The product nuclides then decay with their characteristic half-life. The activity will increase as more and more radionuclides are produced. The system will approach a steady-state situation where the number of nuclides being produced equals the number of nuclides decaying. This amount of activity is called the saturation activity. The growth of activity is governed by the saturation factor. A plot of the growth of activity versus product half-life is shown in Fig. 1. For bombardment times that are short compared to the half-life, growth of activity is roughly linear and the equation can be simplified,

$$D_o = nI\sigma\lambda\tau \quad .$$

The decay constant, λ, can be expressed in terms of the half-life and is given by

$$\lambda = \frac{\ell n\, 2}{t_{1/2}} \quad .$$

The beam intensity is usually measured as a beam current, in microamperes, striking the target. The particle intensity is obtained by knowing the charge state of the incident ions and using the following equation.

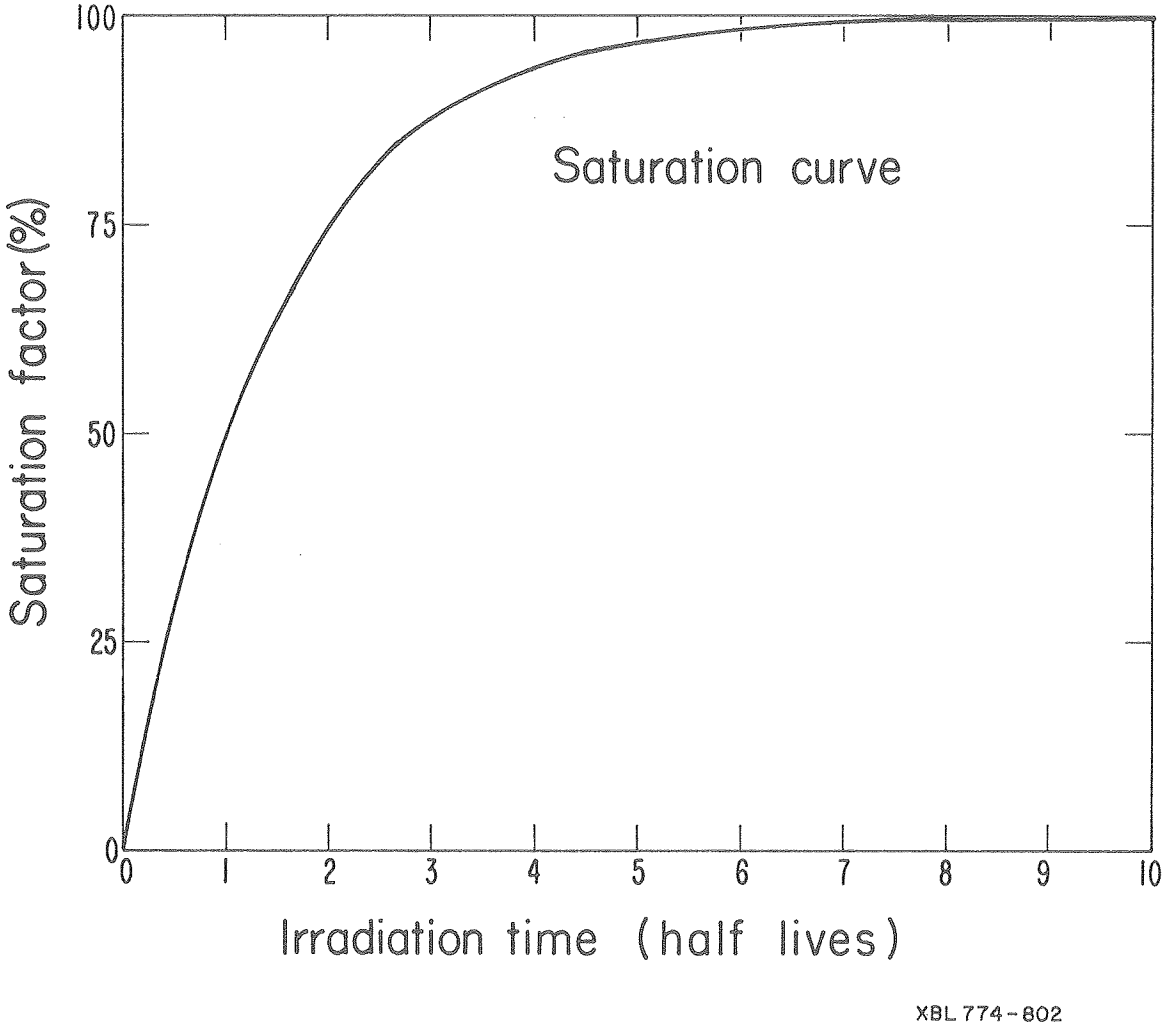

Fig. 1. The growth of activity toward saturation during an irradiation.

$$I \text{ (particles/minute)} = \frac{\text{current } (\mu A) \times 3.744 \times 10^{14}}{\text{charge state of beam}} .$$

The probability of a nuclear process is expressed in terms of the cross section, σ, which has the dimensions of area. (This comes from the picture that the probability for the reaction between a nucleus and an impinging particle is proportional to the cross-sectional area of the target nucleus.) There are many processes occurring during an irradiation and a cross section may be expressed for each one. For example, one may speak of the total cross section for interaction which is just the probability of a particle interacting with a target nucleus by any mechanism. Cross sections may also be defined and measured for particular processes, such as elastic scattering, inelastic scattering, or specific nuclear reactions. Sometimes the distribution of particles as a function of angle for a particular process is desired. In this case the differential cross section is used. The differential cross section expresses the probability for particles from a certain process being emitted into unit solid angle at a particular angle.

The knowledge of the variation of the cross section of a particular reaction with incident particle energy is often required in charged-particle activation analysis. This is called the "excitation function." The absolute cross section is determined at each incident energy with a foil containing a known number of target atoms and by determining accurately the other factors in the general activation equation.

A precise knowledge of the absolute cross section is required if the general activation equation is to be used as the basis for an elemental analysis. This type of analysis is called an "absolute analysis." A

common practice, however, is to use a "relative method" of analysis in which only the relative cross sections of a reaction at different incident particle energies are required.

If the absolute method of analysis is to be used, the absolute cross section for the reaction of interest is first determined in a separate experiment. For the analysis of an unknown sample the important parameter to be determined is the end-of-bombardment disintegration rate. In general, the amount of activity detected by the counting system does not equal the number of disintegrations. This is because the counting system is not 100% efficient for the detection of the radiation and because the nuclide may not emit exactly one particle or photon per decay. Hence, the end-of-bombardment activity, A_0, determined by the counter does not equal the end-of-bombardment disintegration rate, D_0. The equation relating these two quantities is

$$D_0 = \frac{A_0}{ODC} \quad .$$

The overall detection coefficient (ODC) includes all of the counter factors such as counter efficiency, geometry, decay scheme, adsorption, and scattering. It is independently measured for each product nuclide and detector system. The result of an absolute analysis is the determination of n, the number of atoms of the unknown nuclide per square centimeter. This is related to m, the elemental mass per square centimeter, by the following equation.

$$m = \frac{nA}{fN_0}$$

where A = the atomic weight of the element, in grams/mole

f = the fractional isotopic abundance of the target nuclide

N_0 = Avogadro's Number, 6.02×10^{23} $mole^{-1}$.

The relative method of analysis may be carried out by simultaneously bombarding a standard and an unknown in the same beam. The standard is a target of known composition that contains the same element as the element being determined in the unknown. The standard and the unknown are counted under identical conditions. This is done by alternately counting the sample in the same counter and geometry. In any irradiation only a small fraction of the beam particles are actually taken out of the beam by reactions and hence the beam intensity is roughly constant throughout a stack of foils. For the two foils irradiated and counted under identical conditions, several important factors are identical. These factors are the beam intensity, saturation factor, and overall detection coefficient. The atomic weight, fractional abundance, and Avogadro's number, of course, will be the same because the same element is irradiated in both foils. From the previous equations an equation of relative analysis can be obtained:

$$\frac{m(x)}{m(std)} = \frac{A_0(x)}{A_0(std)} \frac{\sigma(std)}{\sigma(x)}$$

where $\sigma(std)/\sigma(x)$ = the ratio of the reaction cross sections at the standard (std) and at the unknown (x). In the relative method of analysis the need for the determination of the absolute cross sections, the beam intensity, the length of bombardment, and the overall detection coefficient is eliminated.

In a foil stack it is necessary to know the energy of the beam at any position. The charged-particle beam will lose energy as it traverses the stack. The primary process responsible for the loss of energy as the

charged particles move through matter is by interaction with electrons. This electronic stopping results in the electronic excitation and ionization of the stopping material. Near the end of its range the energy-loss mechanism becomes a collision with target material nuclei. This is called nuclear stopping. The range of a charged particle depends on the energy of the particle and the stopping material. The range of a particle of energy, E, can be determined by integrating

$$R(E) = \int_0^E \left(-\frac{dE}{dx}\right)^{-1} dE$$

where $-dE/dx$ = the rate of loss of energy, in MeV per mg/cm^2.
An expression for the rate of energy loss which holds at nonrelativistic energies is given by

$$-\frac{dE}{dx} = \frac{4\pi z^2 e^4 n}{mv^2} \ln \frac{2m v^2}{I}$$

where I = the effective ionization potential of the stopping material, in eV

z = the atomic number of the incident ion

m = the mass of the ion, in grams

v = the velocity of the ion, in cm/s

e = the elementary charge, in esu

n = the number of electrons per unit volume in the absorber, in cm^{-3}.

In general, ranges and stopping powers for ions in a specific material are experimentally determined and the theoretical expressions are used to extrapolate into regions where no measurements have been made. The

range-energy determinations are then tabulated. It is these range-energy tables that the experimenter in charged-particle activation will use to determine ranges and energies. The tables of Williamson, Boujot and Picard, and Northcliffe and Schilling are the most widely used for this purpose.[17,18]

The case may arise where the range-energy relationship needs to be known for a material that is not in the tables. In this case the approximation is made that the stopping power of a compound or a homogeneous mixture is given by the sum of the stopping effects of all the component atoms. This rule due to Bragg is given by the following equation

$$\frac{1}{R_t} = \frac{w_1}{R_1} + \frac{w_2}{R_2} + \frac{w_3}{R_3} + \cdots$$

where R_t = the total range in the compound or mixture

$R_1, R_2, R_3, \ldots$ = the range of each component element

$w_1, w_2, w_3, \ldots$ = the weight fraction of each of the elements.

The range-energy relationship for an ion in a specific material obtained from the tables or by using the Bragg rule can be used to determine the energy of an ion as it traverses a foil stack. The residual range, R_r, of an ion after traversing a degrader of thickness t is given by the following expression.

$$R_r = R_i - t$$

where R_i = the range of the incident ion with energy E_i. The energy of the ion after traversing the degrader is that energy which corresponds to the residual range, R_r. The range-energy relationship for protons,

deuterons, and ^{3}He ions in aluminum are shown in Figs. 2, 3 and 4. These are taken from the tables of Williamson, Bujot and Picard.

An important concept in charged-particle activation analysis is that of the Q-value. The Q-value of a nuclear reaction is the amount of energy absorbed or released for that reaction. This is expressed by adding the Q term to the right-hand side of

$$A + a \rightarrow B + b + Q \quad .$$

In nuclear shorthand, the same equation is written as

$$A(a,b)B + Q$$

where A = target atom

a = projectile atom

B = target-like product atom

b = projectile-like product atom.

A positive Q-value corresponds to the release of energy (exoergic reaction) and a negative Q-value corresponds to the absorption of energy (endoergic reaction). The Q-value is determined using

$$Q = (M_A + M_a) - (M_B + M_b)$$

where M = the mass of each atom.

The Q-value of a reaction is not generally determined using mass tables, but rather by using mass excess tables. The mass excess is given by

$$\Delta = M - A$$

where Δ = mass excess, in MeV

M = mass of the nuclide

A = mass number of the nuclide.

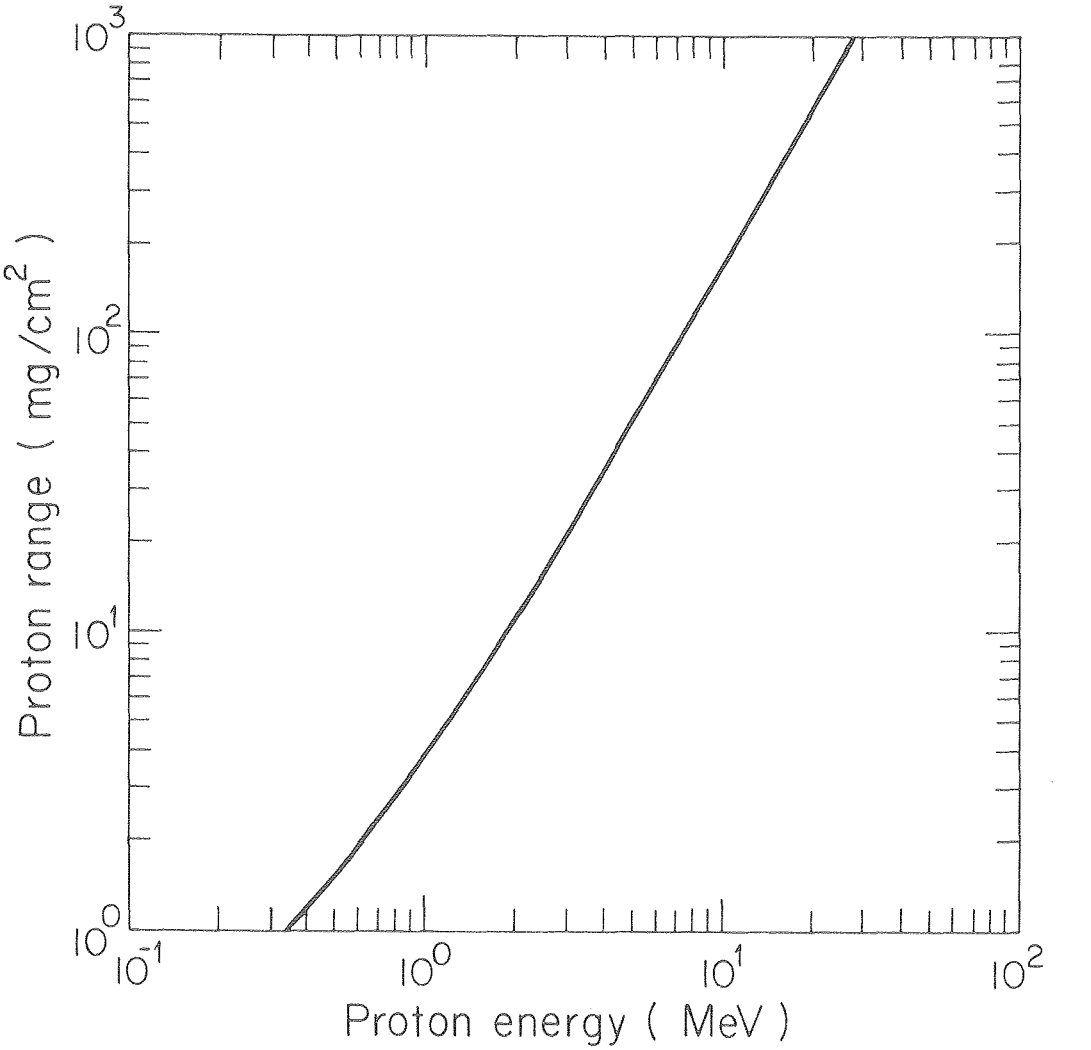

Fig. 2. The range-energy relationship for protons moving through aluminum.

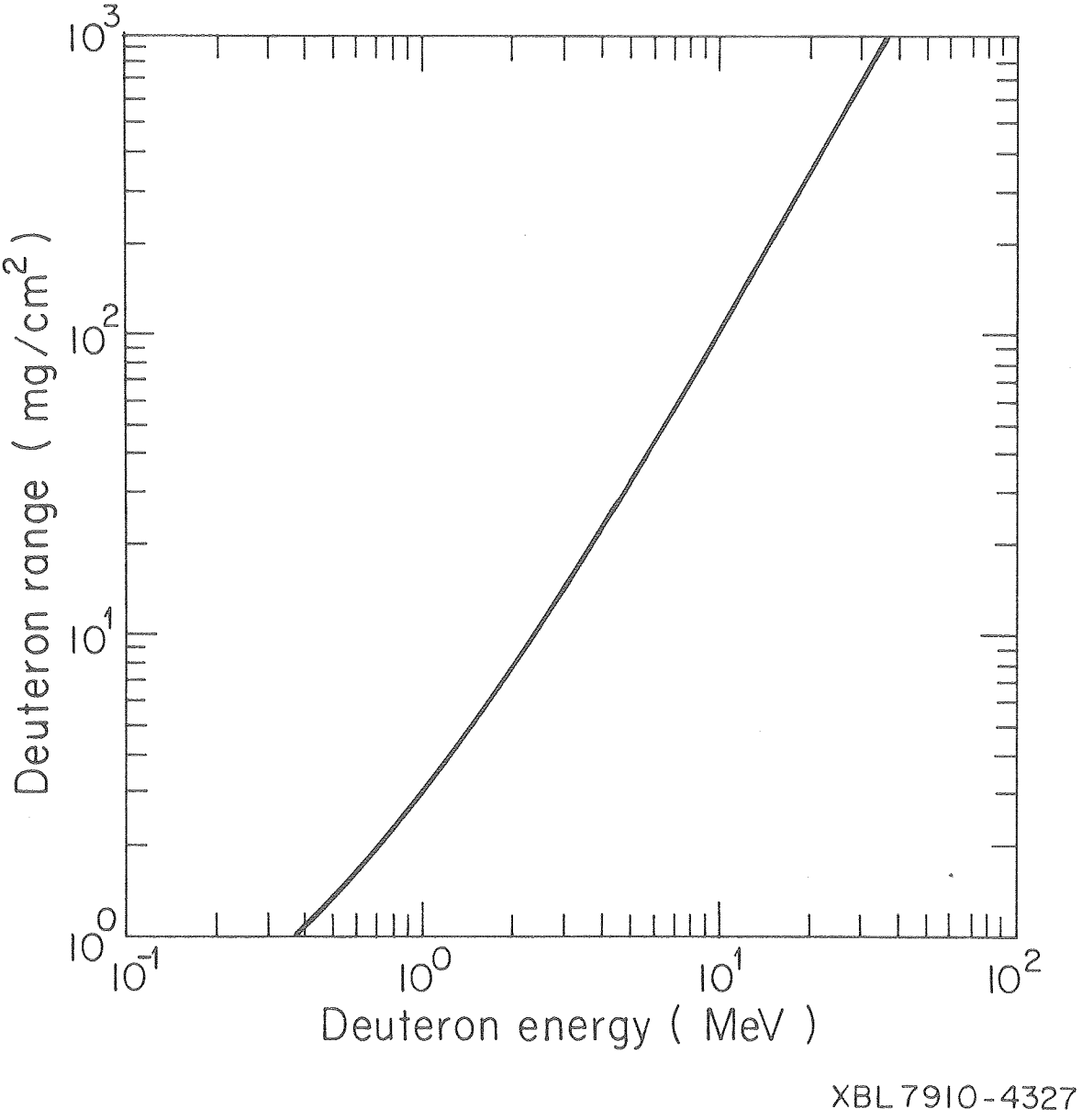

Fig. 3. The range-energy relationship for deuterons moving through aluminum.

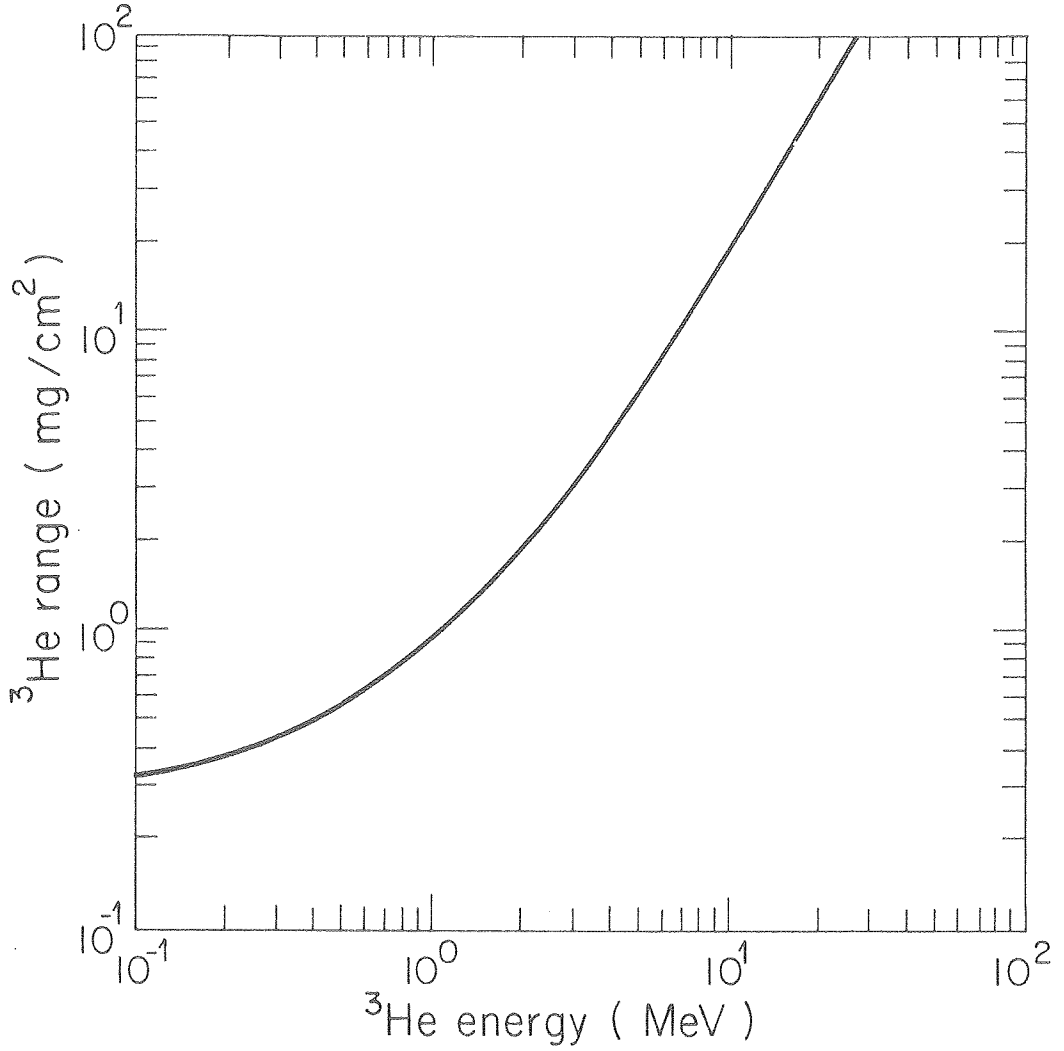

Fig. 4. The range-energy relationship for ^{3}He ions moving through aluminum.

The Q-value is then determined using

$$Q = (\Delta_A + \Delta_a) - (\Delta_B + \Delta_b) \quad .$$

Using this expression, the Q-value is obtained directly in MeV. The mass excess of most known nuclides is included in the Table of Isotopes.[19]

The Q-value gives the amount of energy required by the incident particle to make an endoergic reaction proceed in the center-of-mass system. A higher particle energy, however, will be required in the laboratory system because part of the energy will be lost to movement by the center of mass. The laboratory energy capable of making the reaction energetically possible is called the threshold energy. The threshold energy is given by

$$T = -Q\left(\frac{M_A + M_a}{M_A}\right) \quad .$$

The threshold energy for an endoergic reaction is expressed as a positive quantity while the Q-value is a negative quantity. Exoergic reactions have a threshold equal to zero.

Another important physical concept in charged-particle activation analysis is that of the Coulomb barrier. When a charged projectile approaches a target nucleus there will be an electrostatic force which tends to push the two positively charged nuclei apart. In order for a nuclear reaction to occur the two nuclei must come within range of the nuclear force. The "height" of the potential barrier, V, may be estimated as the Coulomb-repulsion energy when the two particles are just in contact. The nuclei are presumed to be perfect spheres. This is given by the well known Coulomb energy equation

$$V = \frac{Z_a Z_a e}{R_A + R_a} \quad ,$$

where Z_A = atomic number of the target

Z_a = atomic number of the projectile

R_A = radius of nucleus A

R_a = radius of nucleus a .

The nuclear radius can be obtained using the following empirical expression.[9]

$$R = 1.6\ A^{1/3}\ \text{fm}$$

where $1\ \text{fm} = 1 \times 10^{-13}$ cm.

The Coulomb-energy equation, expressed in units of MeV, is given by

$$V = \frac{1.44\ Z_A Z_a}{1.6\ (A_A^{1/3} + A_a^{1/3})}\ \text{MeV} \quad .$$

The Coulomb barrier for protons and ^{3}He ions as a function of target atomic number is shown in Figs. 5 and 6.

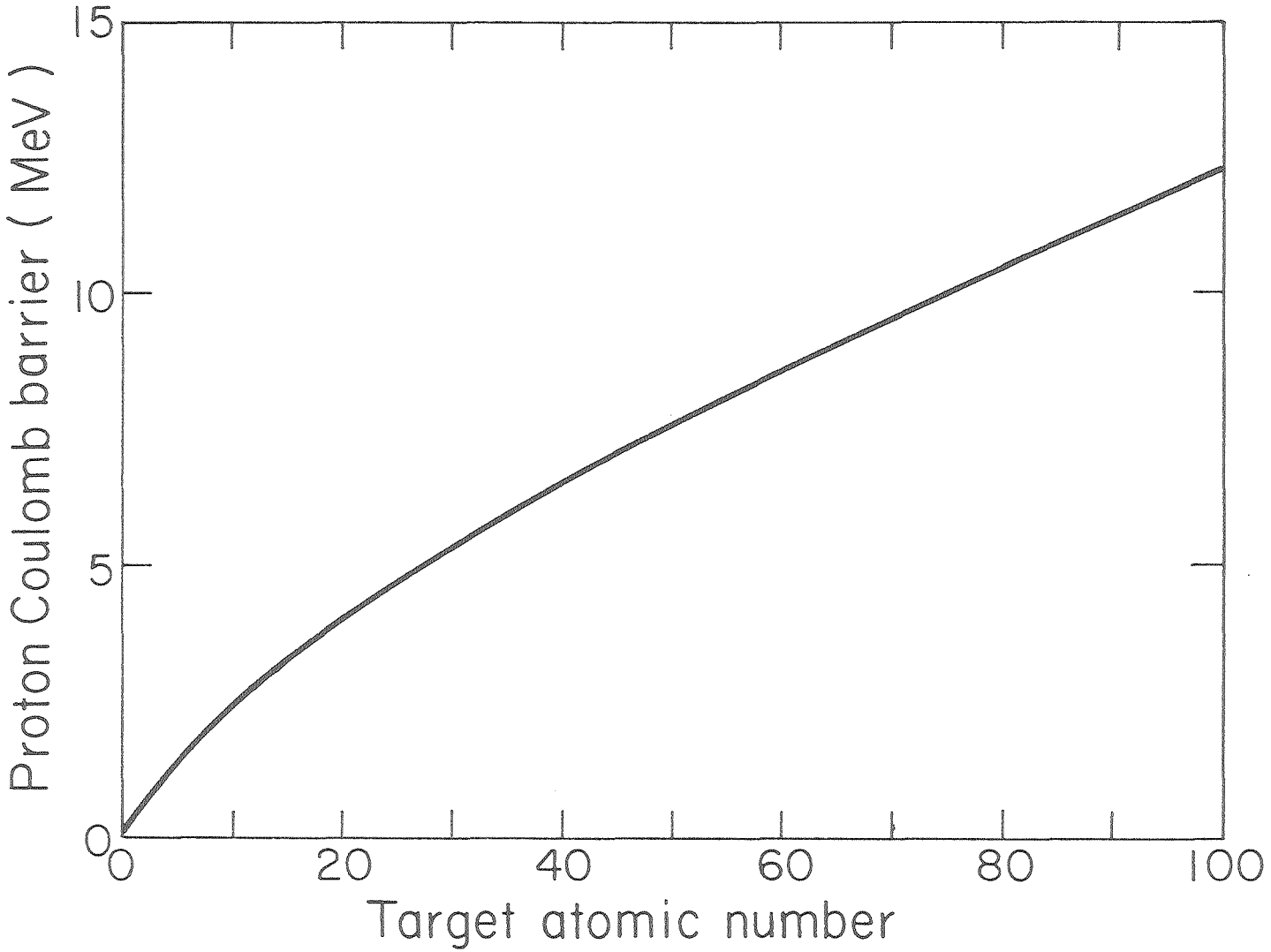

Fig. 5. The center-of-mass Coulomb barrier encountered by a proton touching a target nucleus.

XBL 7910-4330

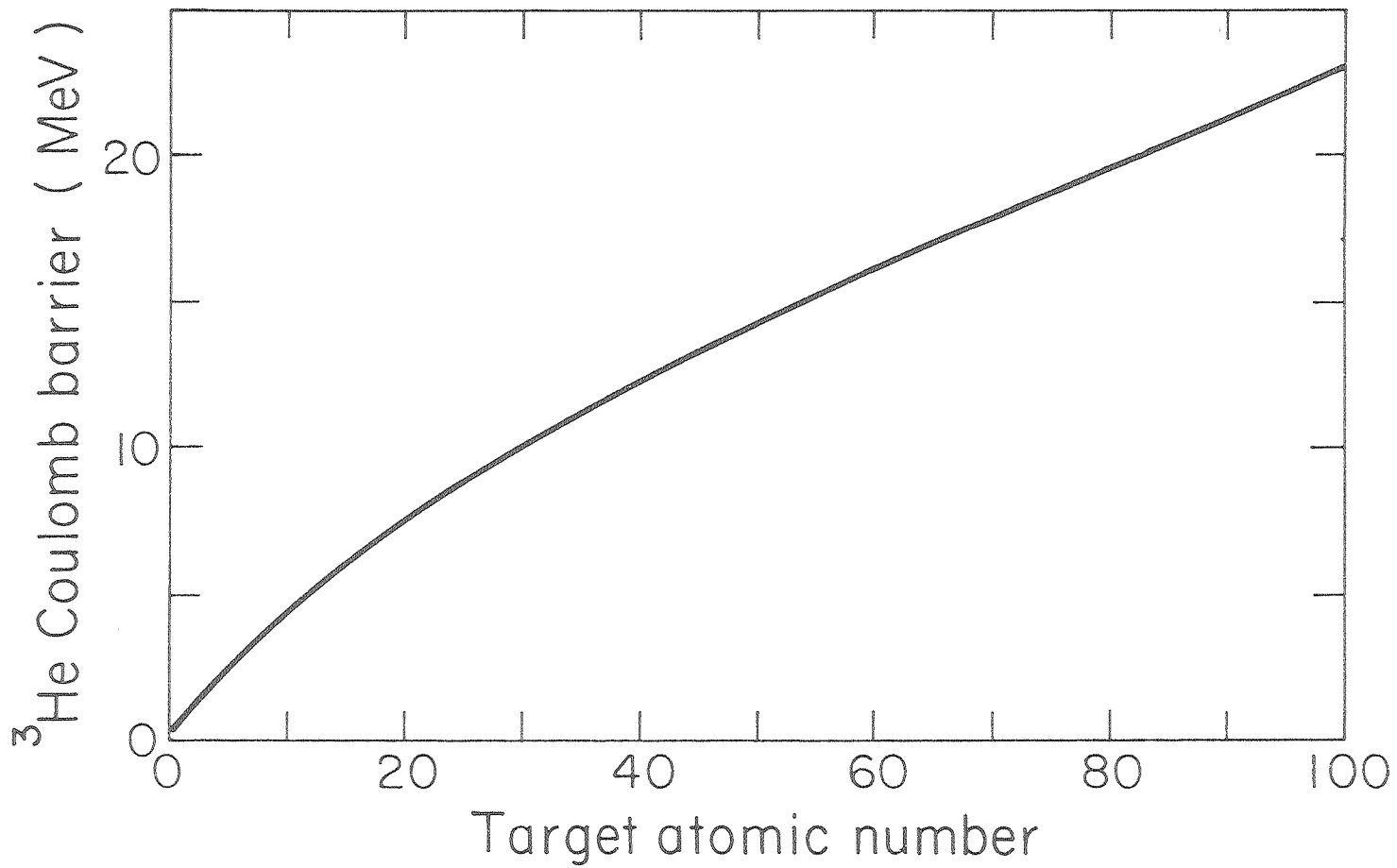

Fig. 6. The center-of-mass Coulomb barrier encountered by a ^{3}He ion touching a target nucleus.

XBL 7910-4328

II. EXPERIMENTAL

A. The 88-Inch Cyclotron

There are many different machines available for the acceleration of charged particles. These machines include Van de Graaf accelerators, linear accelerators, synchrotrons, and cyclotrons. The cyclotron is the most widely used device for generating medium-energy beams and hence the most useful for activation analysis. The first cyclotron was built in 1931 by Lawrence and Livingston (for which Lawrence won the 1939 Nobel Prize) and had a magnet pole diameter of 4 inches.[20] The modern sector-focused 88-inch cyclotron is a third generation cyclotron that combines the advantage of high beam currents of conventional cyclotrons with the high energies of synchrotrons.

Conventional cyclotrons use a constant radio-frequency potential to accelerate ions in small increments. The ions are constrained to move in a spiral path by a magnet field. The ions accelerate as they cross a gap between two electrodes called the dees; the high frequency potential is applied across the dees. The positive ions are accelerated toward the dee which is at the negative potential and away from the dee which is at the positive potential. The ions feel no electric force in the interior of the dee and move in a circular path under the force from the perpendicular magnetic field. If radio-frequency oscillation reverses the dee potentials just when the ions reach the gap, then the particles will be accelerated toward the other dee. The ions will now have a greater velocity and move in a larger circular path inside the other dee. The ion packet then spirals its way outward, increasing in energy at every dee crossing. The ions are then extracted from the machine by a deflector

plate which is held at a high negative potential.

The equation of motion shows that the cyclotron principle is based on the fact that the angular velocity of the particle is independent of the radius and at which the particle is found.

$$\omega = \frac{He}{M}$$

where ω = angular velocity, in sec^{-1}

H = magnetic field strength, in gauss $\times 10^{-4}$

M = ion mass, in kg

e = ion charge, in coulombs.

This also shows that all ions of the same charge-to-mass ratio will be accelerated together. The final energy attainable for a given ion varies as the square of the cyclotron radius,

$$KE = \frac{H^2 e^2 r^2}{2M} \quad .$$

This would indicate that the larger the cyclotron the higher the attainable particle energy. This is true up to a certain point. As the particles increase in energy their mass also increases due to relativistic effects. While the particle energy is low enough (~10 MeV for deuterons) this mass increase is small and does not affect cyclotron operation. At higher energies the mass increase causes the ions to get out of synchronization with the radio-frequency oscillations. This can be seen from the cyclotron equation of motion, where the angular velocity is dependent on the charge-to-mass ratio at constant magnetic field strength, H. The magnetic field strength can be increased as a function of radius to try to compensate for the mass increase, but axial defocusing is an unfortunate consequence.

In 1938, L. H. Thomas proposed a method for overcoming the energy limitations of cyclotrons.[21] He showed that azimuthal variations of the magnetic field can be used to provide axial focusing while letting the average field increase with radius to compensate for the relativistic mass increase. The azimuthal variations are obtained by built-up sections of the magnet pole face which leads to strong (hill) and weak (valley) field regions. A cyclotron of this type is called a sector-focused cyclotron.

The Lawrence Berkeley Laboratory 88-inch cyclotron is one such sector-focused cyclotron.[22] It can produce protons beams up to an energy of 60 MeV as well as heavy-ion beams in the several hundred MeV range. The maximum external power is 3 kilowatts which corresponds to 60 μA of 50-MeV protons. The external unanalyzed beam has an energy spread of 0.3%. The ion source for light-ion beams is a hooded hot-arc source and for heavy-ion beams it is a Penning ionization gauge.

The irradiations in this work were carried out at the LBL 88" cyclotron. Three different particles and several different energies were used for the irradiations. Some beams were used more than others, but the list includes 21-MeV protons, 16-MeV protons, 11-MeV protons, 15-MeV deuterons, and 15-MeV ^{3}He ions. Beam currents used for this work were in the one-half to one μA range. These beams were routinely tuned up in 1 to 1½ hours; since the bombardments were for one minute on target, the entire cyclotron time used for one run was about two hours.

B. The Irradiation Apparatus

Targets to be irradiated were mounted on water-cooled copper blocks

known as TAG-target blocks. One is shown in Fig. 7. There were several targets on each block. This foil stack was isolated from the cyclotron vacuum by a large top foil which was sealed using O-ring seals. The beam was collimated to a ½-inch diameter circle using an upstream collimator. The beam did not actually strike the collimator ring shown in Fig. 7, which had an inside diameter of 7/8 inch, but was used primarily for holding the stack in place and for forming the top seal. The foil stack was arranged such that the beam was stopped in the copper and the heat carried away by the water-cooling system. The power deposited by the beam in a foil is 1 watt per μA per MeV of energy lost in passing through the foil. Since all the beam degraders were aluminum foils, the aerosol samples were collected on silver filters and standard targets were prepared by depositing a thin layer of material on an aluminum foil; there was good heat conduction in the stack. Targets irradiated using this system were observed to be completely undamaged by the beam. This was checked by having a combustion analysis performed on a target of 2 mg/cm^2 melamine, $C_6H_6N_3$, deposited on a 0.001-inch aluminum foil after it had been used in several runs. The correct elemental composition for the melamine within experimental error was found.

The TAG-target block was also used as the back end of the Faraday cup. The TAG-target block fits into an apparatus at the end of the beam line. This is shown in Fig. 8. The front end of this apparatus is a collimator which could be used to center the beam in the up-down and side-to-side directions. The back end of the apparatus is a Faraday cup. The integrator lead is attached directly to the TAG-target block. The cold-water hoses are well insulated from ground. The total charge received

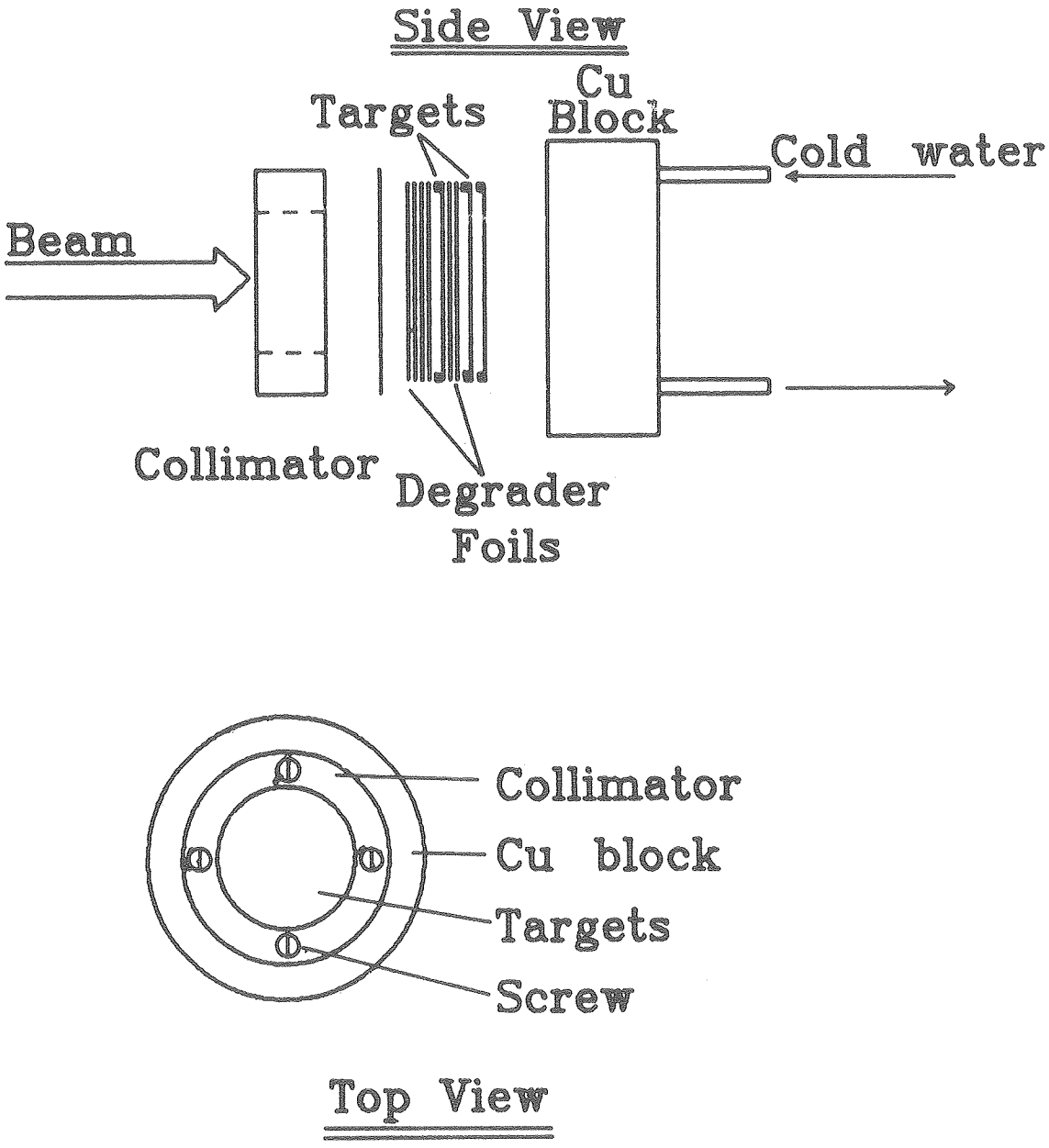

Fig. 7. The TAG-target block used to hold the targets for irradiation.

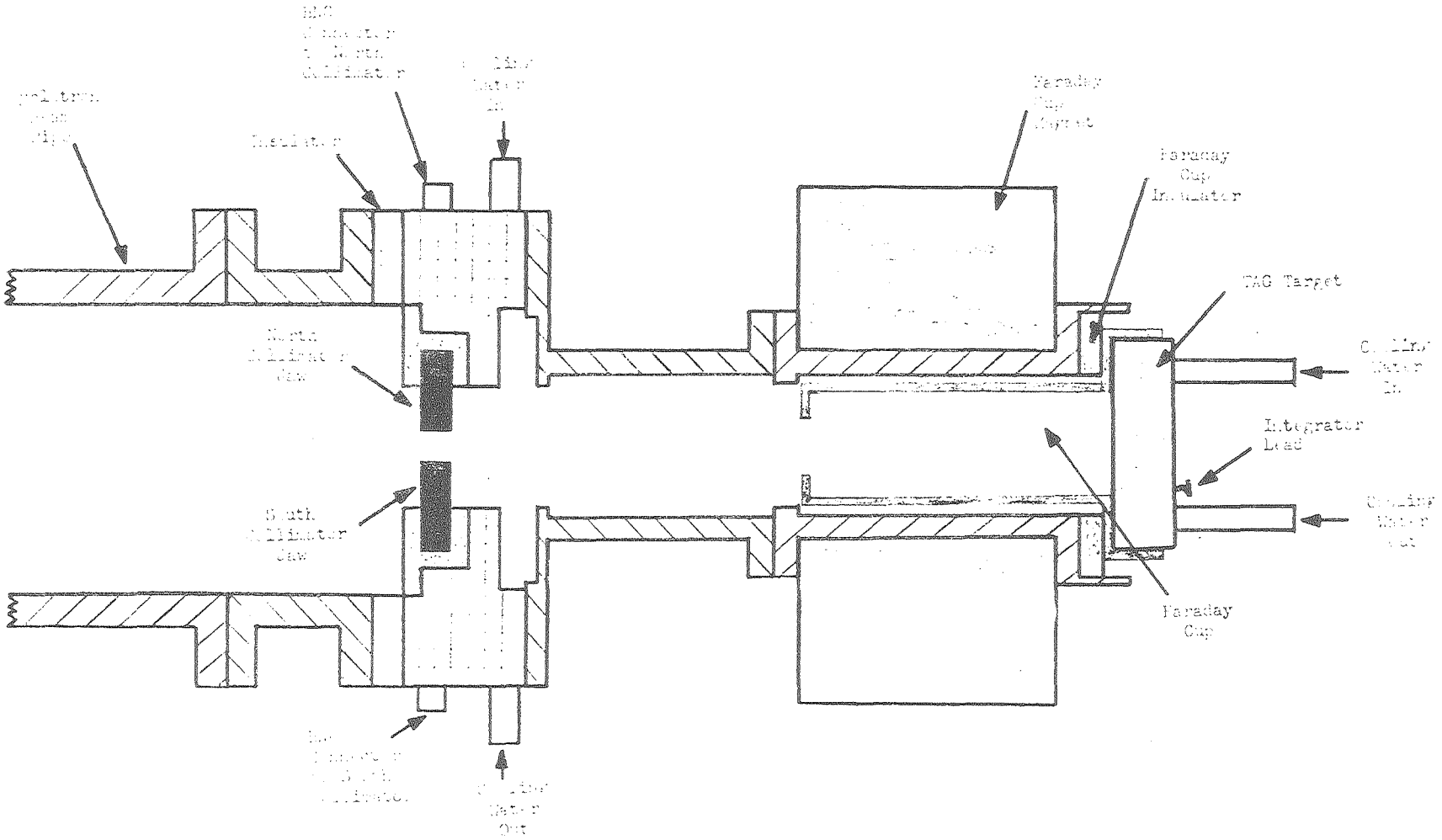

Fig. 8. The irradiation apparatus for hold the TAG-target. The TAG-target itself forms the back end of the Faraday cup.

from the Faraday cup is measured by a calibrated integrating electrometer. The advantages of using this irradiation apparatus is that the foil stacks could be mounted ahead of time on the TAG-target blocks and quickly changed after each stack irradiation. The time between stack irradiations was typically 5 minutes, including cave entry and pump-down time.

C. Detectors and Counting Equipment

There are many different counting systems that one may use for assaying an irradiated sample depending on the half-life and decay characteristics of the radionuclides involved. If the produced radionuclide has a short half-life ($t_{\frac{1}{2}} < 1$ minute) then the assay will have to be carried out at the irradiation facility. Radionuclides with longer half-lives allow the sample to be assayed outside the irradiation facility under low-background conditions. In many cases it is desirable to allow the short-lived isotopes to decay and to assay the longer-lived components at a later time. Radionuclides decay primarily by three processes. These processes are α-decay, β-decay, and spontaneous fission. The γ-decay of an excited nucleus may accompany any one of these processes. The type of counter to be used depends on the radiation to be detected. An ionization chamber or a surface-barrier detector can be used to detect α-rays and fission fragments. The β-rays are detected with Geiger counters or proportional counters. The γ-rays are detected primarily with NaI(Tl) scintillation counters and Ge(Li) semiconductor detectors.

The specificity of nuclear radiation is an important advantage in activation analysis. Such nuclear-decay properties as half-life, beta-

decay energy and gamma-ray energy are generally characteristic of a nuclide and it is possible by measuring these quantities to ensure that the activity that is being measured is appropriate to the element being determined. Direct detection of beta particles for an activation analysis is complicated by the beta-decay process itself. The beta-decay process is a three-body process involving the decaying nucleus, the beta particle and the normally undetectable neutrino. This means that even though there is a definite beta-decay energy (Q-value) the observed beta particle has a range of kinetic energies. There is really no use for energy analyzing the beta particles since the energy is not characteristic of a given nuclide. All radionuclides used in this work and indeed, most radionuclides of importance in the field of activation analysis, decay by the beta-decay process. The direct detection of the beta rays in a counter such as a gas-flow proportional counter must primarily use decay-curve-resolution methods and in some cases beta absorption methods to separate the different nuclides present. This is a difficult process at best, in all but the most simple cases, since most radionuclides decay by beta emission.

A more specific radiation to use for assay purposes is the gamma radiation associated with the beta-decay process. A beta-decay event will generally have a branch that leaves the product nucleus in an excited state. The most common way for the nucleus to deexcite is by the emission of electromagnetic radiation (internal conversion is an alternate mechanism). This gamma ray will be characteristic of the emitting nucleus and can be used to separate the decay event from decay events involving other nuclei. This is a common strategy in activation

analysis and has made gamma spectroscopy an important part of the field.

There are three types of beta-decay events. There is the beta decay of neutron-rich nuclides which involves the emission of a β^- particle and a $\bar{\nu}$ particle (antineutrino). This decay results in a daughter nucleus that has the same mass number, but has its atomic number increased by one. The neutron-deficient nuclides may decay by two processes which have the same effect of decreasing the atomic number by one while keeping the mass number the same. One process is positron decay which involves the emission of a β^+ particle and the simultaneous emission of a ν particle (neutrino). The other process is electron capture where the nucleus captures an orbital electron to achieve the same effect. Since the K-shell electrons are the most likely to be captured this process is also called K-capture. This is the only process that can occur for a decay energy (Q-value) of less than 2 M_e (1.02 MeV). For Q-values over 1.02 MeV, positron emission competes effectively with electron capture.

As a general rule, charged-particle activation analysis produces neutron-deficient nuclides. This may be a prime reason for choosing charged-particle activation analysis. This was certainly the case with the proton, deuteron and ^{3}He irradiations of this work. This means that the radionuclides will be decaying by either positron emission or electron capture. In the region below Z = 10 the neutron-deficient nuclides all decay by almost 100% positron emission (the notable exception is ^{7}Be). Another general characteristic of this region is that the radionuclides directly off the line of beta stability have no nuclear gamma rays accompanying their decay. This includes the important activation products ^{11}C, ^{13}N, ^{15}O, ^{17}F, and ^{18}F. There is, however, one important gamma ray

accompanying the decay of these nuclides. This is the 0.511-MeV positron-annihilation radiation. The positrons are emitted into the surrounding medium, quickly coming to rest via collisions with electrons and the electron-positron pair annihilates. The primary result is the formation of two quanta of gamma radiation each with an energy of one electron rest mass (0.511 MeV). Conservation of momentum requires the photons to be emitted in directions 180° apart from each other. This gives the positron-annihilation event a unique angular correlation. An important point is that nearly all annihilation events involve positrons that have slowed to thermal energies. The mean life of positrons in most metals is about 1.5×10^{-10} second.[9]

The 0.511-MeV positron-annihilation radiation was used exclusively in this work as the assay radiation. The irradiated samples were placed on aluminum counting cards of sufficient thickness to stop the positrons. A thin Saran cover was placed over the target to keep it in place while counting as well as to keep the sample from being contaminated. Finally a copper cover with a thickness of 850 mg/cm^2 was placed over the sample in order to stop all the positrons emitted in that direction. The positrons were hence stopped in the material directly surrounding the target. This meant that the annihilation events were occurring in a compact and well defined region of space.

The two primary detectors available for the detection of the 0.511 MeV annihilation radiation are the solid-state Ge(Li) diode detector and the NaI(Tl) scintillation detector. Each detector has its advantages, but the main comparison between the two detectors is that the Ge(Li) detector offers a high resolution (2 to 3 keV) and the NaI(Tl) detector

offers a high detection efficiency (approximately ten times that of the Ge(Li) detector). For work involving just the detection of 0.511-MeV radiation the cheaper and more efficient NaI(Tl) detector seems like the obvious choice. A single-channel analyzer and a scaler would suffice as the data collection electronics. For routine work involving many samples this simple system should be used. For development work, however, where resolution rather than efficiency is required, the Ge(Li) detector is the most useful detector. This high-resolution detector can be used to check for possible nuclear gamma rays in the 0.511 MeV region that would otherwise not be seen with the NaI(Tl) detector. The information obtained using a Ge(Li) detector also permits a more complete identification of the other radionuclides produced during the irradiation. For these reasons the Ge(Li) detector was used for gamma-ray detection throughout this work.

There were several different Ge(Li) detection units used during the course of the experiments. All detectors were coaxial Ge(Li) detectors and have active volumes of approximately 60 cm^3. The efficiency for each counter at 0.511 MeV was determined with a ^{22}Na calibrated standard obtained from the International Atomic Energy Authority, Vienna. The overall detection coefficient for a 100% positron emitter positioned 5 cm from the face of the crystal was approximately 2%. The decay characteristics data for all nuclides was were taken from the Table of Isotopes.[17]

An LBL-built multichannel analyzer system was used for most of the data collection. Some experiments were carried out using a recently received Tracor-Northern multichannel analyzer system.[23] Both systems are similar so only the LBL analyzer and electronics will be described. A block diagram of the analyzer system is shown in Fig. 9. An Ortec

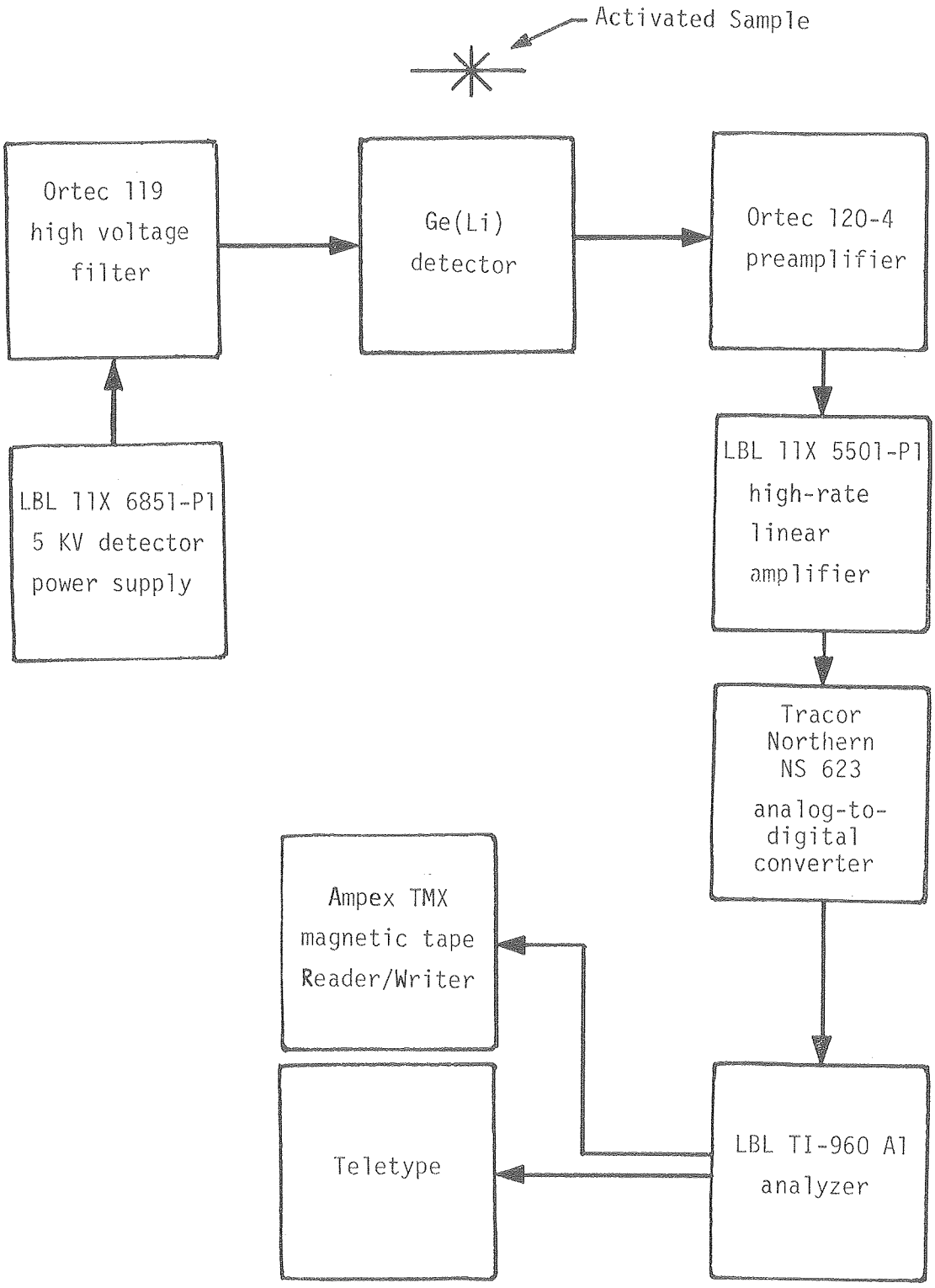

Fig. 9. Block diagram of the counting system used for assaying samples.

Ge(Li) detector is operated at a bias of +4000 volts d.c. This bias is delivered by an LBL-built high voltage supply. The output of the Ge(Li) crystal goes into a charge-sensitive dc-coupled preamplifier. The preamplifier has a sensitivity of 170 mV/MeV. This means that for every MeV of energy that is deposited in the Ge(Li) crystal the preamplifier emits a pulse of 170 mV. The output of the preamplifer goes to an LBL-built high-rate linear amplifier. The high-rate linear amplifier is operated at a gain of about 29 and emits a unipolar pulse. This pulse then goes to a Tracor-Northern 100 MHz analog-to-digital converter (ADC). The ADC converts the 0 to 10 volt analog signal and sends it to the analyzer's 4096-channel memory. The TI-960 Al analyzer is an LBL-built analyzer that uses a Texas Instruments 960 minicomputer as the heart of the system.[24] It is capable of many simple functions such as arithmetic operations, peak integration and peak-centroid determination. The computer greatly facilitated rapid data collection. For each individual count the computer would mark the time of day, determine net counting rate, determine the 0.511-MeV peak centroid (for possible gain shifts) and automatically write the data on magnetic tape. The important data for the 0.511-MeV peak was output to teletype during the data collection period. The decay curves could be constructed from this hard copy in case anything was wrong with the magnetic tape data. The entire spectrum was stored on magnetic tape as well as all important timing information. The usual method of data analysis was to use the LBL main computing facility (the CDC-7600 system) to analyze the data from the magnetic tape.

D. Data Analysis

The decay of the 0.511-MeV annihilation radiation for each sample was followed for several hours using the described counting system. The determination of the A_0 value for each component present in the decay curve was done in the following manner.

The spectrum was analyzed to determine the net number of counts in the peak. The 0.511-MeV peak "sits" on a background of Compton events caused by higher-energy gamma rays. This Compton background must be removed from the peak area. This is done by a simple linear-background subtraction. A region on the high energy side of the full energy peak and one on the low energy side of the peak are defined. A typical value of 20 channels was used to define the full energy peak. A region of 20 channels on the immediate high-energy was then defined and likewise a region of 20 channels on the immediate low-energy side was defined. The net counts in the peak is determined by

$$C_n = C_p - \frac{(C_h + C_l)}{2}$$

where C_n = net counts in the peak

C_p = total counts in the peak

C_h = total counts in the high-energy region

C_l = total counts in the low-energy region.

This simple background subtraction works well for spectra where the peaks are well separated, as in this case. The method yields very consistent results and more complicated computer-determined polynomial background determinations are not really needed.

It is not possible to measure the counting rate at an instant in time, but only over a period of time. The start time or stop time of the interval are not the correct times corresponding to the observed counting rate. There is, however, a point during the counting interval that corresponds to the measured counting rate. Cook and Duncan have shown that using the midpoint time of the counting interval results in very small errors as long as the count time is less than one half-life.[25] The error is 2% for a count time equal to the half-life and only 0.1% for a count time equal to 0.2 half-life. In most cases the count time used in this work was approximately 0.2 half-life. The midpoint time of the interval was used as the time point representing the measured count rate in this work. Another method for determining true-time representation has been offered by Hoffman and Camerik.[26]

The plot of the observed counting rate versus time is called a decay curve. In this work the decay curve is a mixture of independent activities which must be separated into individual components. For a mixture of independent activities the plot or log of activity versus time is always a curve that is concave upward. This curvature results because the shorter-lived components contribute relatively less to the activity as time passes. After a sufficiently long time, the longest-lived activity will dominate the decay curve and its half-life can be read directly.

The decay curves were resolved by the least-squares computer code CLSQ.[27] The code has been adapted for use on the CDC-7600 computer at LBL. The program can read data directly from magnetic tape or from punched cards. The program utilizes the following mathematical method. The decay curve consists of n measurements of the counting rate, A_i, of the sample

at time t_i. The m independent radioactive species present satisfy a set of n equations of the form

$$A_i = \sum_{j=1}^{m} A_{0j} e^{-\lambda_j t_i} + r_i$$

where $A_{0j} e^{-\lambda_j t_i}$ = the contribution of the j^{th} component to the total activity at time t_i

r_i = the residual.

The residual is due to the statistical fluctuations and experimental errors. The m number of coefficients A_{0j} enter these equations in a linear manner. This means that a least-squares solution is possible. The condition for that solution is given by

$$\sum_{i=1}^{n} P_i r_i^2 = \text{minimum}$$

where P_i = the weight assigned to each residual.

The weight factor is given by

$$P_i = \frac{1}{\sigma_i^2}$$

where σ_i = the standard deviation of the i^{th} count.

The statistical considerations of radioactive decay yield an important property between total counts measured in an interval and the standard deviation of the error.

$$\sigma = \sqrt{N}$$

where N = number of counts measured.

Where a background subtraction is required the statistical error of the net number of counts is determined by the error in the total peak

counts and the error in background measurement. This is given by

$$\sigma_i = \sqrt{\sigma_{it}^2 + \sigma_{ib}^2}$$

where σ_{it} = the error in the total counts in the peak of the i^{th} count

σ_{ib} = the error in the total counts in the background of the i^{th} count

The standard deviations σ_{it} and σ_{ib} are given by

$$\sigma_{it} = \sqrt{N_{it}} \qquad \text{and} \qquad \sigma_{ib} = \sqrt{N_{ib}} \quad .$$

The standard deviation for net number of counts is given by

$$\sigma_i = \sqrt{N_{it} + N_{ib}} \quad .$$

Using this method the computer code determines the best fit values for the end-of-bombardment counting rate, A_0, for all given components. The code also determines the X^2 per degree of freedom. The standard deviation of the end-of-bombardment counting rate is the total of the statistical and decay curve analysis errors. The computer code could usually determine the A_0 value to an error of approximately one percent since the desired radiation was almost always the major component. An example of the CLSQ computer output is shown in Fig. 10.

Calculation of the amount of the element being determined was done by the relative method of analysis for all determinations performed in this work. This method of analysis was discussed in Section I, part G. This method of analysis yields a more accurate answer since many of the possible systematic errors cancel out. The precision and accuracy of each method of elemental analysis was obtained by the comparison of activation

BBD 77- DECAY CURVE FOR B 1 -511 KEV GAMMA 9/20/79

NUMBER OF COUNTS	RUNNING TIME	BACKGROUND	MIDPOINTTIME	COUNTING RATE	VARIANCE IN COUNT. RATE
4.56765E+03	1.00000E+00	7.73500E+01	9.11166667E+00	4.56765E+03	6.85221E+01
3.51660E+03	1.00000E+00	6.24000E+01	1.31283333E+01	3.51660E+03	6.01628E+01
2.86855E+03	1.00000E+00	4.74500E+01	1.71450000E+01	2.86855E+03	5.42848E+01
2.28215E+03	1.00000E+00	4.48500E+01	2.09950000E+01	2.28215E+03	4.85402E+01
1.84580E+03	1.00000E+00	3.12000E+01	2.50783333E+01	1.84580E+03	4.35578E+01
1.49895E+03	1.00000E+00	3.70500E+01	2.90533333E+01	1.49895E+03	3.94979E+01
1.36125E+03	1.00000E+00	3.57500E+01	3.09866667E+01	1.36125E+03	3.76860E+01
2.47645E+03	2.00000E+00	6.95500E+01	3.35283333E+01	1.23822E+03	2.54520E+01
2.20515E+03	2.00000E+00	5.78500E+01	3.64783333E+01	1.10257E+03	2.39823E+01
1.97845E+03	2.00000E+00	5.65500E+01	3.94116667E+01	9.89225E+02	2.27583E+01
1.75155E+03	2.00000E+00	4.74500E+01	4.23116667E+01	8.75775E+02	2.13883E+01
1.57560E+03	2.00000E+00	4.94000E+01	4.52616667E+01	7.87800E+02	2.03538E+01
1.48120E+03	2.00000E+00	4.68000E+01	4.81533333E+01	7.40600E+02	1.97384E+01
1.15340E+03	2.00000E+00	4.16000E+01	5.45783333E+01	5.76700E+02	1.74788E+01
9.52350E+02	2.00000E+00	3.96500E+01	6.37783333E+01	4.76175E+02	1.59513E+01
1.28910E+03	3.00000E+00	6.89000E+01	7.30366667E+01	4.29700E+02	1.24846E+01
1.22505E+03	3.00000E+00	5.39500E+01	7.90283333E+01	4.08350E+02	1.20834E+01
1.80795E+03	5.00000E+00	8.90500E+01	9.71033333E+01	3.61590E+02	8.84281E+00
1.62595E+03	5.00000E+00	8.90500E+01	1.18228333E+02	3.25190E+02	8.42112E+00
1.53110E+03	5.00000E+00	9.49000E+01	1.50120000E+02	3.06220E+02	8.21629E+00
1.42415E+03	5.00000E+00	9.68500E+01	1.78853333E+02	2.84830E+02	7.95978E+00

NP= 21 NC= 3 NV=0 CNV=0. BGD= 0. SBGD= 0. BLOCK= 0. SCOFF= .1 RJT= 5.0 KCS=0

	HALF LIFE	SIGMA H		CPM AT EOB	SIGMA	DECAY FACTOR
COMP(1)	9.980M	0.	M	7.03726E+03	1.53967E+02	1.00000E+00
COMP(2)	20.400M	0.	M	5.71502E+02	6.98707E+01	1.00000E+00
COMP(3)	390.000M	0.	M	3.89877E+02	5.79055E+00	1.00000E+00

FIT= .688

T(I)	F(I)	FCALC(I)	V(I)	SIGMA(I)	RATIO(I)	PCINT	CNTR NO.
9.11167E+00	4.56765E+03	4.54031E+03	2.73372E+01	6.85221E+01	.40	1	=
1.31283E+01	3.51660E+03	3.57427E+03	-5.76679E+01	6.01628E+01	-.96	2	=
1.71450E+01	2.86855E+03	2.83655E+03	3.19973E+01	5.42848E+01	.59	3	=
2.09950E+01	2.28215E+03	2.29291E+03	-1.07641E+01	4.85402E+01	-.22	4	=
2.50783E+01	1.84580E+03	1.84962E+03	-3.81925E+00	4.35578E+01	-.09	5	=
2.90533E+01	1.49895E+03	1.51875E+03	-1.97958E+01	3.94979E+01	-.50	6	=
3.09867E+01	1.36125E+03	1.38638E+03	-2.51345E+01	3.76860E+01	-.67	7	=
3.35283E+01	1.23822E+03	1.23585E+03	2.37208E+00	2.54520E+01	.09	8	=
3.64783E+01	1.10257E+03	1.08947E+03	1.31061E+01	2.39823E+01	.55	9	=
3.94117E+01	9.89225E+02	9.68913E+02	2.03122E+01	2.27583E+01	.89	10	=
4.23117E+01	8.75775E+02	8.65869E+02	5.90056E+00	2.13883E+01	.28	11	=
4.52617E+01	7.87800E+02	7.86021E+02	1.77875E+00	2.03538E+01	.09	12	=
4.81533E+01	7.40600E+02	7.17464E+02	2.31357E+01	1.97384E+01	1.17	13	=
5.45783E+01	5.76700E+02	5.96389E+02	-1.96890E+01	1.74788E+01	-1.13	14	=
6.37783E+01	4.76175E+02	4.97417E+02	-2.12420E+01	1.59513E+01	-1.33	15	=
7.30367E+01	4.29700E+02	4.34290E+02	-4.58976E+00	1.24846E+01	-.37	16	=
7.90283E+01	4.08350E+02	4.06851E+02	1.49861E+00	1.20834E+01	.12	17	=
9.71033E+01	3.61590E+02	3.57457E+02	4.13273E+00	8.84281E+00	.47	18	=
1.18228E+02	3.25190E+02	3.28188E+02	-2.99808E+00	8.42112E+00	-.36	19	=
1.50120E+02	3.06220E+02	3.02266E+02	3.95449E+00	8.21629E+00	.48	20	=
1.79853E+02	2.84830E+02	2.85050E+02	-2.20362E-01	7.95978E+00	-.03	21	=

ALL DATA POINTS OK.

Fig. 10. A typical computer output for the CLSQ code.

results with the results of an independent method. In the case of the oxygen analyses two activation methods were compared since a completely independent method for oxygen analysis at levels found in aerosols was not available. These errors are discussed in the results section for each elemental analysis method.

Excitation functions were determined using the general activation equation. The errors in precision for these determinations are estimated to be 2 to 3% for the beam intensity measurement and 2 to 3% for the overall detection coefficient. Errors in timing, target weight and A_0 determination are all small (~1% each). Overall precision for each cross section determination in the excitation functions is 5 to 8%.

III. RESULTS

A. Nitrogen Determination

There are several possible ways that nitrogen could be determined by charged-particle activation. The primary considerations in the selection of a suitable nuclear reaction are that a) the product nuclide has the appropriate half-life and decay characteristics, b) there are no interfering reactions, and c) the optimum sensitivity is obtained. The optimum sensitivity can be obtained only by using the high abundance isotope of an element. The highest possible sensitivity is especially important in analysis of aerosols where sample sizes are small. For nitrogen this means that one should select a nuclear reaction that employs the ^{14}N nuclide. The product nucleus must have a half-life between 10 minutes and several hours and decay by positron emission or preferably have a high-abundance nuclear gamma ray. The short half-life nuclides are ruled out because the assay is done away from the cyclotron and they decay away before an assay is possible. Of course, a special apparatus at the cyclotron could be constructed to detect activities of shorter half-lives but this defeats the purpose of designing a simple analysis method that uses a minimum of accelerator time. The longer half-lives are ruled out because the assay would take too long and a longer irradiation would be required to get a comparable activity relative to a shorter half-life nuclide (from the saturation curve).

The possibility of interfering reactions is also an important consideration. Two types of interferences must be considered in an activation analysis using gamma-ray spectroscopy. The first type of interference is from the production of activities of similar half-life

and gamma-ray energy to the activity of interest. This type of interference can usually be minimized by use of high-resolution Ge(Li) detectors but this presents a potential problem in this work because the gamma ray being counted is the 0.511-MeV positron annihilation radiation. There will be contributions to this photopeak from all other positron-emitting nuclides that may be created in the bombardment depending on the half-lives. This type of interference is overcome by selecting the appropriate reaction and particle energy so the activity of interest is the dominant positron-emitting nuclide.

The second type of interference which must be considered is the production of the radionuclide of interest from an element other than the one under analysis. In this case if the radionuclide of interest is produced from any element other than nitrogen, then the amount that is measured is not proportional to the amount of nitrogen in the sample and an error in the analysis will result. The selection of a nuclear reaction will be made only after the possible interfering reactions in both aerosol and filter have been identified and their importance determined. This is an important consideration in a sample as complex as an aerosol which contains many elements in widely varying proportions. The possible nuclear reactions with their associated interfering reactions, half-lives and Q-values are listed in Table 1.

The $^{14}N(p,\alpha)^{11}C$ reaction was selected as the analysis reaction for nitrogen. There are several reasons for this selection. The first one is that the product is the ^{11}C nuclide which has a half-life of 20.4 minutes and decays by 100% positron emission. This makes the product activity easy to assay and sensitivity will be high because of the decay

TABLE 1. Possible reactions for determination of nitrogen and the corresponding interfering reactions.

Reaction	Half-life (min)	Q-Value (MeV)	Potential interfering reactions	Half-life (min)	Q-value (MeV)
$^{14}N(p,\alpha)^{11}C$	20.4	-2.9	$^{11}B(p,n)^{11}C$	20.4	- 2.7
			$^{12}C(p,pn)^{11}C$	20.4	-18.7
			$^{16}O(p,\alpha d)^{11}C$	20.4	-23.6
			$^{19}F(p,2\alpha n)^{11}C$	20.4	-17.8
			$^{107}Ag(p,pn)^{106}Ag$	24.1	- 9.5
$^{14}N(p,n)^{14}O$	1.17	-5.93	$^{16}O(p,t)^{14}O$	1.17	-20.4
			$^{19}F(p,\alpha 2n)^{14}C$	1.17	-20.8
$^{14}N(d,n)^{15}O$	2.03	+5.1	$^{16}O(d,dn)^{15}O$	2.03	-15.7
			$^{16}O(d,n)^{17}F$	1.10	- 1.6
			$^{29}Si(d,n)^{30}P$	2.5	+ 3.4
$^{14}N(^{3}He,\alpha)^{13}N$	10.0	+10.0	$^{12}C(^{3}He,d)^{13}N$	10.0	- 5.8
			$^{11}B(^{3}He,n)^{13}N$	10.0	10.2

property. There is really only one significant interfering reaction, the $^{11}B(p,n)^{11}C$ reaction. All the other reactions can be eliminated by using a proton energy of less than 9.5 MeV. The silver reaction is included in the list since silver was selected as the preferred filter material for reasons that will be discussed. Most notably, there is *no interference from carbon*, which constitutes a large fraction of the bulk aerosol. The boron interference cannot be eliminated by a proper choice of beam energy because the Q-value for this reaction is actually less than for the nitrogen reaction. Large concentrations of boron will interfere with the nitrogen analysis. It has been shown, however, that boron concentrations are at least *two orders of magnitude lower* than nitrogen concentrations in typical urban aerosols;[28] therefore, boron is not a significant interference.

The $^{14}N(p,n)^{14}O$ reaction was not used because of the short half-life (70 sec) of the ^{14}O nuclide. To use this reaction would require special apparatus at the accelerator. Otherwise, it is an interference-free reaction for proton energies below 20 MeV. It also has a nuclear gamma ray (2.31 MeV, 99%) which would be ideal to use as the assay radiation.

The $^{14}N(^{3}He,\alpha)^{13}N$ reaction produces a convenient radiation for assay purposes. There is, however, two interfering reactions. The boron interference can be dismissed in the same fashion as for the $^{14}N(p,\alpha)^{11}C$ reaction, i.e., its low concentration in aerosols. The carbon interference is not so easily dismissed. In order to prohibit carbon interference by the $^{12}C(^{3}He,d)^{13}N$, the ^{3}He energy would have to be below 6 MeV. Over 6 MeV, the $^{12}C(^{3}He,d)^{13}N$ reaction cross section rises quickly and reaches 120 mb at 10 MeV.[29] Although there is cross section for the $^{14}N(^{3}He,\alpha)^{13}N$ reaction below 6 MeV, it is small (~10 mb).[30]

The absolute cross sections at several energies were determined for the $^{14}N(p,\alpha)^{11}C$ reaction. The excitation function for this reaction has been reported.[31,32] The excitation function was repeated in this work to check the other published results and to gain confidence and experience in the irradiation and counting techniques. The excitation function must be known in order to determine the optimum energy for production of the assay radionuclide. The excitation function is shown in Fig. 11. The excitation function agrees well with the one recently measured by Wolf et al.[31] and reasonably well with that of Epherre and Seide.[32]

The targets used to determine the $^{14}N(p,\alpha)^{11}C$ excitation function were prepared by vacuum evaporation of melamine, $C_3N_6H_6$, onto 0.001-inch aluminum foils. Melamine was selected because it has a high nitrogen content (66.6% by weight) and is stable in the beam. The thickness of the melamine ranged from 0.5 to 3.5 mg/cm^2.

A silver membrane filter was found to be the best type of filter for collection of the ambient aerosol. This is because it is only slightly activated during the proton irradiation. This permits the most sensitive detection of gamma radiation from activation of the aerosol itself. The silver filter was only slightly activated because the irradiations were carried out below the Coulomb barrier of 8.4 MeV for protons on silver. There is some activation of the silver, but it is small and can be easily identified in the decay curves. Carbon- and oxygen-containing filters were found to be unsuitable because of large amounts of ^{13}N and ^{18}F that were formed from the $^{16}O(p,\alpha)^{13}N$, $^{13}C(p,n)^{13}N$ and $^{18}O(p,n)^{18}F$ reactions. The production of 10.0-minute ^{13}N and 109.8-minute ^{18}F in quartz and Nucleopore filters interferes with the detection of 20.4-minute ^{11}C from the activation of the nitrogen in the relatively small mass of aerosol on

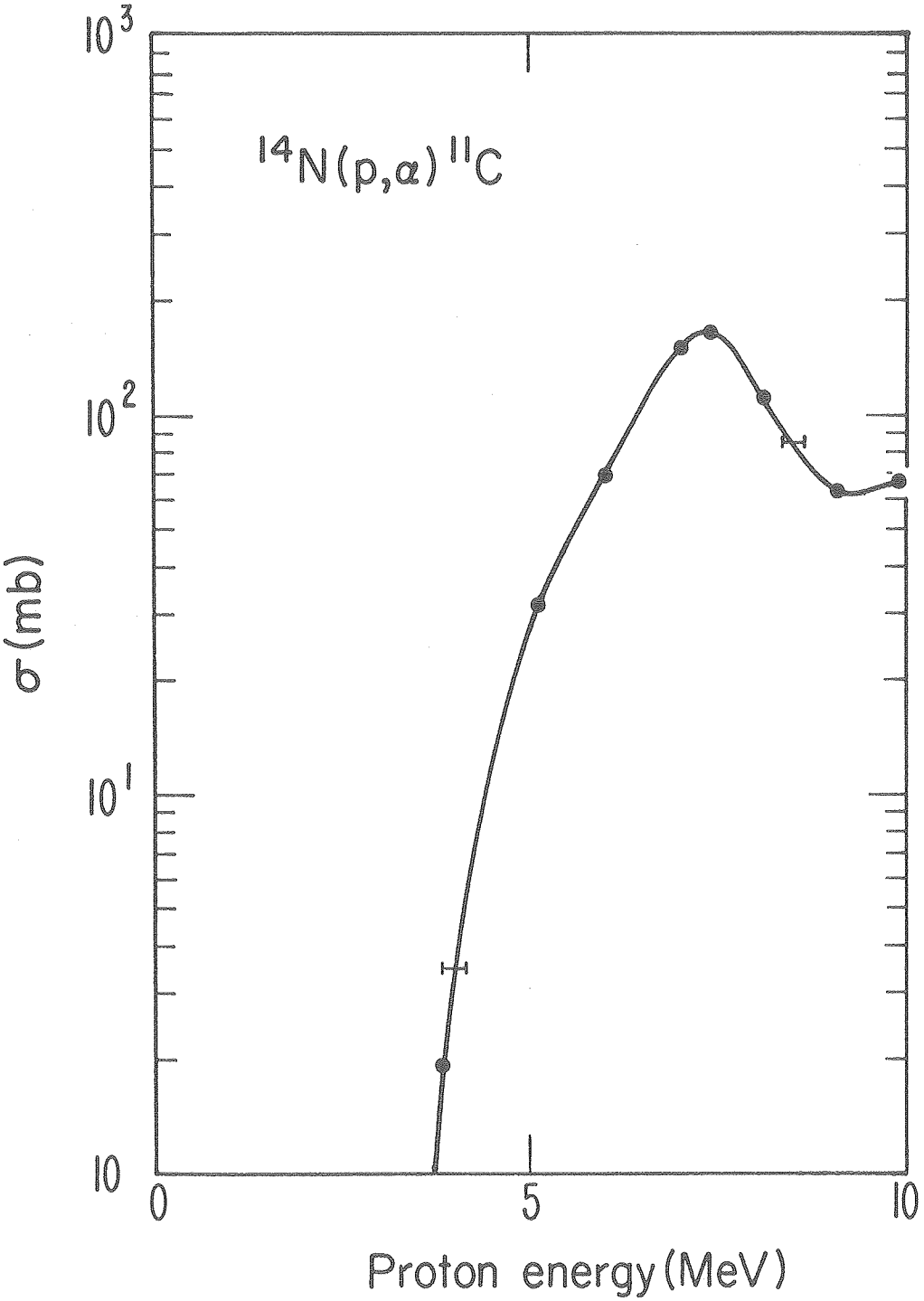

XBL 774-800

Fig. 11. Excitation function for the $^{14}N(p,\alpha)^{11}$ reaction.

the filters. The aerosol loading on the silver filters ranged from 100 to 500 $\mu g/cm^2$ on the samples used in this work. Using a pump which draws 75 liters/minute and assuming a total suspended particulate of 25 to 50 $\mu g/m^3$, we required between 4 hours and 2 days to collect a sample depending on the thickness needed. Time resolution in aerosol collection is also an important consideration and this may limit the time available for collection and hence the loading on the filter.

The filter samples were irradiated in a foil stack as previously described. In the stack there were two filter samples and a melamine standard. A typical stack arrangement is shown in Fig. 12. Using the information obtained from the excitation function, the standard and two filter samples were irradiated at specific energies in the stack. The standard was irradiated at a proton energy of 9.2 MeV. This is a portion of the excitation function that is relatively flat. Because the standard has a large nitrogen content, a high cross section is not required. This is the best energy at which to irradiate the standard. The two filter samples should be irradiated at the highest possible cross section to maximize production of the ^{11}C activity. A maximum in the excitation function appears at 7.5 MeV. One filter sample was irradiated at a proton energy of 7.5 MeV and the other at 6.0 MeV. The sensitivity is not as high for the sample irradiated at 6.0 MeV, but is sufficiently high for all but the most lightly-loaded samples. The lightest load samples were always irradiated at a proton energy of 7.5 MeV for maximum sensitivity. The ratio of the cross sections at the standard ($E_p = 9.2$ MeV) and at the samples is shown below.

$$\frac{\sigma(\text{std})}{\sigma(7.5)} = 0.40 \quad , \qquad \frac{\sigma(\text{std})}{\sigma(6.0)} = 0.86 \quad .$$

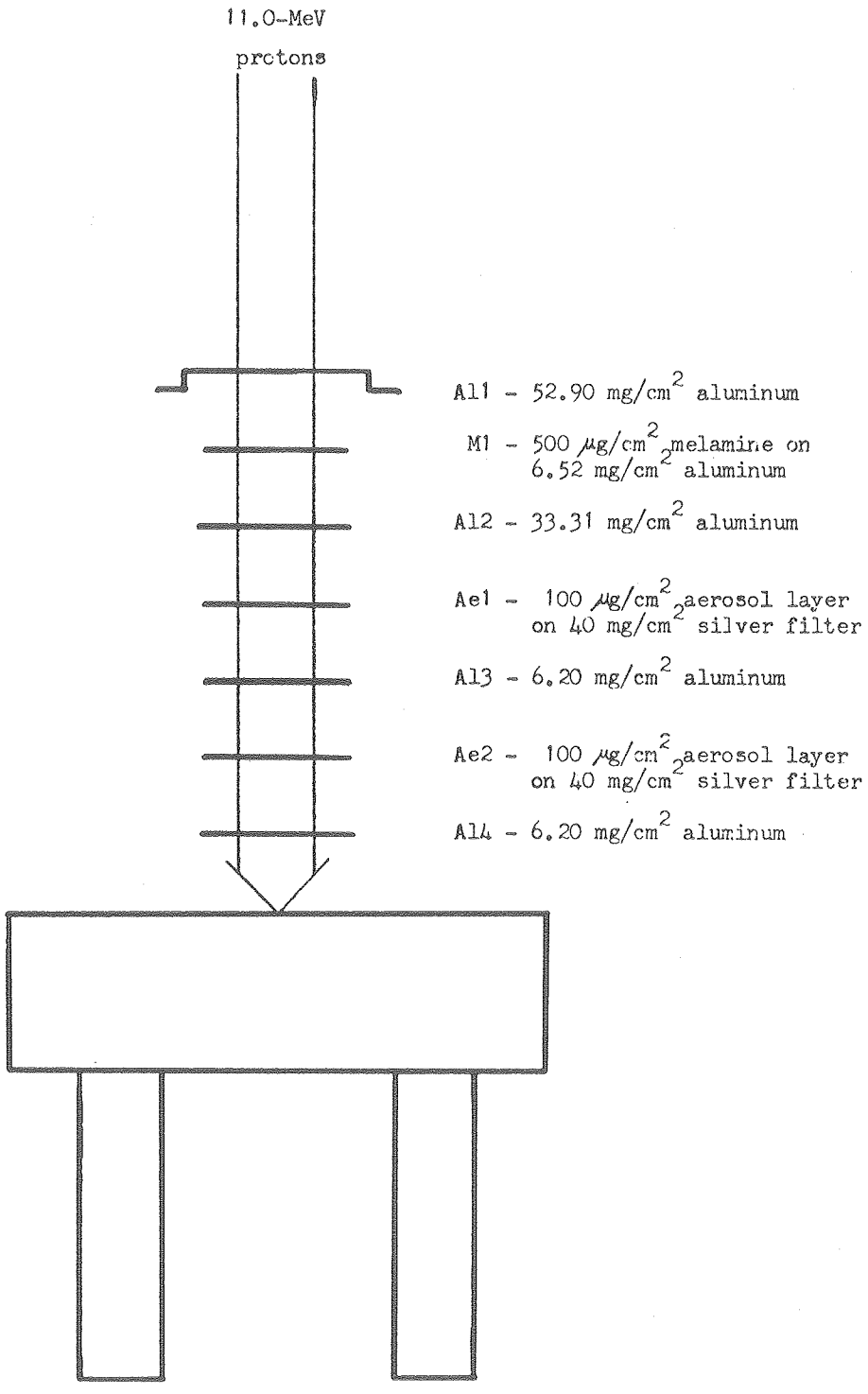

Fig. 12. Diagram of the stack set-up for nitrogen determination by proton activation analysis.

The recoiling ^{11}C nuclei were caught in the thick silver backing. The aluminum foil backing of the melamine standard was sufficient to stop those ^{11}C recoils. The range-energy tables of Williamson, Boujot and Picard[17] were used to calculate the required aluminum thickness. Aluminum is a good degrader foil to use since it has good heat conduction properties and only slightly activates. The two principle reactions on aluminum produce 4.2-second ^{27}Si and stable ^{24}Mg. The stack was typically irradiated for 1 minute at a beam intensity of 1 μA.

The irradiated samples were then assayed using the 0.511-MeV annihilation radiation as previously described. The decay of the 0.511-MeV annihilation radiation in the melamine standard is shown in Fig. 13. The decay is a single component with a 20.4-minute half-life corresponding to the decay of ^{11}C in the target. Therefore the standard in later irradiations was only counted at four times during the decay. This allowed more time to measure the decay of the aerosol samples.

The aerosol samples were counted in the same geometry as the standard. The decay of the 0.511-MeV annihilation radiation was followed at short intervals for 3 or 4 hours. A typical gamma-ray spectrum for an aerosol sample is shown in Fig. 14. Besides the annihilation peak, several other gamma rays are present. All of these other gamma rays are a result of the activation of the silver membrane filter. These gamma rays are a result of the decay of ^{107}Cd which is produced by the $^{107}Ag(p,n)^{107}Cd$ nuclear reaction. A typical decay curve for the integrated 0.511-MeV peak is shown in Fig. 15. There are four components present in the decay curve:

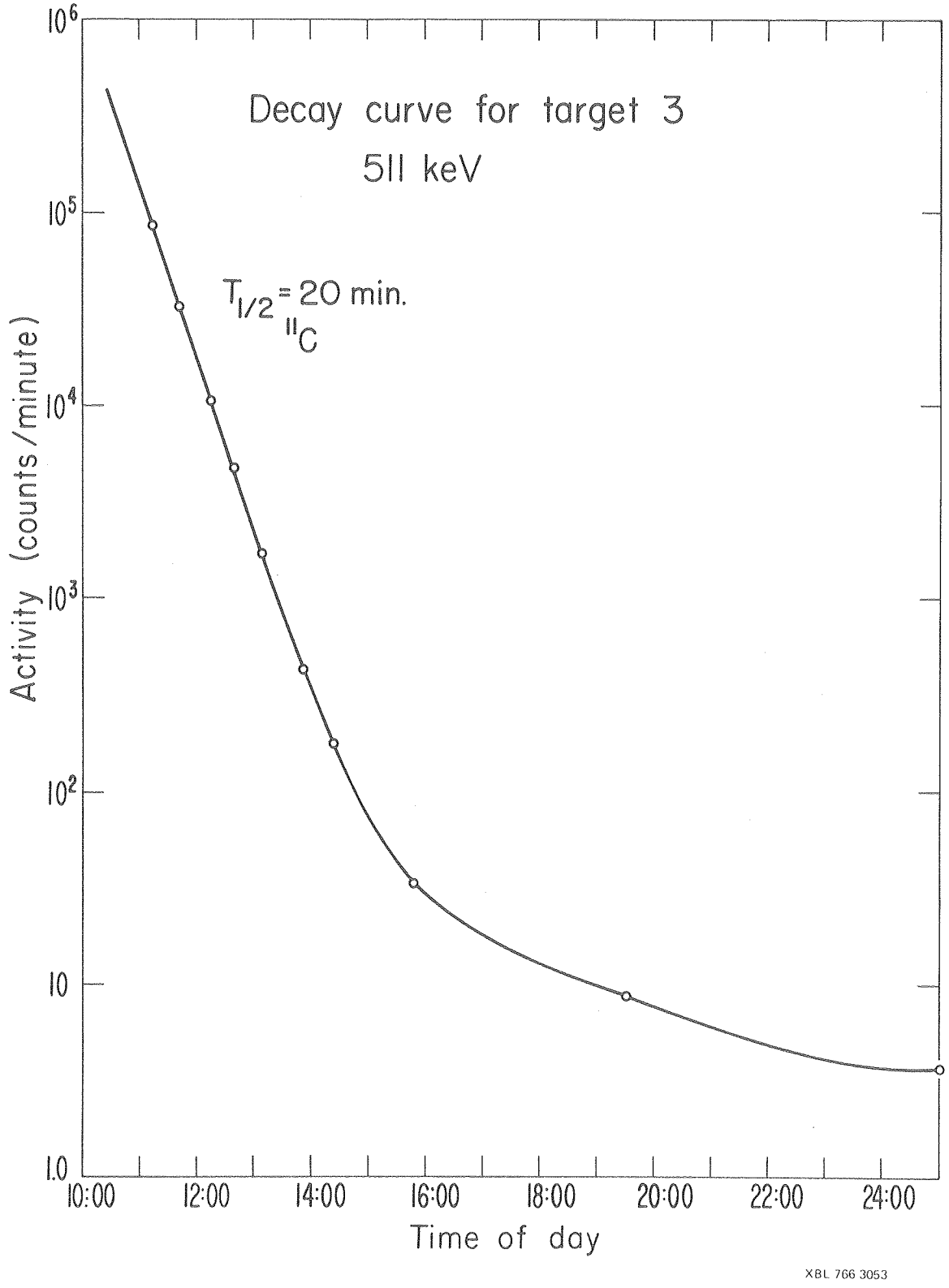

Fig. 13. Decay curve of the 20.4-minute ^{11}C annihilation radiation for a melamine target.

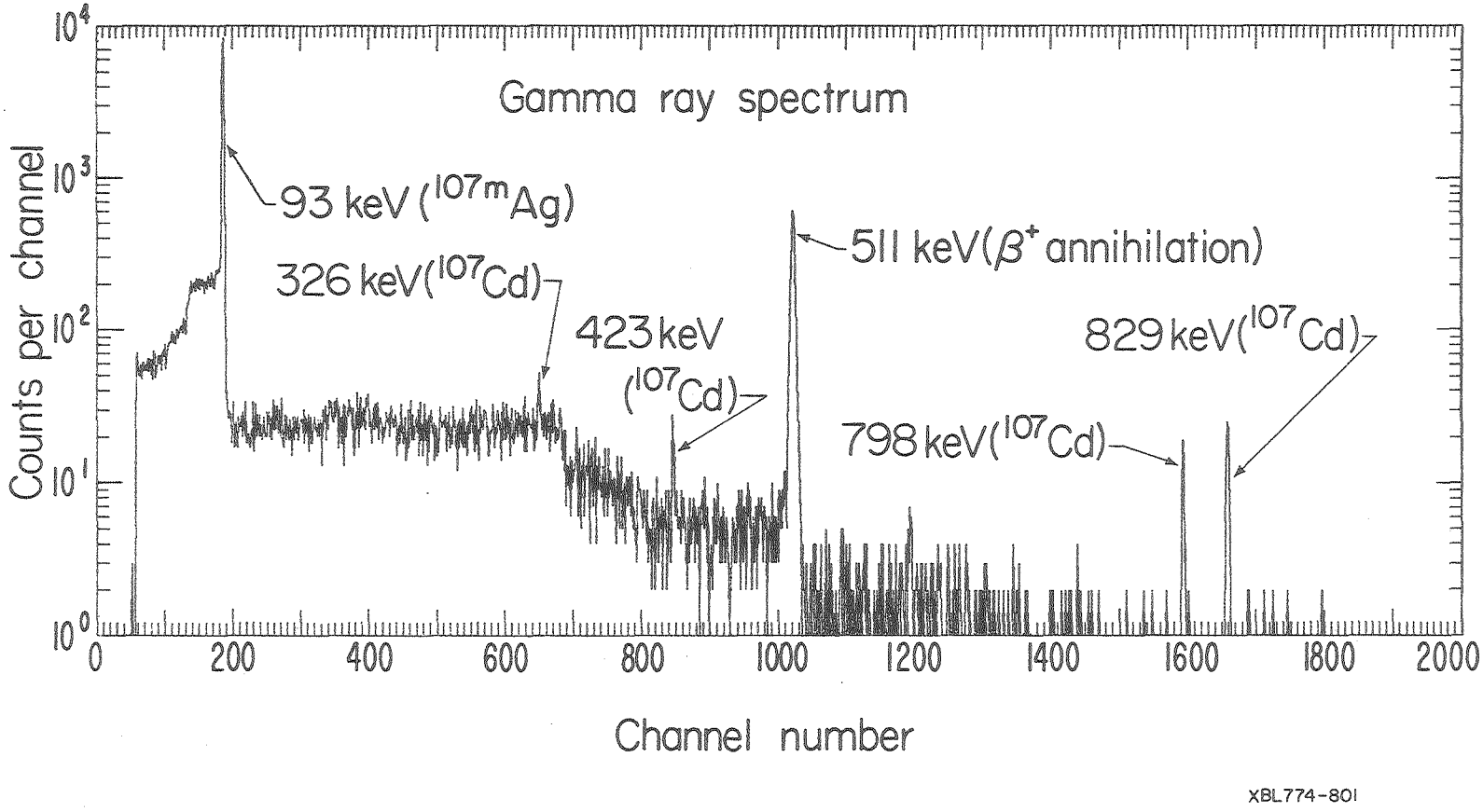

Fig. 14. Gamma-ray spectrum of at atmospheric aerosol sample collected on a silver filter following proton irradiation.

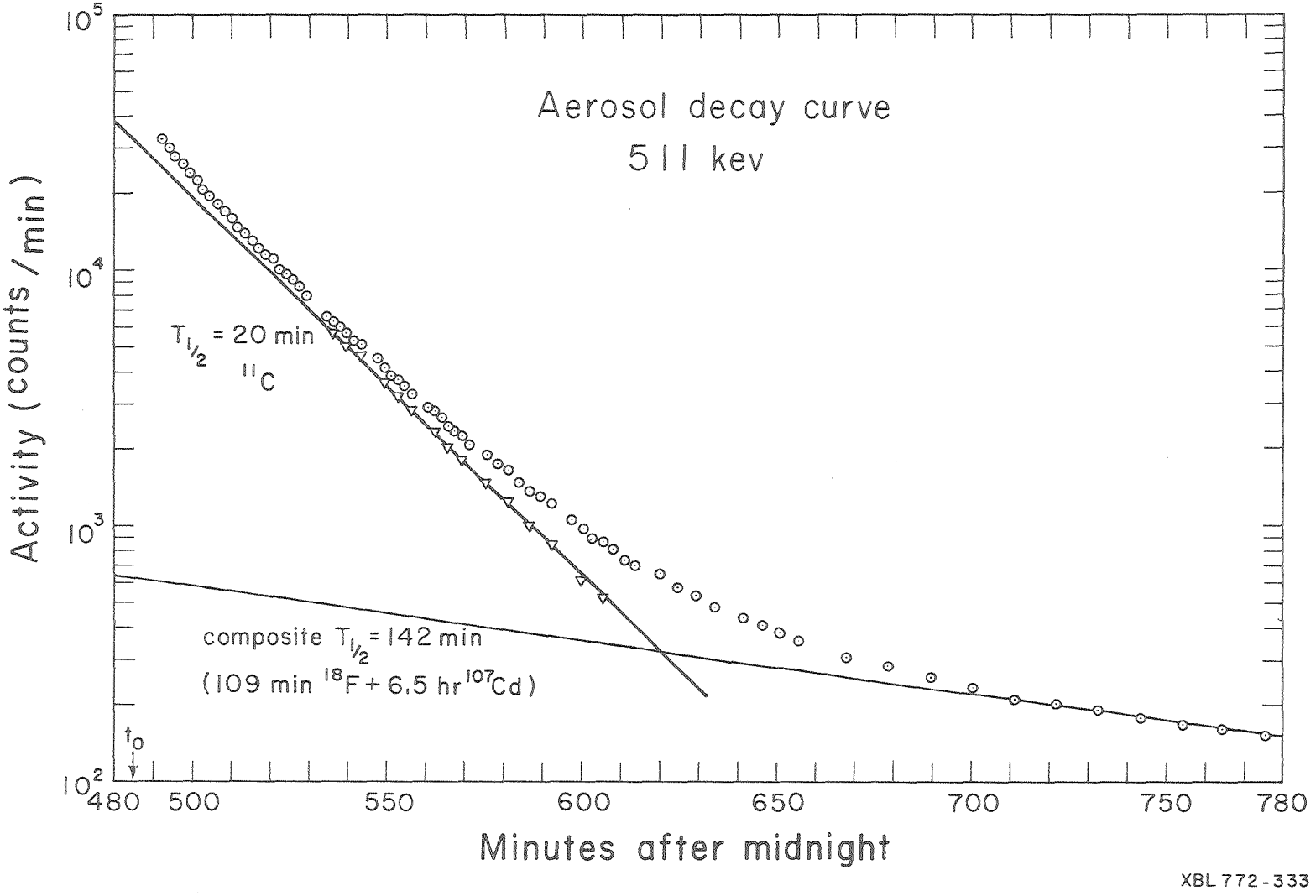

Fig. 15. Decay of the 0.511-MeV annihilation radiation activity following irradiation of an atmospheric aerosol sample with 7.5-MeV protons.

a) a 10.0-minute component due to ^{13}N produced from the $^{16}O(p,\alpha)^{13}N$ and $^{13}C(p,n)^{13}N$ reactions,

b) a 20.4-minute component from the $^{14}N(p,\alpha)^{11}C$ reaction,

c) a 109.8-minute component due to ^{18}F produced by the $^{18}O(p,n)^{18}F$ reaction,

d) a 6.5-hour component due to activation of the silver filter to produce ^{107}Cd by the $^{107}Ag(p,n)^{107}Cd$ reaction.

By far the most dominant component in this decay curve is the 20.4-minute component, ^{11}C, which results from the activation of nitrogen present in the aerosol. The amount of nitrogen present was calculated following the relative method of analysis as previously described. The important quantities determined by the decay curve analysis are the A_0 value for the ^{11}C component in the standard and the A_0 value for the ^{11}C component in the aerosol. Several blank filters were also analyzed for nitrogen and found to contain approximately 0.5 $\mu g/cm^2$; this is normally a very small correction to the total nitrogen found. The precision and accuracy of the method was checked by nondestructively analyzing samples using the proton activation method, followed by analysis of the same samples by an independent method. The independent method used to check the proton activation results was combustion analysis. The samples can be divided into two groups. One group of samples was prepared in the laboratory by depositing either ammonium sulfate, $(NH_4)_2SO_4$, or ammonium oxalate, $(NH_4)_2C_2O_4$, on a silver membrane filter. These are nitrogen-containing compounds that have the other low-Z elements commonly found in aerosols. The ability to measure nitrogen in the presence of high concentrations of neighboring elements would indicate the ability to do so in aerosols.

These samples correspond to the first nine reported in Table 2. The second group of samples are ambient aerosols collected in the San Francisco Bay area under widely varying atmospheric conditions. Aerosols are very complex chemically and contain a wide variety of elements. The ability to measure nitrogen in this matrix is the goal of this work and must be successfully demonstrated. The results of these analysis on eight samples are shown in the latter part of Table 2.

Comparison of the nitrogen found by proton activation analysis and that found by the independent combustion method shows an average percent difference of 14% for the 17 samples. This difference is essentially the same whether one compares only the laboratory-prepared samples or the ambient aerosol samples. It should also be noted that the agreement between the two methods holds over a range which spans two orders of magnitude in nitrogen concentration.

In order to estimate the sensitivity of the method, a set of irradiation conditions approximating those normally used will be considered. One must also consider the lowest amount of activity which can be detected accurately with the given detection system. Using this approach, we can calculate an estimated detection limit for nitrogen. The irradiation conditions are a proton beam intensity of 1 μA and an irradiation time of 4 minutes; the proton energy is 7.5 MeV, which is at the peak of the $^{14}N(p,\alpha)^{11}C$ excitation function (σ = 165 mb). The overall detection coefficient for the 0.511-MeV gamma ray is approximately 2%. The minimum amount of activity that could be counted is approximately 500 counts/minute of ^{11}C (full-energy peak) at the end of bombardment. This minimum A_0 value takes into account the contribution of the other positron-emitting nuclides

TABLE 2. Comparison of methods for nitrogen determination in atmospheric aerosols.

Sample	Material	N found, μg/cm² — Proton activation	combustion	Ratio (Actv./Comb.)
AS-1	ammonium sulfate	129	144	0.89
AS-2	ammonium sulfate	110	130	0.85
AS-3	ammonium sulfate	326	368	0.89
AS-4	ammonium sulfate	68	52	1.31
AO-1	ammonium oxalate	162	147	1.10
AO-2	ammonium oxalate	210	207	1.01
AO-3	ammonium oxalate	261	279	0.94
AO-4	ammonium oxalate	134	143	0.94
AO-5	ammonium oxalate	136	133	1.02
AA-1	aerosol	4.0	3.5	1.14
AA-2	aerosol	8.0	6.5	1.23
AA-3	aerosol	15	13	1.15
AA-4	aerosol	76	99	0.77
AA-5	aerosol	16	18	0.89
AA-6	aerosol	59	59	1.00
AA-7	aerosol	36	37	0.97
AA-8	aerosol	46	54	0.85
				$\bar{R} = 1.00 \pm 0.14$

that are always present. These conditions correspond to a nitrogen detection limit of approximately 0.1 $\mu g/cm^2$, corresponding to 200 ppm in an aerosol sample of thickness 500 $\mu g/cm^2$. This detection limit could be lowered by an increase in proton beam intensity or a longer irradiation time. The use of more intense beams, however, increases the risk of sample alteration. Considering the complexity of the aerosol, we suggest that this represents a reasonable lower limit to nitrogen sensitivity in a nondestructive analysis.

B. Carbon Determination

Carbon is a very important element in aerosol studies. It is the major elemental constituent of all fossil fuels. The determination of carbon in aerosols is usually carried out by destructive combustion analysis. There are several reactions that could be used to measure carbon. The most sensitive reactions should use the ^{12}C nuclide. A list of possible nuclear reactions employing ^{12}C is given in Table 3.

The proton reaction on the ^{12}C nucleus has a very high threshold energy. The 20-MeV protons required to make this reaction proceed would produce a host of interfering reactions, the most notable being the $^{14}N(p,\alpha)^{11}C$ and $^{16}O(p,\alpha d)^{11}C$ reactions. These high abundance elements constitute a serious and unavoidable interference. The proton irradiation of the silver filter would also produce a large amount of 24.1-minute ^{106}Ag which would also interfere with the detection of the ^{11}C activity. The $^{12}C(p,pn)^{11}C$ reaction is not a suitable reaction for the analysis of carbon in atmospheric aerosol samples.

The $^{12}C(^3He,\alpha)^{11}C$ reaction is another possible analysis react

TABLE 3. Possible reactions for determination of carbon and the corresponding interfering reactions.

Reaction	Half-life (min)	Q-value (MeV)	Potential interfering reactions	Half-life (min)	Q-value (MeV)
$^{12}C(p,pn)^{11}C$	20.4	-18.7	$^{11}B(p,n)^{11}C$	20.4	- 2.7
			$^{14}N(p,\alpha)^{11}C$	20.4	- 5.9
			$^{16}O(p,\alpha d)^{11}C$	20.4	-23.6
			$^{107}Ag(p,pn)^{106}Ag$	24.1	- 9.5
$^{12}C(d,n)^{13}N$	10.0	- 0.28	$^{14}N(d,dn)^{13}N$	10.0	-10.5
			$^{14}N(d,t)^{13}N$	10.0	- 4.3
			$^{16}O(d,\alpha n)^{13}N$	10.0	- 7.4
$^{12}C(^{3}He,\alpha)^{11}C$	20.4	+ 1.9	$^{16}O(^{3}He,2\alpha)^{11}C$	20.4	- 5.8
			$^{14}N(^{3}He,\alpha d)^{11}C$	20.4	- 8.4
			$^{11}B(^{3}He,t)^{11}C$	20.4	- 2.0
			$^{9}Be(^{3}He,n)^{11}C$	20.4	+ 7.6

There are interferences from boron and beryllium which cannot be avoided. These elements are present, however, only in very low concentrations in aerosols and do not constitute a realistic interference. The potential carbon and nitrogen interferences that exist must be avoided. The threshold for the $^{16}O(^{3}He,2\alpha)^{11}C$ reaction is 6.9 MeV and is 10.2 MeV for the $^{14}N(^{3}He,\alpha d)^{11}C$ reaction. The peak of the $^{12}C(^{3}He,\alpha)^{11}C$ excitation function occurs at 10.0 MeV ($\sigma = 65$ mb) and samples should be irradiated near this energy in order to take advantage of the high cross section.[29] At 10 MeV, however, the $^{16}O(^{3}He,2\alpha)^{11}C$ reaction has a significant cross section (~20 mb). The irradiation could be carried out below 10 MeV where the $^{16}O(^{3}He,2\alpha)^{11}C$ reaction has a low cross section, but the cross section for the $^{12}C(^{3}He,\alpha)^{11}C$ reaction also drops off sharply below 10 MeV. If the region of the $^{12}C(^{3}He,\alpha)^{11}C$ excitation function below 10 MeV is used, then the sensitivity for detection of carbon is being reduced. Also, it is not reliable to use the steep part of the excitation function. This reaction could be used to analyze for carbon, but the $^{12}C(d,n)^{13}N$ reaction would be a better choice.

The reaction chosen for the analysis of carbon in aerosols is the $^{12}C(d,n)^{13}N$ reaction. There are two possible interfering reactions that are potentially important: the $^{14}N(d,dn)^{13}N$ reaction with a threshold of 12.1 MeV and the $^{16}O(d,\alpha n)^{13}N$ reaction with a threshold of 8.4 MeV. As long as the sample is irradiated below 8.4 MeV these reactions will not interfere with the $^{12}C(d,n)^{13}N$ reaction. There may be some interference below 8.4 MeV from the $^{14}N(d,t)^{13}N$ reaction, but this reaction has a very low cross section and is not a significant interference. This was checked by irradiating GaN targets with deuterons of energy 7.0 and 8.0 MeV. The

cross section for the $^{14}N(d,t)^{13}N$ reaction was found to be 0.5 mb at both energies. The deuteron reactions with oxygen and nitrogen, in general, produce only short-lived nuclides ($t_{1/2} < 2$ minutes) or stable nuclides. This means that the ^{13}N activity produced from the carbon in an aerosol sample should be the dominant component in the decay curve. The $^{12}C(d,n)^{13}N$ reaction is a sensitive method of analysis that produces a nuclide that is easily detected from other matrix products and is interference free.

The absolute cross sections for the $^{12}C(d,n)^{13}N$ reaction at several energies were determined. This excitation function is shown in Fig. 16. The excitation function agrees with that of Brill and Sumin.[33] The targets used to determine the excitation function were foils of polystyrene. The thickness of the polystyrene foils was 2.2 mg/cm^2. Polystyrene was chosen for its high carbon content (92.26%), high purity, and easy availability.

The silver membrane filter was again found to be the best filter for collection of the ambient aerosol. Deuteron irradiations on the filter sample were carried out below the Coulomb barrier of 8.4 MeV for deuterons on silver. There was only a slight amount of activity produced from deuteron reactions in the silver filter. This permits a higher sensitivity for the detection of ^{13}N activity from the deuteron activation of carbon in the aerosol.

The filter samples were irradiated in a foil stack. In the stack there was one filter sample, a polystyrene standard, and aluminum degrader foils. A typical stack is shown in Fig. 17. The excitation function data showed the best energies at which to irradiate the sample and standard. The excitation function is quite flat in the region between 5 and 9 MeV. An energy-independent part of the excitation function is the preferable

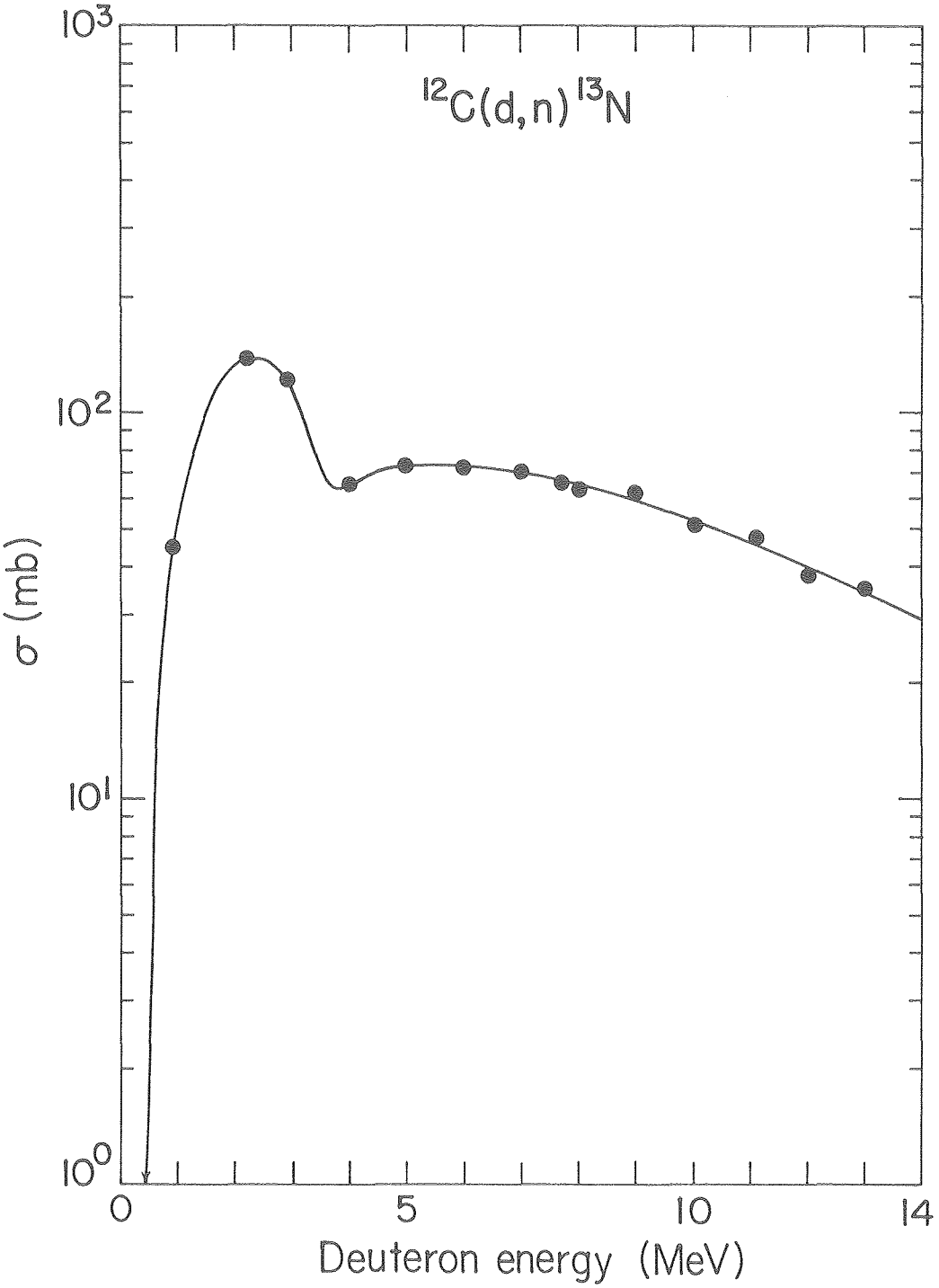

XBL 797-2331

Fig. 16. Excitation function for the $^{12}C(d,n)^{13}N$ reaction.

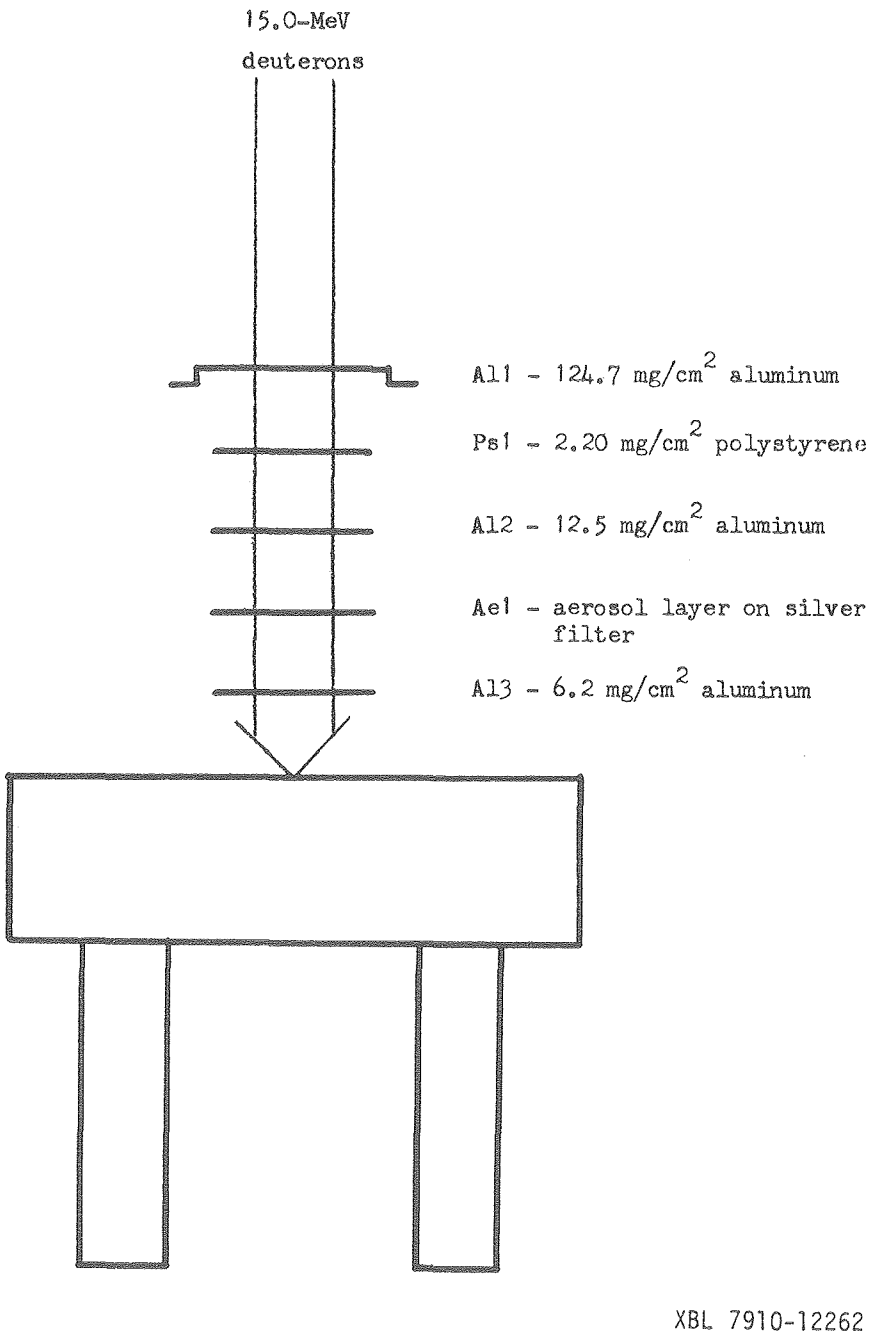

Fig. 17. Diagram of the stack set-up for carbon determination by deuteron activation analysis.

place to do the irradiation, if such a flat region is present. In such a region a slight shift in beam energy has little effect on the cross section. The standard was irradiated at a deuteron energy of 8.6 MeV. The filter sample was irradiated at a deuteron energy of 7.6 MeV. The cross section ratio for the $^{12}C(d,n)^{13}N$ reaction at the standard and the sample is given below.

$$\frac{\sigma(std)}{\sigma(x)} = 0.78$$

The recoil products from the deuteron reactions in the aerosol were caught in the silver filter. The recoils from the reactions in the polystyrene were caught in a 0.001-inch aluminum foil behind the polystyrene foil. The aluminum recoil catcher and the polystyrene foil were counted together. The range-energy tables of Williamson, Boujot and Picard[17] were used to calculate the required aluminum thicknesses to achieve the desired energies in the stack. There was one important deuteron reaction occurring in the aluminum foils that was not occurring with the proton beam — the $^{27}Al(d,p)^{28}Al$ reaction. This reaction produces 2.27-minute ^{28}Al in large amounts. There is a 1.779-MeV gamma ray (100%) that accompanies the decay of ^{28}Al. This gamma ray is observed in copious amounts in the aluminum recoil catcher of the polystyrene foil. It is, however, almost totally decayed by 20 minutes after the end of bombardment and the polystyrene can then be assayed. The stacks were typically irradiated for one minute at a deuteron beam intensity of ½ μA.

The irradiated samples were assayed using the 0.511-MeV annihilation radiation. The decay of the integrated annihilation peak in the polystyrene standard is shown in Fig. 18. The decay is a single component with a 10.0-minute half-life corresponding to the decay of ^{13}N in the target.

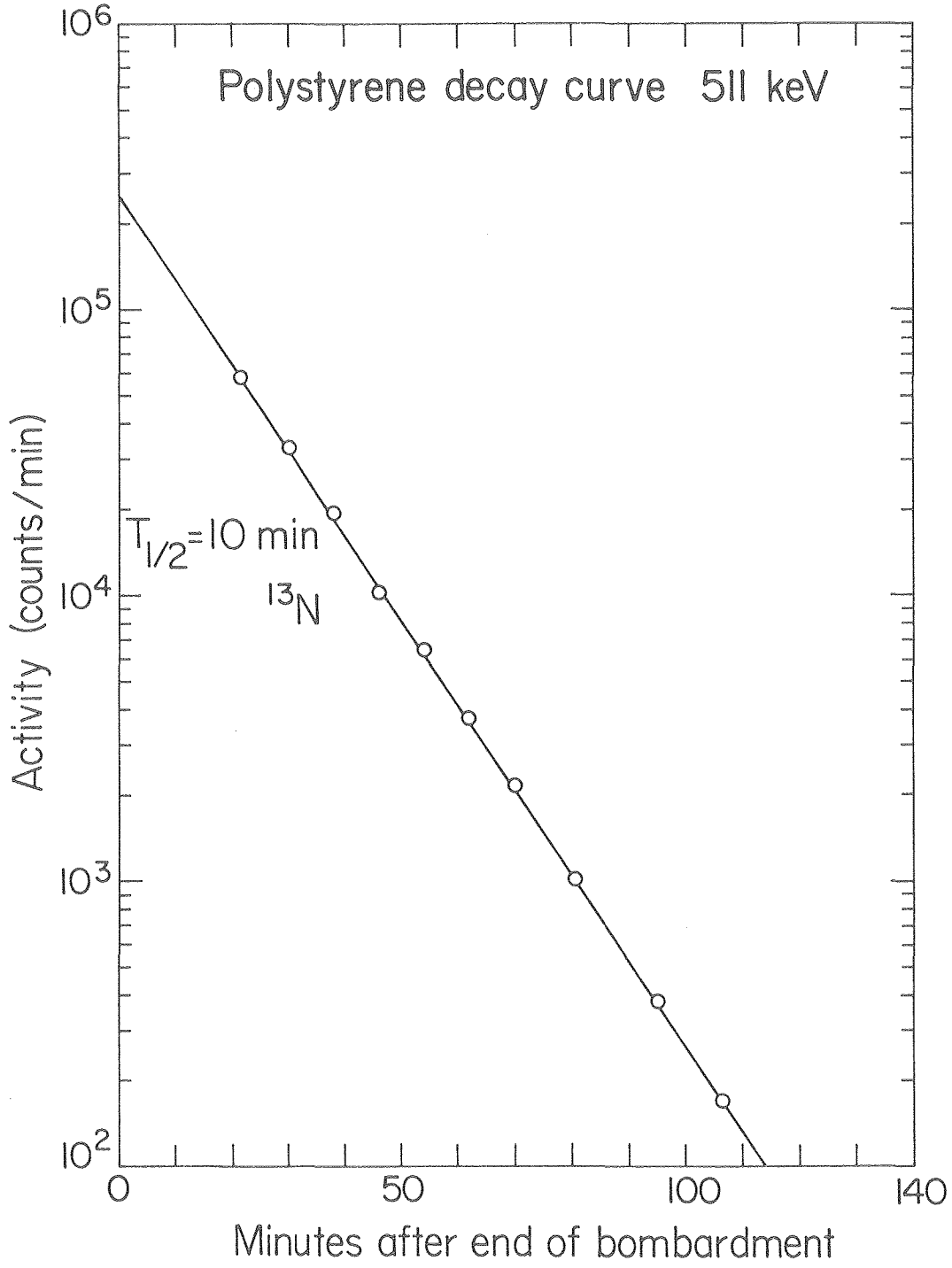

XBL 797-2330

Fig. 18. Decay of the 0.511-MeV annihilation radiation activity following deuteron irradiation of a polystyrene foil.

The single-component decay permitted the standard to be checked only four times in subsequent irradiations. This means that more counter time can be devoted to the assay of the filter sample. A typical gamma-ray spectrum of an irradiated polystyrene foil is shown in Fig. 19. There are two peaks in the spectrum which are located at 0.511 MeV and at 0.844 MeV. There is also some additional broad structure around 0.18 MeV. The gamma rays at 0.844 and 0.18 MeV are from ^{27}Mg which is produced by the ^{27}Al(d,2p)^{27}Mg (Q = -4.06 MeV) reaction in the aluminum recoil catcher foil. The peak at 0.511 MeV is the expected positron-annihilation radiation.

The aerosol sample was counted in the same geometry as the standard. The decay of the integrated 0.511-MeV peak was followed at short intervals for 2 to 3 hours. A typical gamma-ray spectrum for an aerosol sample is shown in Figs. 20 and 21. All of the nuclear gamma rays observed in the region below 1 MeV (Fig. 18) are due to deuteron activation of the silver filter. The reactions leading to the observed gamma rays are ^{107}Ag(d,2n)^{107}Cd (Q = -4.42 MeV) and ^{107}Ag(d,p)^{108}Ag (Q = +5.05 MeV). The gamma-ray spectrum between 1 and 2 MeV (Fig. 19) shows three peaks. The gamma ray at 1.368 MeV is due to ^{24}Na which is produced by the ^{27}Al(d,αn)^{24}Na (Q = -6.14 MeV) reaction. The ^{24}Na activity results from deuteron reactions on aluminum in the aerosol and from recoils from deuteron reactions in the aluminum degrading foil that is immediately upstream from the aerosol sample. The gamma ray at 1.642 MeV is from ^{38}Cl which is produced by the ^{37}Cl(d,p)^{38}Cl reaction on chlorine in the aerosol. The peak at 1.779 corresponds to a gamma ray emitted in the decay of ^{28}Al. This nuclide is produced by the ^{27}Al(d,p)^{28}Al reaction on aluminum in the aerosol and degrading foils.

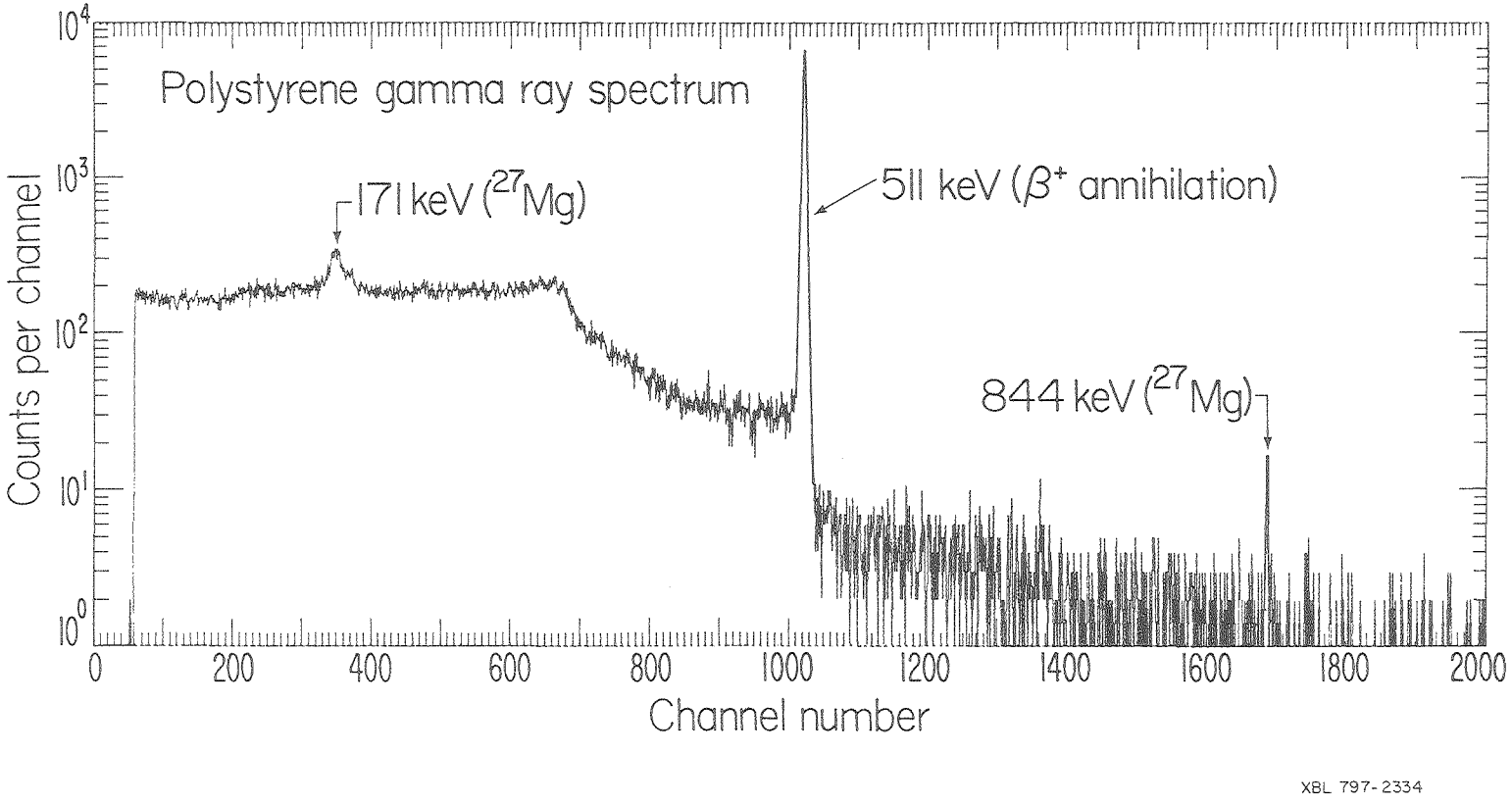

XBL 797-2334

Fig. 19. Gamma ray spectrum of the polystyrene standard following deuteron irradiation.

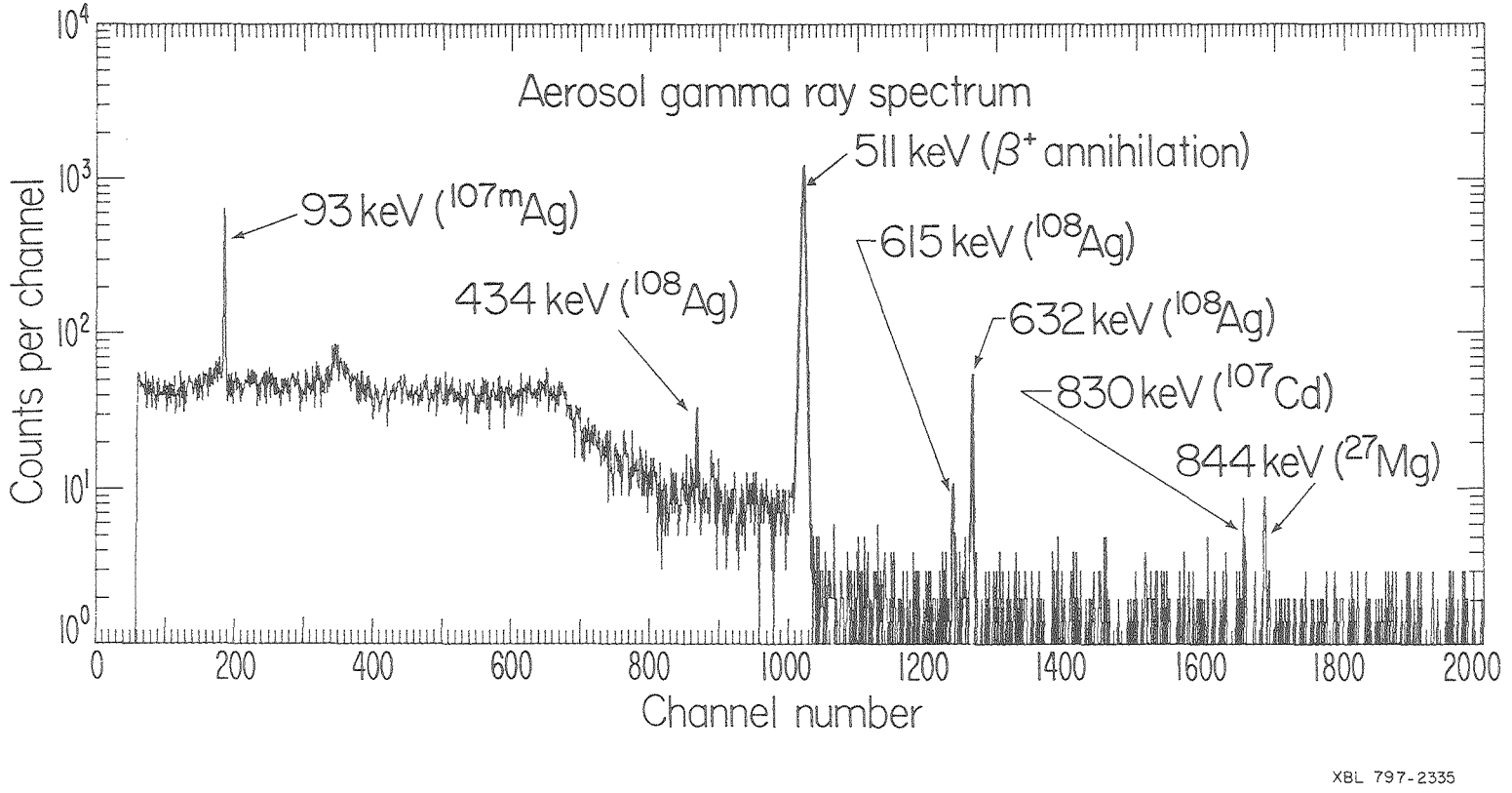

Fig. 20. The region from 0 to 1 MeV in the gamma ray spectrum of an aerosol sample following deuteron irradiation.

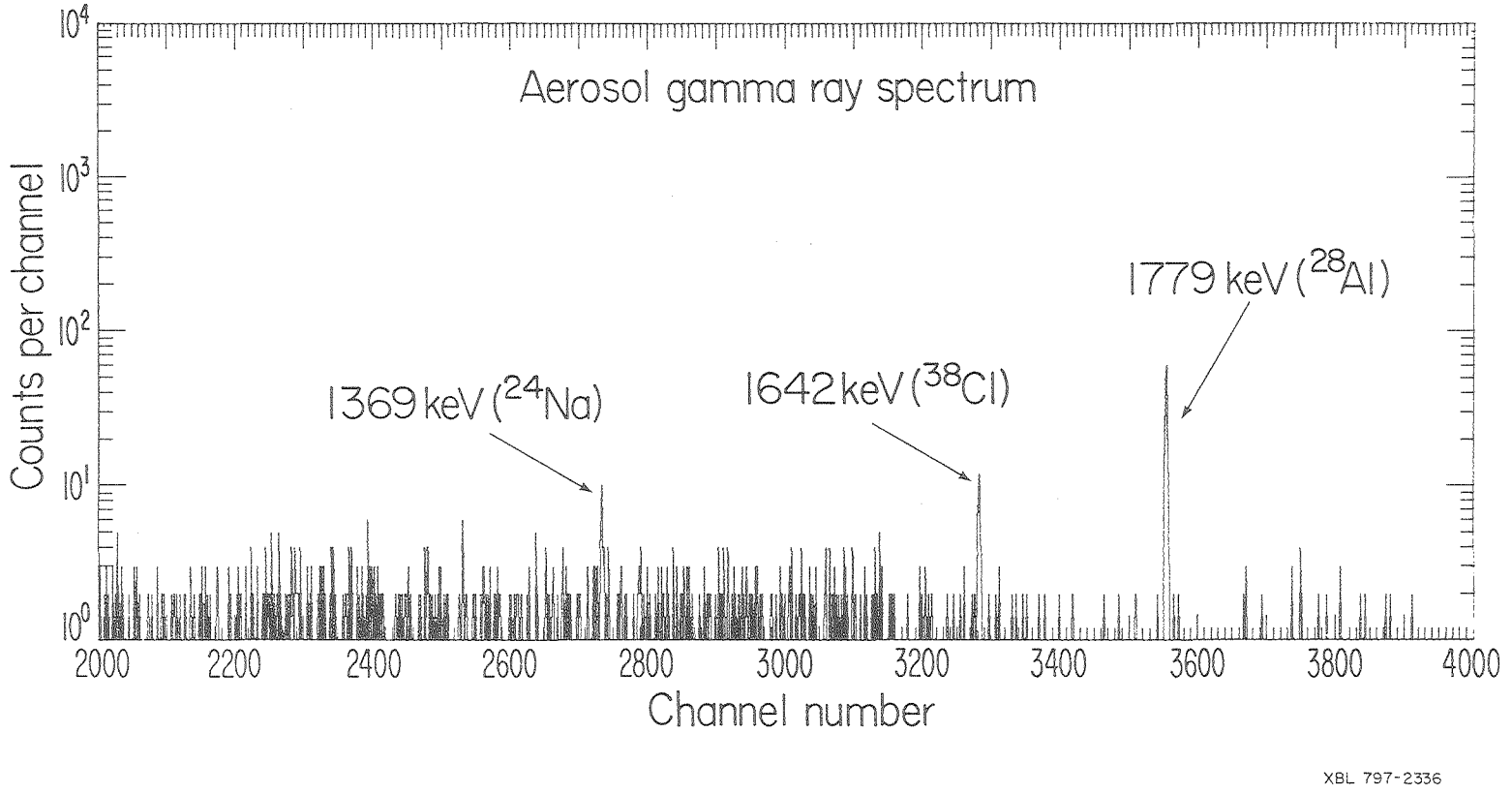

XBL 797-2336

Fig. 21. The region from 1 to 2 MeV in the gamma ray spectrum of an aerosol sample following deuteron activation.

A typical aerosol decay curve for the integrated 0.511-MeV peak is shown in Fig. 22. There are four components that are resolved by decay-curve analysis:

a) a dominant 10.0-minute component due to ^{13}N produced from the $^{12}C(d,n)^{13}N$ reaction,

b) a 24.1-minute component due to the $^{107}Ag(d,t)^{106}Ag$ reaction,

c) a 109.8-minute component due to the $^{17}O(d,n)^{18}F$ (Q = +3.38 MeV) and the $^{18}O(d,2n)^{18}F$ (Q = -4.66 MeV) reactions,

d) a 6.5-hour component due to ^{107}Cd produced by the $^{107}Ag(d,2n)^{107}Cd$ reaction in the silver filter.

Other decay curves from samples with much less carbon content show a short-lived component present in the decay. This is the 2.41-minute ^{108}Ag whose corresponding nuclear gamma ray is observed at 0.434 MeV. The contribution to the peak at 0.511 MeV from ^{106}Ag is due to its positron decay mode as well as a nuclear gamma ray of energy 0.512 MeV.[19] The amount of carbon present was calculated following the relative method of analysis as previously described. The A_0 value for ^{13}N in the standard and the aerosol are the important quantities that were determined from the decay-curve analysis. Both of the A_0 values can be determined with great precision since the ^{13}N activity dominates both decay curves. Several blank silver filters were analyzed for carbon and found to contain approximately 5 $\mu g/cm^2$. This blank carbon can be reduced by "firing" the silver filters at 300°C for 24 hours. This reduces the blank value to approximately 0.5 $\mu g/cm^2$.

Samples containing varying amounts of carbon were nondestructively analyzed using the deuteron activation method. The same samples were then destructively analyzed by combustion. The samples are divided into

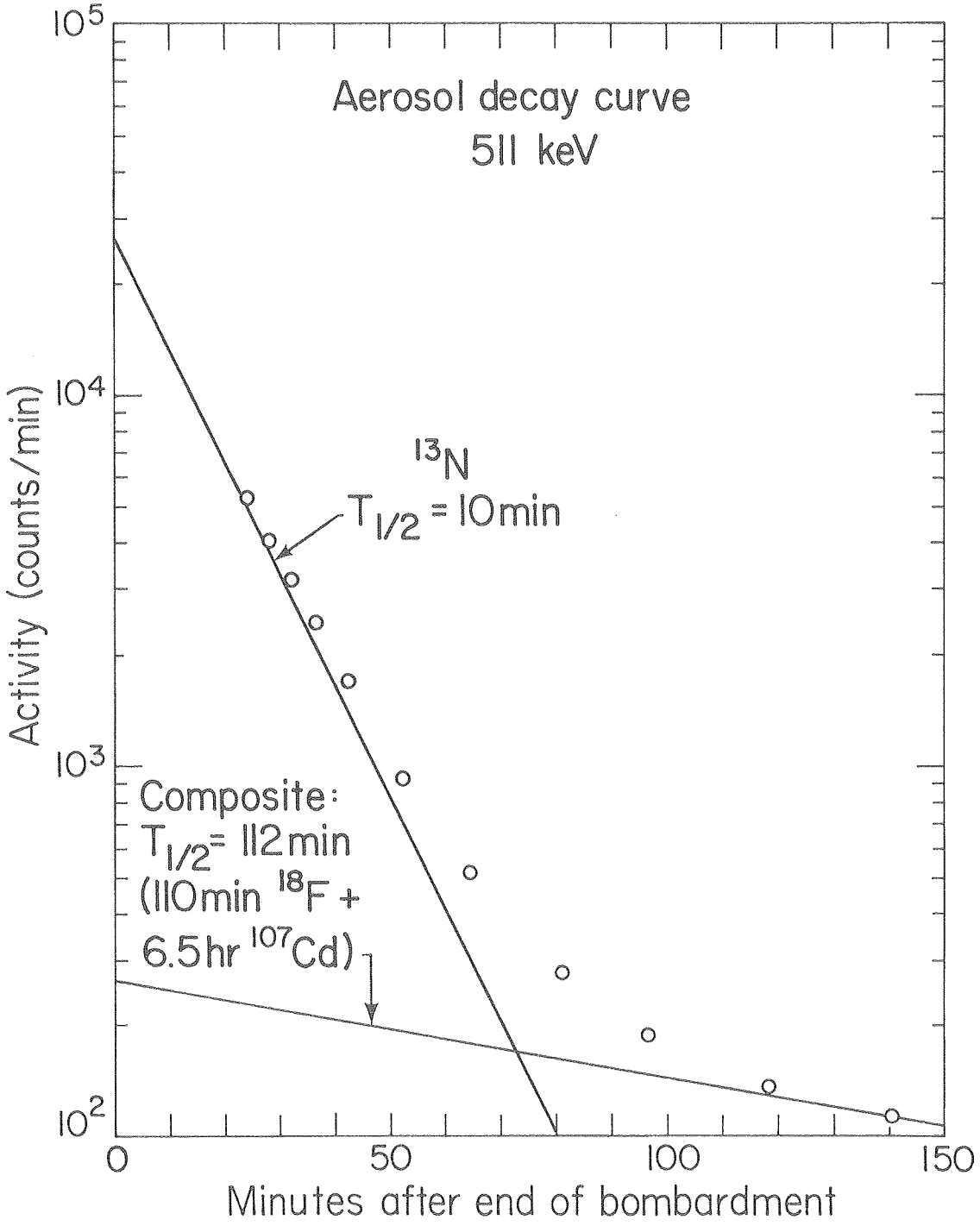

XBL 797-2332

Fig. 22. Decay of the 0.511-MeV annihilation radiation activity following deuteron irradiation of an atmospheric aerosol sample.

two groups: the first group of samples were prepared in the laboratory by deposition of a known compound onto a silver filter, the second group of samples were ambient aerosols collected on silver filters in the San Francisco Bay area. The laboratory samples were prepared by depositing a layer of ammonium oxalate, $(NH_4)_2C_2O_4$, on a silver filter. This carbon-containing compound contains a known concentration of the other elements found in aerosols. An accurate determination of carbon in high concentrations of other low-Z elements, such as in ammonium oxalate, would indicate the ability to do so in actual ambient aerosols. The results of the deuteron activation analysis of the laboratory-prepared samples and ambient aerosol samples and the corresponding independent combustion checks are shown in Table 4.

The comparison of the carbon found by the deuteron activation method and that found by the independent combustion method shows an average percent difference of 10% for the 15 samples analyzed. The agreement holds over a wide range of carbon concentrations and is good for both the laboratory-prepared samples and the actual ambient aerosol samples.

The sensitivity is estimated by considering a reasonable set of irradiation and counting conditions that permits the best detection of carbon. Irradiation is carried out at a deuteron beam intensity of ½ μA, and the length of the irradiation is three minutes. The filter sample is irradiated at a deuteron energy of 7.6 MeV which corresponds to a $^{12}C(d,n)^{13}N$ cross section of 65 mb. The overall detection coefficient for detection of the annihilation radiation of ^{13}N is approximately 2%. The minimum activity that can be detected with reasonable precision is approximately 1000 counts/minute of ^{13}N at the end of bombardment and the

TABLE 4. Comparison of methods for carbon determination in atmospheric aerosols.

Sample	Material	C found, $\mu g/cm^2$ — Deuteron activation	combustion	Ratio (actv./comb.)
AO-1	ammonium oxalate	218	210	1.04
AO-2	ammonium oxalate	268	224	1.20
AO-3	ammonium oxalate	131	122	1.07
AO-4	ammonium oxalate	74	62	1.19
AO-5	ammonium oxalate	109	113	0.96
AA-1	aerosol	84	85	0.99
AA-2	aerosol	100	99	1.01
AA-3	aerosol	106	111	0.95
AA-4	aerosol	76	76	1.00
AA-5	aerosol	103	100	1.03
AA-6	aerosol	93	93	1.00
AA-7	aerosol	5.2	4.8	1.08
AA-8	aerosol	0.6	0.7	0.86
AA-9	aerosol	57	62	0.92
AA-10	aerosol	28	32	0.88
				$\bar{R} = 1.01 \pm 0.10$

minimum A_0 value takes into account the contribution of the other positron-emitting nuclides that are always present. Most notably, the activation of the silver to make 2.41-minute ^{108}Ag and 24.1-minute ^{106}Ag most seriously limits the minimum detectable A_0 value of ^{13}N. Under these conditions the carbon detection limit is approximately 0.5 $\mu g/cm^2$.

C. Oxygen Determinations

Oxygen has been the least investigated of all the elements in atmospheric aerosols. This is mainly due to the remarkable difficulty in finding a simple method to analyze samples for this common and reactive element. The study of the oxygen content of atmospheric aerosols could yield valuable new insight into the origin and reaction of aerosols. This section describes two methods based on activation analysis to analyze aerosol samples for oxygen. One method is based on proton activation analysis and the other is based on ^3He activation analysis. An independent method that could be used to analyze the samples for oxygen at the concentrations found in aerosol samples is not readily available. The analytical laboratory of the University of California chemistry department will not analyze samples for oxygen at any level and the two companies that were contacted could measure oxygen at the milligram level but not at the microgram level.[7,10] This meant that the only way to check the accuracy of one charged-particle activation method was to use another charged-particle method. Both methods of charged-particle activation analysis are unchecked by a completely independent method such as combustion, but the relative agreement between the two methods will give a measure of the accuracy and precision. The proton and ^3He activation methods for deter-

mination of oxygen are independent to the extent that the projectiles are different and the induced radioactivities are different. They are not completely independent in that they are both charged-particle activation-analysis methods and the same equipment and personnel were used in both cases. The introduction of a systematic error is a serious consideration when the same equipment and personnel are used to check one another even though the methods are otherwise independent. The development of methods for determination of carbon and nitrogen in aerosols using this same equipment and the good agreement found by independent combustion analysis is a good reason for believing that systematic errors in the two oxygen methods is not a problem. Considering the limitations imposed by the lack of completely independent checks, the development of two charged-particle methods was considered the best way to proceed.

There are several possible projectiles and reactions that could be used to determine oxygen. For sensitivity reasons only the reactions involving the ^{16}O nuclide will be considered. The possible reactions and Q-values along with the principle interfering reactions are shown in Table 5.

The deuteron reaction on oxygen, $^{16}O(d,n)^{17}F$, produces a short-lived (65 sec) isotope that is not convenient to count. There will also be counting and decay-curve resolution problems from the production of large amounts of ^{15}O activity (2.1 min) from the $^{14}N(d,n)^{15}O$ reaction. The production of the ^{15}O nuclide, which has similar half-life and decay properties to ^{17}F, could interfere with the accurate measurement of the ^{17}F activity. This makes the $^{16}O(d,n)^{17}F$ reaction unsuitable for the analysis of oxygen.

TABLE 5. Possible reactions for determination of oxygen and the corresponding interfering reactions.

Reaction	Half-life (min)	Q-value (MeV)	Potential interfering reactions	Half-life (min)	Q-value (MeV)
$^{16}O(p,\alpha)^{13}N$	10.0	-5.2	$^{13}C(p,n)^{13}N$	10.0	- 3.0
			$^{14}N(p,pn)^{13}N$	10.0	-10.6
$^{16}O(d,n)^{17}F$	1.10	-1.6	$^{14}N(d,n)^{15}O$	1.17	+ 5.1
$^{16}O(^{3}He,p)^{18}F$	109.8	+2.0	$^{19}F(^{3}He,\alpha)^{18}F$	109.8	+10.1
			$^{20}Ne(^{3}He,\alpha p)^{18}F$	109.8	- 2.7
			$^{23}Na(^{3}He,2\alpha)^{18}F$	109.8	- 0.3

The $^{16}O(^{3}He,p)^{18}F$ method has been used previously for the determination of oxygen.[12,34] It has not been used, however, for the determination of oxygen in atmospheric aerosols. The ^{18}F activity is very convenient for assay purposes and the reaction is a good choice from that standpoint. The interference from neon can be dismissed since this noble gas undoubtedly is present in very small amounts in aerosols. The fluorine and sodium interferences must be considered much more carefully. The peak of the $^{16}O(^{3}He,p)^{18}F$ excitation function is at approximately 8 MeV and the cross section is about 400 mb.[12] This is the energy at which a sample would be irradiated for an oxygen determination. The first consideration is the values of the cross section for the two interfering reactions at that energy. The $^{19}F(^{3}He,\alpha)^{18}F$ reaction has a considerably smaller cross section than the oxygen reaction at 8 MeV. The cross section at this energy for the fluorine reaction is 20 mb.[35,36] Since fluorine is present in much smaller concentrations in typical urban aerosols[28] and since the cross section is a factor of 20 smaller than the oxygen reaction, the fluorine is not a serious problem. The $^{23}Na(^{3}He,2\alpha)^{18}F$ reaction has a cross section of about 15 mb at 8 MeV.[37] Because the cross section for this reaction is much smaller than that of the oxygen and because sodium concentrations are about a factor of five smaller in typical urban aerosols than oxygen concentrations,[28] the sodium is not a problem in the determination of oxygen by ^{3}He activation analysis. The $^{16}O(^{3}He,p)^{18}F$ reaction was one of the reactions used for the determination of oxygen in atmospheric aerosols.

The $^{16}O(p,\alpha)^{13}N$ reaction was the other reaction used for the analysis of oxygen in aerosols. The proton activation analysis of aerosol samples

for oxygen is very similar to the proton activation method for determination of nitrogen. The irradiation yields the same activities, but for the oxygen determinations the proton energy is selected for maximum production of ^{13}N. Samples are irradiated at a proton energy of 8.1 MeV where the $^{16}O(p,\alpha)^{13}N$ reaction has a cross section of 80 mb. This is below the threshold energy for the $^{14}N(p,pn)^{13}N$ reaction and hence nitrogen is not an interference. The only interference that must be carefully investigated is the $^{13}C(p,n)^{13}N$ reaction. Carbon and oxygen have similar concentrations in ambient aerosols. The ^{13}C nuclide, however, has an abundance of only 1.11% in carbon. At a proton energy of 8.1 MeV the $^{13}C(p,n)^{13}N$ reaction has a cross section of 150 mb as measured in a separate experiment using polystyrene foils. This means that the carbon interference in the oxygen determination can be expected to introduce a 2 to 3% error. This error is not important when compared to the 10 to 15% accuracy that was obtained in the carbon and nitrogen determinations and which is, at best, expected for the oxygen determinations.

The excitation function for the $^{16}O(^{3}He,p)^{18}F$ reaction from the threshold up to 30 MeV was previously measured by Markowitz and Mahony and was not repeated. The absolute cross section was measured, however, at two energies and compared to the Markowitz and Mahony curve. At a ^{3}He energy of 11.9 MeV the cross section was measured to be 225 mb and the published result is 200 mb. An an energy of 7.9 MeV the cross section was measured to be 405 mb and the published result is 400 mb. The peak of the excitation function is at 8 MeV and this is the energy at which the samples were irradiated. The standard was irradiated at the higher

energy of 11.9 MeV. The oxygen standard was 225 μg/cm^2 SiO_2 evaporated onto a 0.001-inch aluminum foil. Quartz is an extremely stable material and is not affected by the beam.

The excitation function for the $^{16}O(p,\alpha)^{13}N$ reaction was measured from the threshold up to 16 MeV and is shown in Fig. 23. The quartz foils were used for the measurement of this excitation function. This excitation function was previously reported by Whitehead and Foster.[38] The resonance structure of the excitation function agrees very well with this previous result, although the absolute cross sections are higher in this work.

The silver membrane filter was used to collect the ambient aerosol. For the ^3He activation analysis the silver filter was not activated at all because the sample was irradiated at 7.9 MeV and the Coulomb barrier for ^3He plus silver is 14.5 MeV. In the case of protons on silver there was some activity produced from reactions with silver since the sample was irradiated at 8.1 MeV and the Coulomb barrier is 8.4 MeV; however, this was only a small amount of activity and was easily resolved from the activities produced from proton reactions on the aerosol material. The silver filter permits a higher detection sensitivity for the activities induced in the aerosol and is the best available filter for the determination of oxygen in aerosols by both methods.

The filter samples were irradiated in a stacked-foil arrangement. The stack used in the ^3He activation analysis is shown in Fig. 24. The aerosol sample was irradiated at the peak of the $^{16}O(^3He,p)^{18}F$ excitation function ($E_{^3He}$ = 7.9 MeV). The quartz standard was irradiated at 11.9 MeV. The circulating cyclotron beam energy was 15 MeV. The whole stack was

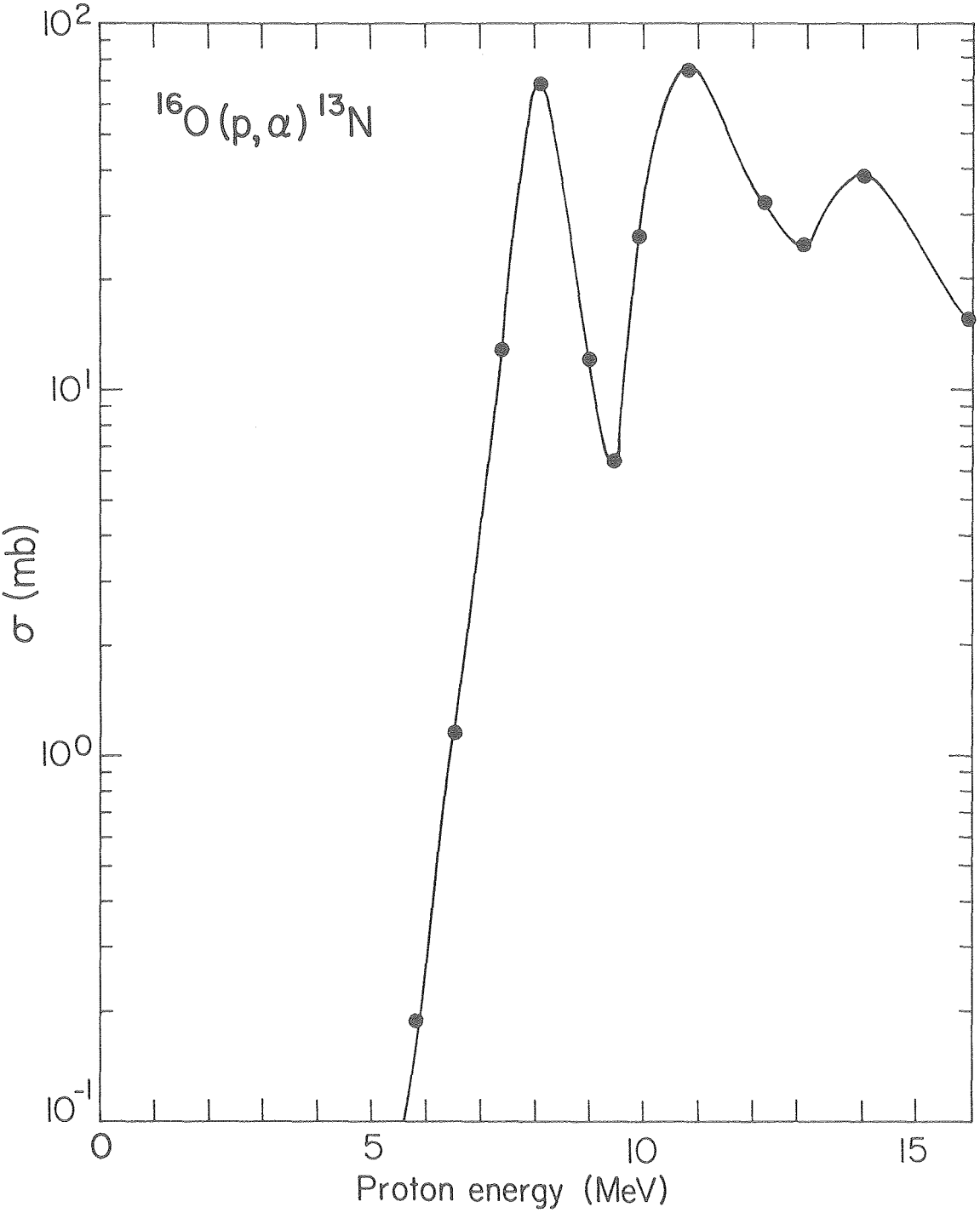

XBL 797-2333

Fig. 23. Excitation function for the $^{16}O(p,\alpha)^{13}N$ reaction.

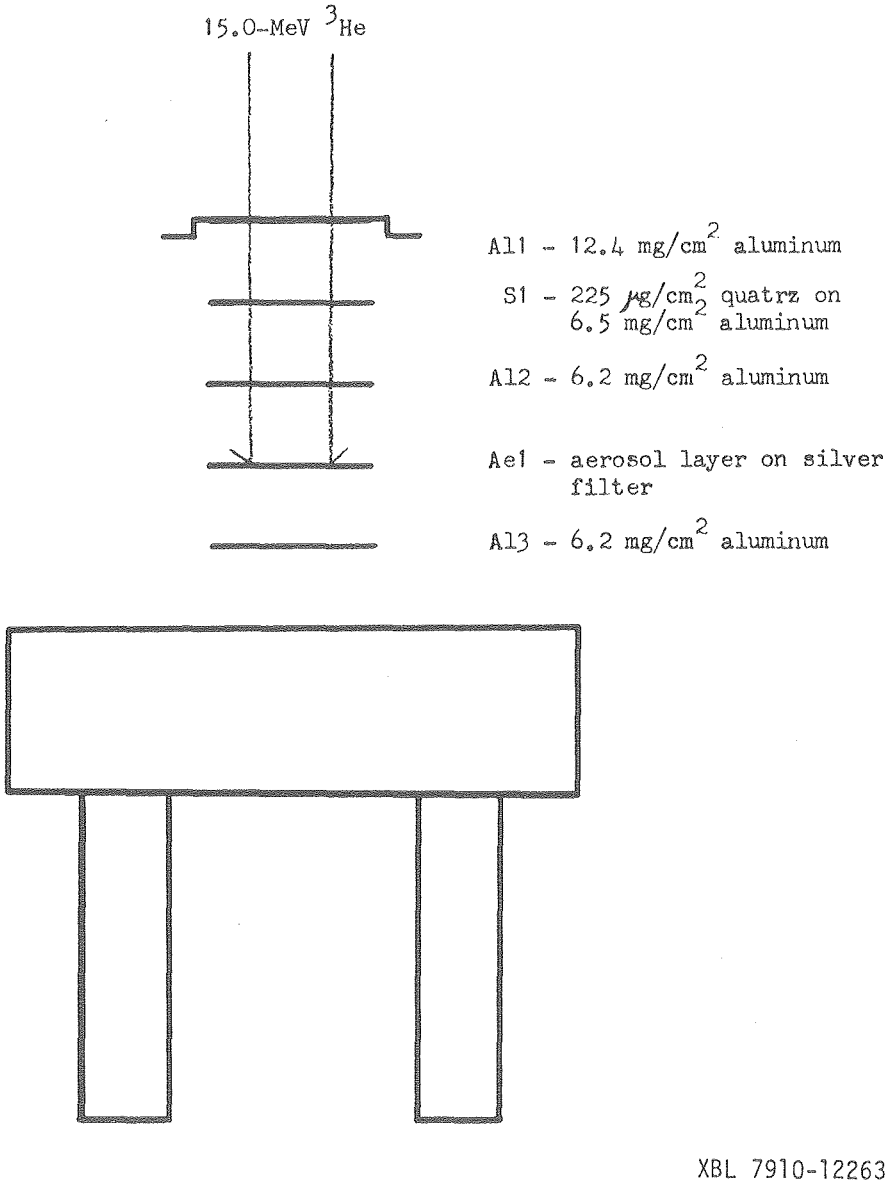

Fig. 24. Diagram of the stack set-up for oxygen determination by ^{3}He activation analysis.

isolated from the cyclotron vacuum by the top aluminum foil and O-ring seals. The cross section ratio for the $^{16}O(^{3}He,p)^{18}F$ reaction at the standard and the sample is given by

$$\frac{\sigma(std)}{\sigma(x)} = 0.55 \quad .$$

The range-energy tables of Williamson, Bujot and Picard were used to calculate the required aluminum thickness for degrading the ^{3}He beam to the proper energy. The stack was typically irradiated for 20 seconds at a beam intensity of ½ μA. Proton activation analyses were also carried out using a stacked-foil arrangement. A diagram of the stack used in the proton activation analysis of aerosol samples for oxygen is shown in Fig. 25. The aerosol sample was irradiated at the peak of the lower-energy resonance in the excitation function. This is at a proton energy of 8.1 MeV. This is the only energy at which the sample could be analyzed. This energy yields the maximum production of ^{13}N from ^{16}O. It would have been better to analyze the sample at the 11-MeV resonance, which is broader and hence less prone to energy dependent changes in the cross section, but the threshold for the $^{107}Ag(p,pn)^{106}Ag$ reaction is at 9.6 MeV and this reaction produces the 24.1-minute ^{106}Ag nuclide which will interfere with the ^{13}N assay. The ^{106}Ag nuclide has a positron decay branching ratio of 70%. Since the majority of the mass of a filter sample is silver, the ^{106}Ag activity would easily dominate the decay curve. The aerosol sample must be irradiated below a proton energy of 9.5 MeV. The quartz standard was irradiated at an energy of 10.9 MeV. The range-energy tables of Williamson, Boujet and Picard were used to calculate the required aluminum thickness to degrade the proton beam to the desired energy. The

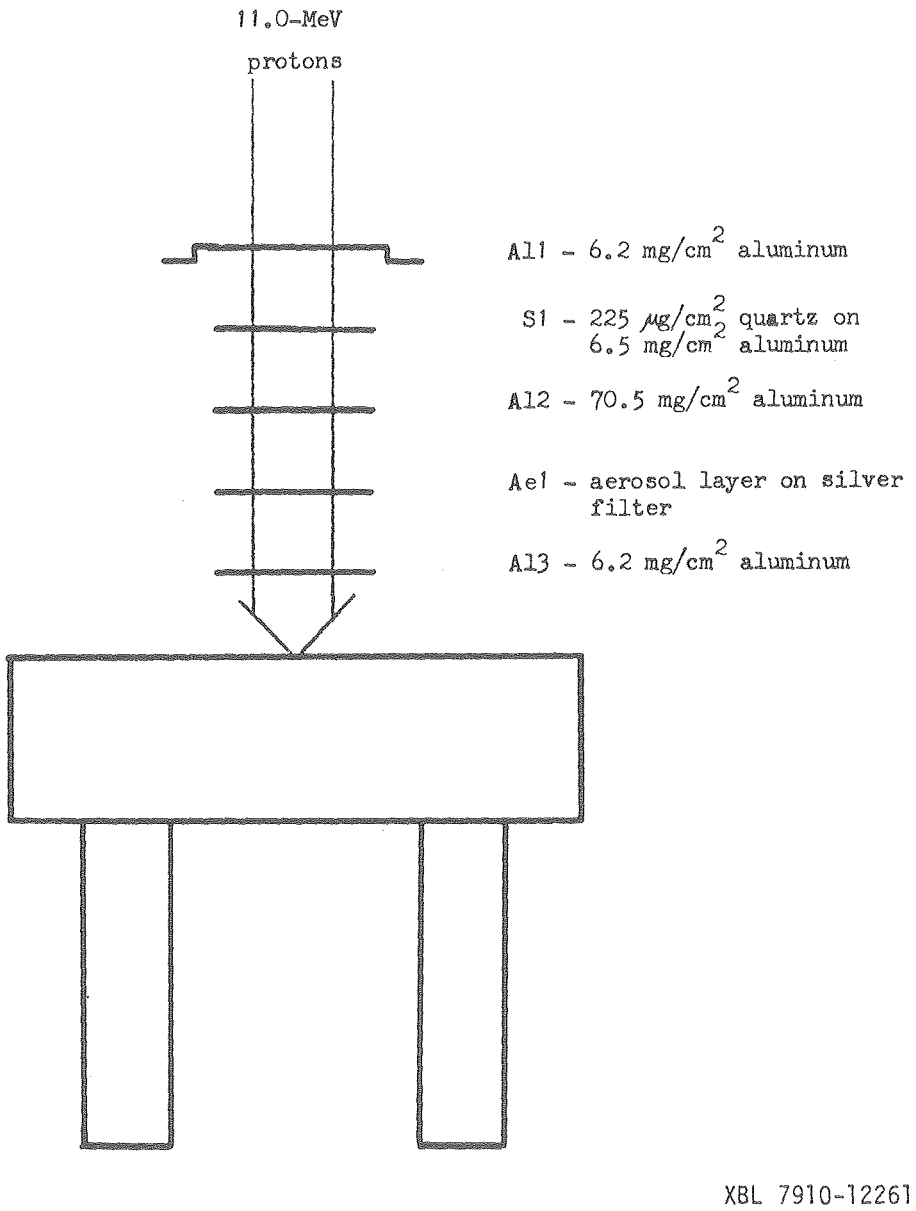

Fig. 25. Diagram of the stack set-up for oxygen determination by proton activation analysis.

circulating cyclotron beam energy was 11 MeV. The stack was isolated from the cyclotron vacuum by the top aluminum foil and O-ring seals. The stack was irradiated for one minute at a proton intensity of 1 μA.

The irradiated samples were assayed using the 0.511-MeV annihilation radiation for both the ^{3}He activation analysis and the proton activation analysis. The decay of the quartz standard after irradiation with the ^{3}He beam is shown in Fig. 26. The decay is a single component corresponding to the decay of ^{18}F in the target. A typical gamma-ray spectrum of a quartz target following a ^{3}He irradiation is shown in Fig. 27. There is only one peak in the spectrum at 0.511 MeV corresponding to the positron-annihilation radiation. The ambient aerosol sample was assayed in the same geometry as the quartz standard. The decay of the integrated 0.511-MeV peak following the ^{3}He irradiation is shown in Fig. 28. The decay has two components: one component is 20.4-minute ^{11}C produced from the $^{12}C(^{3}He,\alpha)^{11}C$ reaction and the other is 109.8-minute ^{18}F produced from the $^{16}O(^{3}He,p)^{18}F$ reaction. By far the dominant component in the decay curve is the ^{18}F activity. A typical gamma-ray spectrum for an aerosol sample is shown in Fig. 29. The lack of any gamma rays other than the annihilation radiation shows that no reactions of ^{3}He on silver occurred.

The decay curve for the integrated 0.511-MeV peak of the quartz standard following proton irradiation is shown in Fig. 30. The decay curve is dominated by the 10.0-minute ^{13}N activity in the early part of the decay curve, but tails into a 109.8-minute component due to ^{18}F. The ^{13}N activity is produced by the $^{16}O(p,\alpha)^{13}N$ reaction and the ^{18}F activity is produced by the $^{18}O(p,n)^{18}F$ reaction in the quartz. A typical

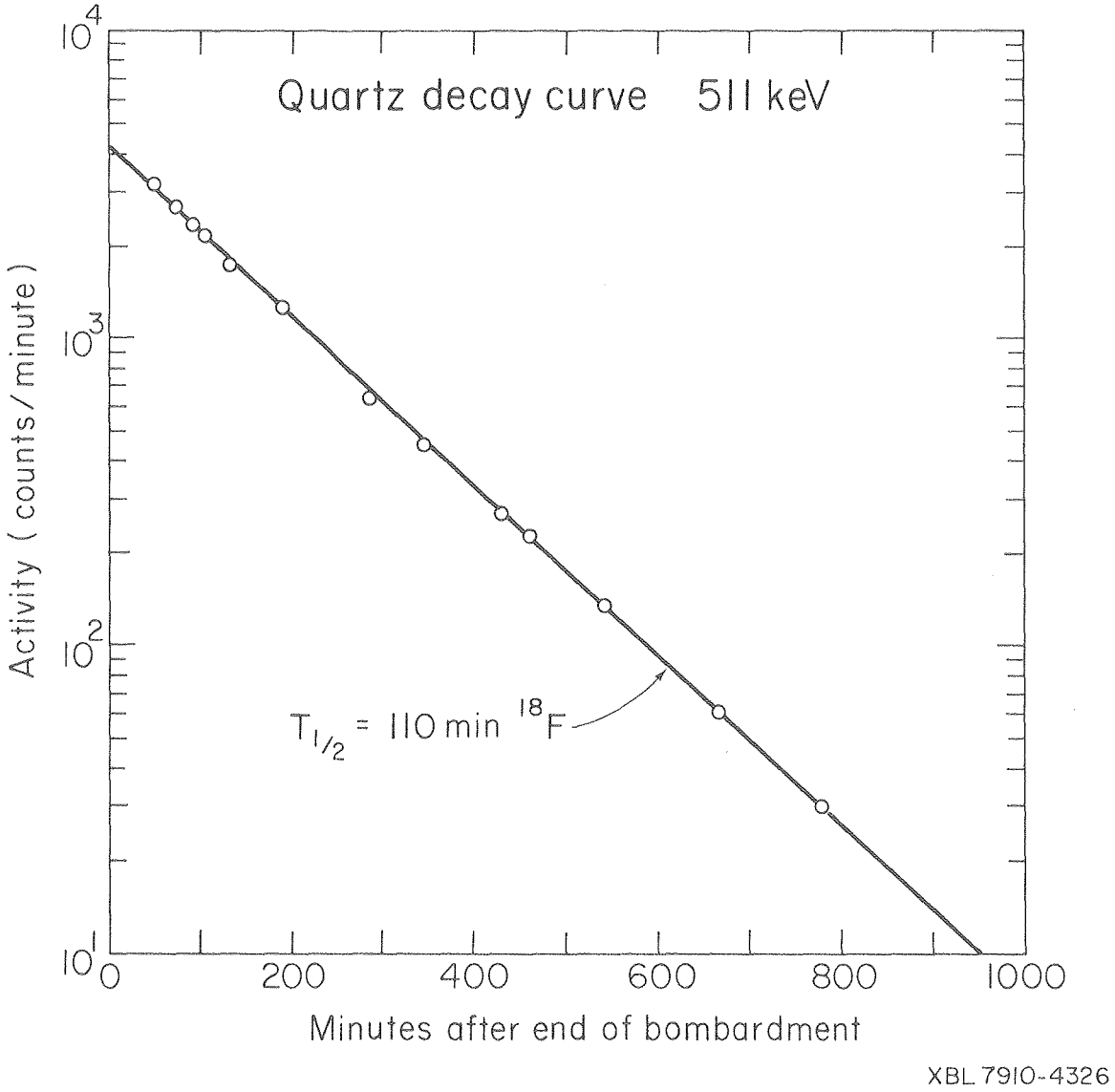

Fig. 26. Decay of the 0.511-MeV annihilation radiation activity following ^3He irradiation of the quartz standard.

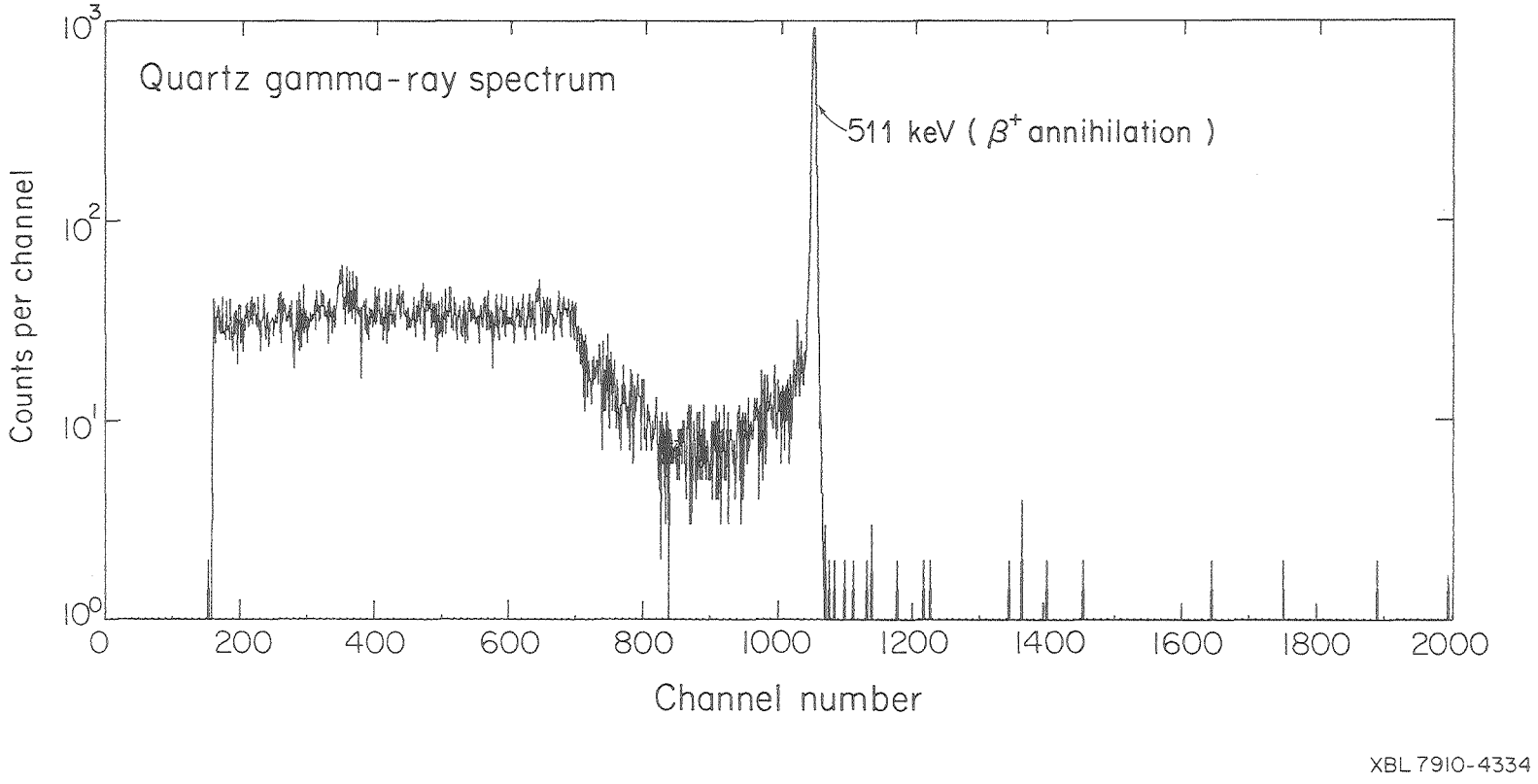

Fig. 27. Gamma-ray spectrum of the quartz standard following ^{3}He irradiation.

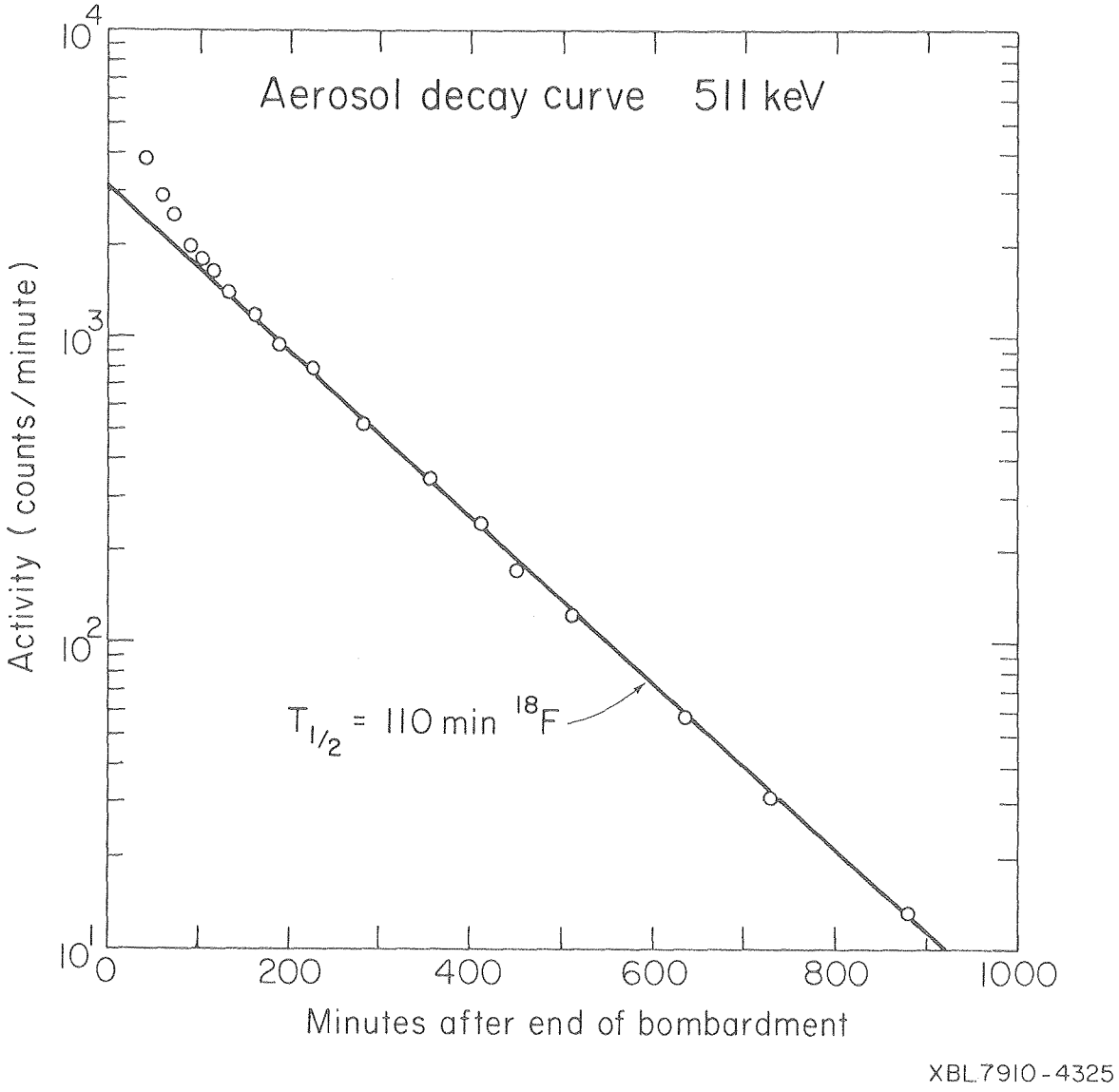

Fig. 28. Decay of the 0.511-MeV annihilation radiation following ^{3}He irradiation of an atmospheric aerosol sample.

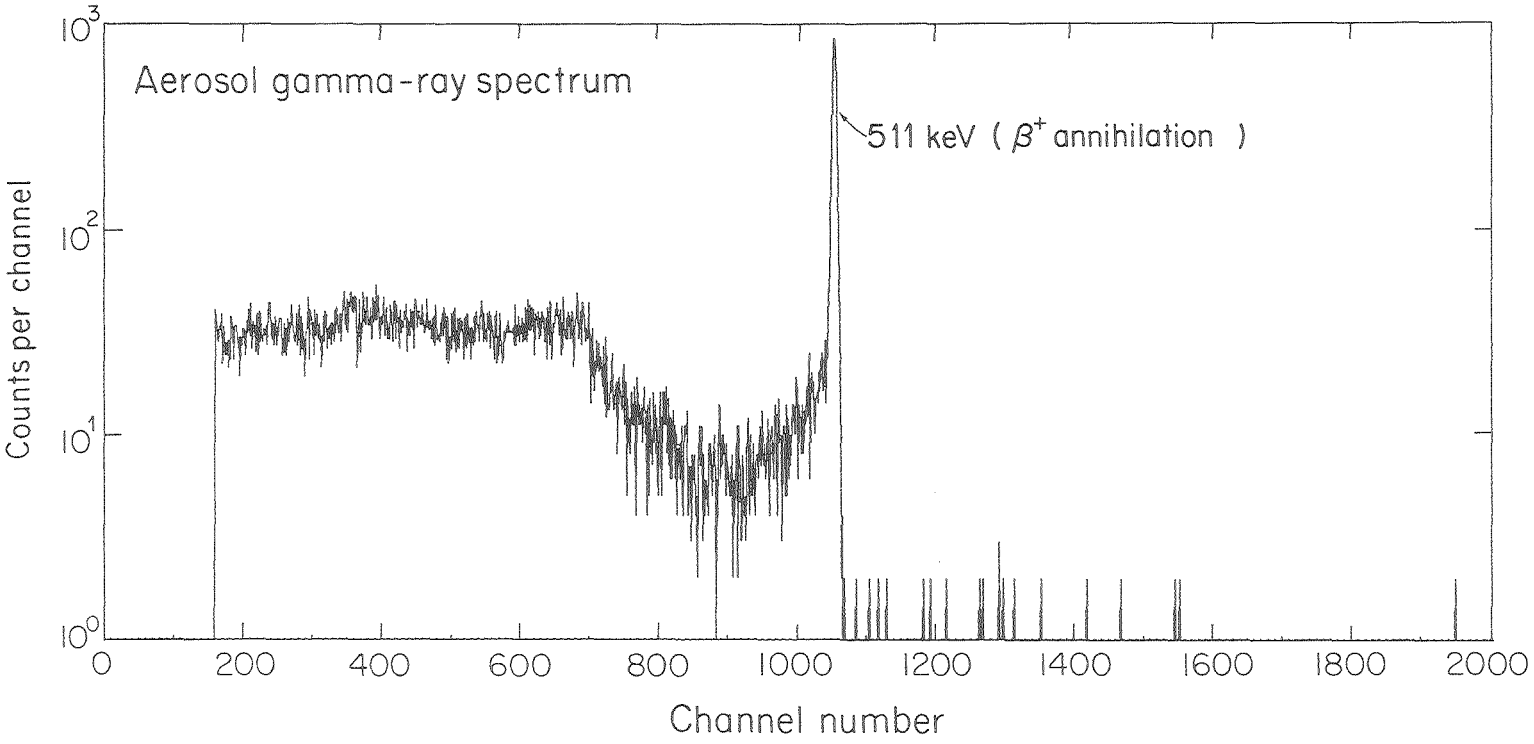

XBL 7910-4331

Fig. 29. Gamma-ray spectrum of an atmospheric aerosol sample collected on a silver filter following irradiation with 7.9-MeV ^{3}He ions.

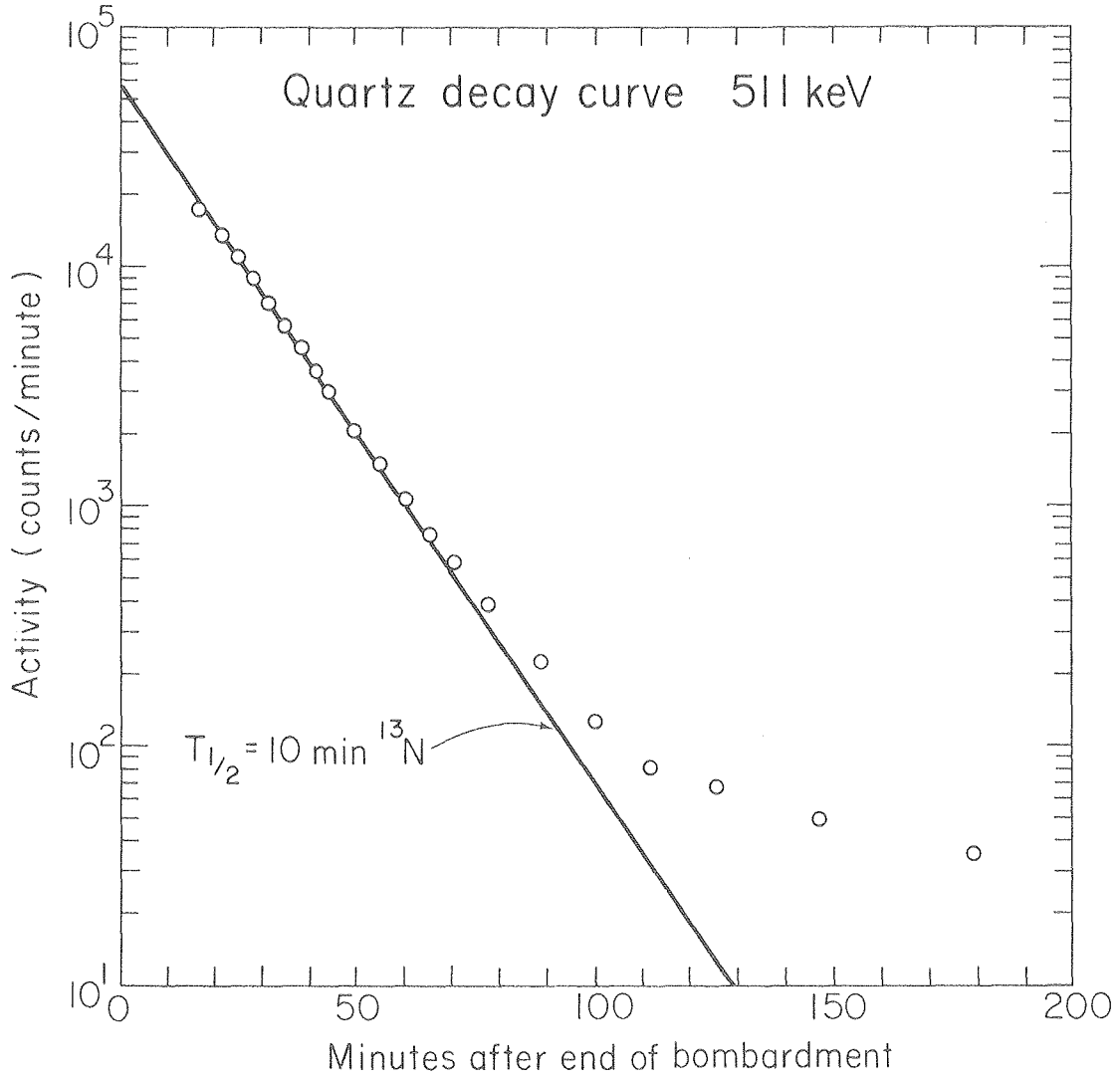

Fig. 30. Decay of the 0.511-MeV annihilation radiation intensity following proton irradiation of the quartz standard.

gamma-ray spectrum is shown in Fig. 31 for the proton irradiation of the quartz standard. The dominant peak in the spectrum is the 0.511-MeV annihilation radiation, but a very small amount of ^{27}Mg can be identified by its gamma rays. This activity results from the $^{27}Al(n,p)^{27}Mg$ reaction of secondary neutrons with the aluminum foil. The decay of the integrated 0.511-MeV radiation in the aerosol sample after proton irradiation was followed at short intervals for several hours. This decay curve is shown in Fig. 32. There are three components in the decay curve: (a) a 10.0-minute component due to ^{13}N produced by the $^{16}O(p,\alpha)^{13}N$ reaction, (b) a 20.4-minute component due to ^{11}C produced by the $^{14}N(p,\alpha)^{11}C$ reaction, and (c) a 6.5-hour component due to ^{107}Cd produced by the $^{107}Ag(p,n)^{107}Cd$ reaction in the silver filter.

The amount of oxygen in the aerosol samples was calculated using the relative method. The important values obtained from the decay-curve analyses are the A_0 value for ^{18}F in the quartz standard and ^{18}F in the aerosol for the ^{3}He activation analysis. The important values obtained from the decay-curve analyses following proton irradiation are the A_0 value for ^{13}N in the quartz standard and ^{13}N in the aerosol. Several blank silver filters were analyzed for oxygen by both ^{3}He and proton activation analysis. The oxygen blank value obtained from these irradiations does not represent the true oxygen content of the silver filter, but only an apparent oxygen content. This is because the silver filters are thick (30 to 40 mg/cm^2) and the beam energy is severely degraded on passage through the filter. In fact, the ^{3}He beam which enters the filter at an energy of 7.9 MeV is stopped in the silver. The range of 7.9 MeV ^{3}He ions in silver is 25 mg/cm^2. The proton beam which enters

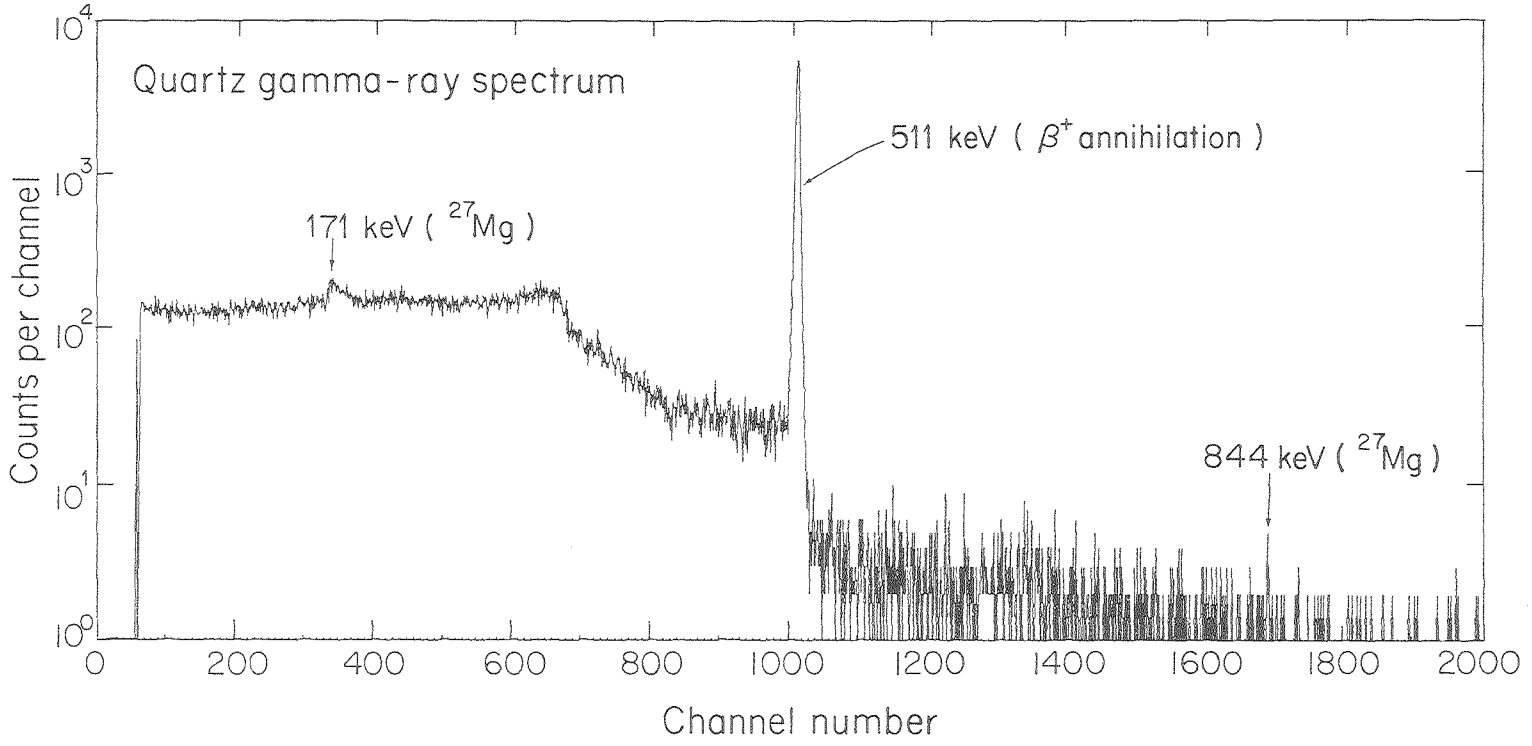

XBL 7910-4333

Fig. 31. Gamma-ray spectrum of the quartz standard following irradiation with 10.9-MeV protons.

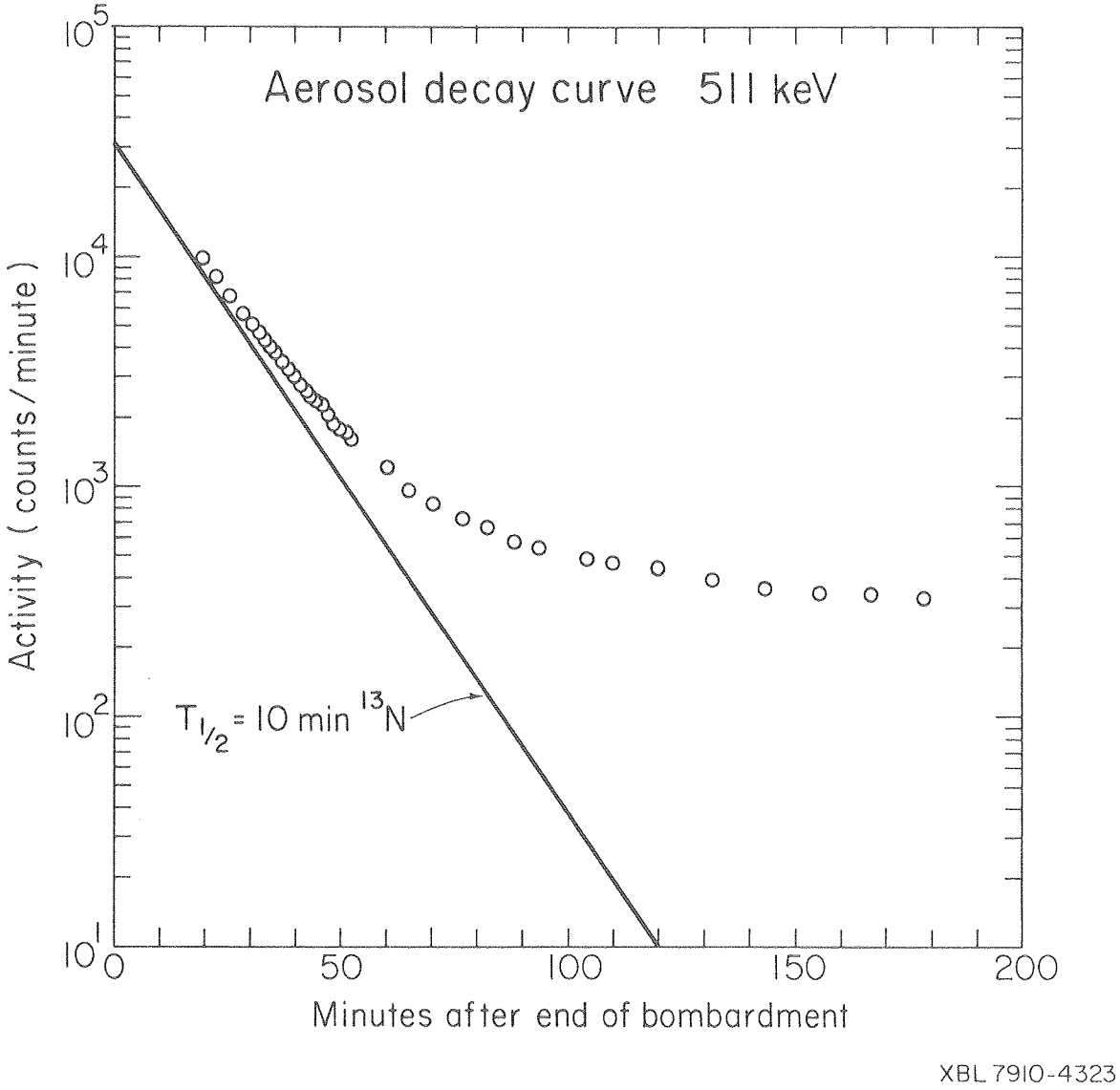

Fig. 32. Decay of the 0.511-MeV annihilation radiation activity following irradiation of an atmospheric aerosol sample with 8.1-MeV protons.

the filter at 8.1 MeV passes completely through the filter. The sharp resonance of the $^{16}O(p,\alpha)^{13}N$ reaction and the fact that the beam is degraded in energy to around 7 MeV means that the ^{13}N activity produced is not indicative of the true oxygen content. The observed ^{13}N activity, however, can be related to an apparent oxygen content on the surface of the silver filter. The same can be done for the ^{18}F activity that is produced in the silver filter following ^{3}He irradiation. This means that the oxygen blank value will differ for the same filter depending on the particle that was used for the activation analysis. The oxygen blank values for silver filters irradiated with protons ranged from 10 to 30 $\mu g/cm^2$. The oxygen blank values for silver filters irradiated with ^{3}He ions ranged from 3 to 8 $\mu g/cm^2$.

Several samples were analyzed by both proton activation analysis and ^{3}He activation analysis. The samples can be divided into two main groups. The first group consists of six laboratory-prepared samples of known composition and varying oxygen content. The second group consists of four ambient aerosols. The laboratory-prepared samples were made by depositing ammonium sulfate on silver filters. Two more were made by depositing disodium (ethylenedinitrilo) tetraacetate (EDTA) on silver filters, and the last two prepared samples were made by depositing ammonium oxalate on silver filters. These compounds have known compositions of low-Z elements commonly found in atmospheric aerosols. The ability to determine accurately oxygen in these samples would indicate the ability to do so in actual ambient samples. The ambient samples were collected for 24 hours at LBL on silver filters. The filters were weighed before and after collection of the aerosol so that the aerosol

loading on the filter could be determined. The results of the analysis of these ten samples by proton and ^{3}He activation analysis are shown in Table 6.

The comparison of results between the two methods shows an average percent difference of 18% for the ten samples. There are several points that must be considered in comparing the two methods and deciding which method would be best in routine use. These points give sufficient reason for believing that the ^{3}He activation analysis yields the more reliable results.

1) The $^{16}O(p,\alpha)^{13}N$ excitation function is characterized by sharp resonances while the $^{16}O(^{3}He,p)^{18}F$ excitation function increases smoothly from the threshold to around 8 MeV and then monotonically decreases out to 30 MeV. This difference in the structure of the excitation function means that the precise energy of the projectile is much less important in the ^{3}He method than in the proton method. A variation in energy of the proton by as little as 0.2 MeV can cause a significant change in the cross section, while this type of variation in the ^{3}He beam energy would have no perceptible effect on the cross section. Although the 88-inch cyclotron is capable of reproducing the beam energy to within this limit from run to run, it is still cause for concern.

2) The apparent oxygen blank value of the silver filter is another concern. The blank value for the proton method is much larger than for the ^{3}He method. The subtraction of this much larger blank value from the total oxygen content leads to net oxygen values with a larger error in the proton method than in the ^{3}He method. This is

TABLE 6. Comparison of methods for nitrogen determination in atmospheric aerosols.

Sample	Material	O found, $\mu g/cm^2$		
		Proton activation	^3He activation	Ratio ($p/^3He$)
AO-1	ammonium oxalate	722	784	0.92
AO-2	ammonium oxalate	210	179	1.17
ED-1	EDTA	225	223	1.01
ED-2	EDTA	20	25	0.80
HO-1	ammonium sulfate	152	133	1.14
HO-2	ammonium sulfate	459	449	1.02
JO-1	aerosol	34	45	0.76
JO-2	aerosol	45	55	0.82
JO-3	aerosol	24	37	0.65
JO-4	aerosol	74	64	1.16
				$\bar{R} = 0.95 \pm 0.18$

especially critical in the ambient aerosol sample analyses where the samples are usually lightly loaded. For determination of oxygen in aerosols the lower apparent blank value of the silver filters in the ^{3}He method is very much preferred.

3) The decay-curve analysis is much simpler for the ^{3}He method than for the proton method. There are only two components that must be resolved in the ^{3}He irradiation and if the ^{11}C is allowed to decay out before counting the sample, the decay is entirely 109.8-minute ^{18}F and the A_0 value is very easy to determine. The decay-curve analysis in the proton case is much more difficult. The 10.0-minute ^{13}N must be separated from the 20.4-minute ^{11}C. This requires getting samples to the counters as soon as possible after the irradiation. It also requires decay curves with many points and good statistics for at least two hours after the end of bombardment and preferably four hours. This uses quite a bit of counter time and requires a very good decay-curve analysis in order to obtain good results.

4) The cross section for the $^{16}O(^{3}He,p)^{18}F$ reaction is 400 mb while the cross section for the $^{16}O(p,\alpha)^{13}N$ reaction is only 80 mb. This much larger cross section means that the samples can be irradiated for a shorter period of time to obtain sufficient activity for accurate results. The proton activations used irradiation conditions of 1 μA for 1 minute for a total integrated charge of 60 μC. The ^{3}He activations used irradiation conditions of ½ μA for 20 seconds for an integrated charge of 10 μC.

The conclusion is that the ^{3}He activation analysis is simpler and more

reliable than the proton activation analysis for determination of oxygen in atmospheric aerosol samples for all the above reasons.

The sensitivity of both methods for determination of oxygen is limited by the blank value of the silver filter. The blank value for each individual silver filter can be determined to approximately 15%. For proton irradiations where blank values run 10 to 30 $\mu g/cm^2$ the blank can be determined to 2 to 5 $\mu g/cm^2$. For ^3He irradiations the blank values can be determined to 0.5 to 1 $\mu g/cm^2$. The precision in determination of the oxygen blank represents the realistic lower limit to the sensitivity of the two methods. As the oxygen content of the aerosol becomes comparable to the blank value then the errors in the analysis become larger. For the ^3He activation method of analysis an aerosol oxygen content of about 5 $\mu g/cm^2$ could easily be determined to 20%. If the aerosol contains less oxygen than this, then the blank contribution to to total oxygen makes an accurate analysis of the aerosol oxygen impossible. If special filters were developed which had oxygen blank values below 0.5 $\mu g/cm^2$, then it would easily be possible to determine the oxygen content of an aerosol sample down to this level.

The possibility of a contribution to the 10.0-minute activity in the blank filter from 9.74-min ^{62}Cu was also considered. This activity could be produced by reactions involving impurities of copper and nickel in the silver filter. The proton reactions involving nickel and copper are $^{62}Ni(p,n)^{62}Cu$ (Q = -4.72 MeV) and $^{63}Cu(p,d)^{62}Cu$ (Q = -8.62 MeV). The ^{62}Cu activity has no nuclear gamma rays that could be used to confirm or dismiss its presence. If copper and nickel impurities are present in sufficient concentration to yield a significant amount of ^{62}Cu, then other reactions

involving copper and nickel must also be detectable. The most important of these reactions are $^{60}Ni(p,n)^{60}Cu$ (Q = -6.90 MeV) and $^{63}Cu(p,n)^{63}Zn$ (Q = -4.15 MeV). The 24-minute ^{60}Cu activity has a nuclear gamma ray with an energy of 1332 keV (87.9%). This gamma ray would be easily detected if there was a significant amount of nickel in the filter. The fact that this gamma ray is not present means that the contribution from the $^{62}Ni(p,n)^{62}Cu$ reaction to the blank activity must also be very small.

The production of ^{62}Cu from the $^{63}Cu(p,d)^{62}Cu$ reaction can be dismissed since the proton energy (8.1 MeV) is less than the Q-value of the reaction. Reactions of other projectiles on copper in the filter, however, could lead to production of the ^{62}Cu nuclide. The most important of these reactions are $^{63}Cu(^{3}He,\alpha)^{62}Cu$ (Q = +9.74 MeV) and $^{63}Cu(d,t)^{62}Cu$ (Q = -4.58 MeV). The presence of copper in the filter can be determined by examination of the gamma-ray spectrum following proton irradiation. The presence of 38.1-minute ^{63}Zn from the $^{63}Cu(p,n)^{63}Zn$ reaction is a good signal for copper. This positron emitter has two nuclear gamma rays with energies of 670 keV (8.44%) and 962 keV (6.64%). These nuclear gamma rays would be easily detected in the gamma-ray spectrum. The absence of these gamma rays indicates that copper impurities in the silver filter are quite small. Therefore, reactions on copper to produce ^{62}Cu activity are also quite small.

IV. DISCUSSION

The methods described in the previous section were developed because the need existed for sensitive and nondestructive methods for the determination of these important low-Z elements in atmospheric aerosols. These experiments demonstrated that activation analysis can be applied to aerosol elemental analysis. These experiments only lay the groundwork for further work in the field and indeed much more work is needed. The important contribution from this project is that a new, hitherto untried, application of activation analysis to the new field of atmospheric aerosol research can and does work. It fulfills a real need where one existed. The methods developed here show the potential for being able to fulfill that need on a routine basis. The majority of the work in atmospheric aerosol research involves the everyday analysis of large numbers of samples. It is important that the methods use a minimum of equipment time for each sample analysis. These activation analysis methods which only use a short amount of accelerator time offer a good solution to a difficult analytical problem.

The next step that is required is the reduction of these methods to everyday practice. This will require the construction of new equipment specifically designed for the determination of low-Z elements in atmospheric aerosols. This includes new beam-line equipment for quickly changing samples and perhaps even a new low-energy particle accelerator since it is not easy to obtain time on a large accelerator on an everyday basis. New and simple assay equipment is also needed. This includes computer-controlled sample changers and single-channel analyzers instead

of the multichannel analyzers used in this work. The simplicity of the gamma-ray spectrum means that NaI detectors may, in many instances, be used to assay the 0.511-MeV radiation. A dedicated computer for decay-curve analysis would also make the system much more practical on a routine basis. All of these things considered together, it should be possible to design and build a system for low-Z element determinations in atmospheric aerosols that can handle a sufficiently large number of samples to be very useful in atmospheric aerosol research. As the method is used more and more on an everyday basis, the precision of the method will certainly improve. The use of equipment specifically designed for the activation analysis of aerosol samples and the experience gained in operating such a system will be the primary contributing factors to such an improvement.

The activation analysis methods developed here for the determination of low-Z elements in atmospheric aerosols have their strong and weak points. A very strong point is that the methods are very sensitive. The accurate determination of these elements to the μg level is an absolute requirement. The activation analysis method ideally fulfills this requirement. This fact was demonstrated for the nitrogen, carbon and oxygen determinations. The fact that the method is nondestructive is another important feature. The nondestructive nature of the analysis was repeatedly demonstrated throughout this work. The samples were first analyzed by activation analysis and then the very same samples were destructively analyzed by other methods. The nondestructive feature of the method will be of great use in future experiments. For example, total nitrogen can be obtained by the proton activation method, then certain nitrogen-containing species can be removed by selective solvent extraction. The sample is then

reanalyzed for nitrogen by proton activation analysis to determine the amount of nitrogen removed by the solvent. This process can be repeated using different solvents. The practical application of this type of analysis has been performed by this author and coworkers and has been reported in the literature.[39] A similar type of analysis can be performed for carbon and oxygen and serves to demonstrate the usefulness of a non-destructive analysis. The single most important weak point of the activation-analysis method is the fact that a particle accelerator is required. It is becoming more and more difficult to secure adequate time at these facilities and, moreover, the cost for that time is rapidly escalating. The activation analysis method, however, uses the least accelerator time per sample of any of the analytical methods relying on an accelerator. For example, the method of Macias and coworkers which uses proton inelastic scattering requires 15 minutes of beam time per sample, while the activation analysis method described here requires only one minute of beam time per sample.[10] For a method which requires the use of an accelerator, the activation analysis method makes the most judicious use of accelerator time.

Activation analysis methods for the determination of low-Z elements can now be used to investigate many properties of aerosols. The first thing that can be done is to attempt to obtain a mass balance of the elements in aerosols. Activation analysis methods can be used to determine the carbon, nitrogen and oxygen that is present in the aerosol, and other methods such as x-ray fluorescence or neutron activation analysis can be used to determine the concentration of heavy elements.

A great deal of information can be learned about aerosols when the

activation analysis method is used with complementary analyses. One way to do this is to use the activation method in conjunction with x-ray photoelectron spectroscopy (ESCA). The activation analysis method can be used to determine the bulk concentration of a certain element and then ESCA, which cannot accurately measure bulk concentrations of elements, can be used to obtain the fraction of a certain chemical form of that element. For example, proton activation can be used to determine the total nitrogen in a sample and ESCA can be used to tell what fraction of that nitrogen is present in a reduced form such as ammonium ion or amide and what fraction is present as nitrate.

The diurnal variation of the low-Z elements in atmospheric aerosols is also an interesting problem that could be studied with the activation analysis method. For example, the fraction of oxygen in aerosols may be strongly dependent on the time of day or ambient conditions, such as the amount of oxidant present.

The concentrations of low-Z elements in size-segregated samples is another interesting problem. Since small-particle sizes are primarily associated with anthropogenic activity, the concentration of low-Z elements in this size range could provide more information on the origin of man-made particles and their chemistry in the polluted troposphere.

There are also additional experiments which could be performed to develop other activation analysis methods for determination of low-Z elements in aerosols. This new work should focus primarily on the use of the short-lived isotopes that were specifically excluded in this work. The short-lived isotopes were not used in this work because special equipment is required to rapidly move samples to a low background environ-

ment for counting. The assay of the samples at the accelerator is mandatory. The use of short-lived isotopes has the additional advantage that assay time is much shorter compared to the longer-lived isotopes.

The $^{14}N(p,n)^{14}O$ reaction is an excellent choice for the determination of nitrogen. It is a truly interference-free reaction which should have excellent sensitivity. The ^{14}O nuclide has a half-life of 71.0 seconds and decays by positron emission. A property of this nuclide is that it is one of the few neutron-deficient nuclides in the region that has a nuclear gamma ray. The 2.313-MeV gamma ray accompanies 99% of the ^{14}O decays. A nuclear gamma ray is preferable to the annihilation radiation since it is generally a unique identification of the emitting nuclide. A very simple and sensitive method for nitrogen determinations in atmospheric aerosols could be developed using the $^{14}N(p,n)^{14}O$ reaction.

Another possible method that could be developed is a multi-element analysis based on a low-energy deuteron irradiation. A facility that produces 3 to 4 MeV deuterons would be ideal for this proposed method. Such a low-energy facility is more commonly available and more readily accessible than the large facilities such as the 88-inch cyclotron. The method would be used to simultaneously measure carbon, nitrogen and oxygen in atmospheric aerosols. The carbon would be detected as it was in this work with the $^{12}C(d,n)^{13}N$ reaction; the oxygen would be detected by the $^{16}O(d,n)^{17}F$ reaction, and the nitrogen by the $^{14}N(d,n)^{15}O$ reaction. All of these reactions are exoergic and would readily proceed at a deuteron energy of 3 MeV. All the reactions would be interference-free at this low deuteron energy. The radionuclides are all positron emitters with no nuclear gamma rays. They would be detected by their 0.511-MeV

annihilation radiation. The ^{13}N nuclide has a half-life of 10.0 minutes, the ^{17}F nuclide has a half-life of 66 seconds, and the ^{15}O nuclide has a half-life of 122 seconds. The difficult part of this experiment would be to accurately resolve the 66-second ^{17}F from the 122-second ^{15}O in the decay curve. This would require good counting statistics and a very good decay-curve analysis. The 10.0-minute ^{13}N should be relatively easy to resolve out in a decay curve analysis, as it was in this work. The samples would have to be counted at the accelerator using a Ge(Li) detector and good counting equipment. Development of such a multi-element determination method would be a valuable and cost-effective contribution to atmospheric aerosol research.

Future research might also concentrate on new methods of aerosol collection to be used in conjunction with activation analysis. The silver membrane filter is currently the best available method for collection of atmospheric aerosols. The blank value of oxygen in the silver filters is, however, high and it would be desirable to have a special low oxygen substrate for aerosol collection. One possible method would be to use an impaction collector and a thin high-Z substrate such as tungsten. A sonic jet of air impacting on the tungsten surface would serve to collect the aerosol from the air stream. The particles could also be size-segregated using this method. The high-Z material would have very low blank values for the low-Z elements and also be activated less than the silver. The result would be an even more sensitive and accurate method for the determination of low-Z elements in atmospheric aerosols.

V. SUMMARY AND CONCLUSIONS

The field of air pollution research has really only existed as a scientific endeavor for about 25 years. The field of atmospheric aerosol research is even younger. Many of the tools required for this new field are still being developed. This project was the development of a new tool for the investigation of atmospheric aerosols. The goal of the work was to develop a method to determine concentrations of carbon, nitrogen and oxygen in these aerosols by a nondestructive method. These are important low-Z elements which constitute the bulk of the mass of ambient aerosols. The methods developed here rely on the use of charged-particle beams for the analysis of aerosol samples. The charged-particle beam induces nuclear reactions in the aerosol material. The radionuclides produced by these reactions are detected by well known nuclear counting methods. The data is analyzed by computer and the concentration of the desired element is obtained following the relative method of analysis.

The method for determination of nitrogen in aerosols uses a proton beam to induce the $^{14}N(p,\alpha)^{11}C$ reaction. The 20.4-minute ^{11}C is followed via its 0.511-MeV annihilation radiation. A target of melamine is used as the nitrogen standard. The results of the proton activation analysis were compared to independent combustion results performed on the same samples. The sensitivity for nitrogen detection is approximately 0.1 $\mu g/cm^2$.

The method for the determination of carbon in aerosols uses a deuteron beam to induce the $^{12}C(d,n)^{13}N$ reaction. The 10.0-minute ^{13}N was followed by its 0.511-MeV annihilation radiation. A carbon standard of polystyrene was employed in this analysis. The results of the deuteron

activation analysis were compared to independent combustion results on the same samples. The sensitivity for detection of carbon is approximately 0.5 $\mu g/cm^2$.

Two methods were developed for the determination of oxygen in atmospheric aerosols. One method uses a ^{3}He beam to induce the $^{16}O(^{3}He,p)^{18}F$ reaction. The 109.8-minute ^{18}F was followed by its 0.511-MeV annihilation radiation. The second method uses a proton beam to induce the $^{16}O(p,\alpha)^{13}N$ reaction. The 10.0-minute ^{13}N was again followed by its 0.511-MeV annihilation radiation. The two methods were used to check one another since another independent method of analysis for oxygen in aerosol samples was not available. The sensitivity for detection of oxygen is about 5 $\mu g/cm^2$ by the more accurate ^{3}He method and is primarily limited by the rather large oxygen blank in the silver filter.

The methods developed here will be useful in the field of atmospheric aerosol research. The determination of carbon, oxygen and nitrogen by a nondestructive method has long been a difficult problem to solve. This research represents one effort at the solution of this problem. It is the useful marriage of basic research in nuclear chemistry and practical applications in air science studies.

There are many new and exciting application of the work that was started with this project. The discussion has dealt with only some of the possibilities. The research goals of this group and in the field of atmospheric pollution research as a whole will be the guide to the direction of future research of this type. It is the hope of this author that the work performed during this project has contributed an important new tool to the investigation of aerosols and will help to fulfill the

desired goal of air pollution research — the complete understanding of air pollution chemistry and the eventual restoration of our air to a pollution-free state.

ACKNOWLEDGMENTS

I wish to thank Professor Samuel S. Markowitz for his most helpful advice and guidance during the course of this work. I also thank the members of the Lawrence Berkeley Laboratory Atmospheric Aerosol Research Group, especially Dr. Tica Novakov, for many helpful discussions and suggestions.

I wish to thank the Lawrence Berkeley Laboratory staff for their indispensable help. I am grateful to the staff of the LBL 88-inch cyclotron and especially grateful to Ruth-Mary Larimer for her help with scheduling my runs and to Harry Harrington for his technical help with the irradiation apparatus.

I appreciated the cooperation of the members of the Glenn Seaborg group with whom I shared the counting facility. I especially wish to thank Diana Lee for her help in scheduling counter time and also for many helpful discussions.

I am grateful to C. Spicer, Battelle Memorial Institute, Columbus, Ohio, and the staff of the analytical laboratory at the University of California Chemistry Department for combustion analyses of many samples. I also wish to thank Gary Mason of the LBL Atmospheric Aerosol Research Group for doing many of the combustion analyses.

The encouragement of my family has been a sustaining force. I especially thank my mother, Cathryn, for her love and support. I also thank my grandmother, Irene, for the many letters of love and encouragement. A powerful force in my life is the love of God through Jesus Christ and the strength that I have received from this relationship is immeasurable.

This work was supported by the National Science Foundation and the Division of Biomedical and Environmental Research of the U.S. Department of Energy under contract W-7405-ENG-48.

APPENDIX A

TI 960 DATA COLLECTION PROGRAM AND SAMPLE DATA OUTPUT

TI 960 INSTRUCTION CODES

1	Read tape
2	Write tape
3	Go to end of data on tape
7	Search tape for specified tag
10	Turn on ADC
11	Turn off ADC
12	Time for one period on interval timer
13	Multiparameter data mode
14	Set data taking origin
15	Clear spectrum. All or part
16	Input tag from teletype
17	Output heading (tag) on teletype
30	Add immediate
31	Subtract immediate
32	Multiply immediate
33	Divide immediate
34	Add two heading slots
35	Subtract two heading slots
36	Move heading slot P1 to heading slot P2 P2 restricted to slots 6 thru 25, P1 not restricted
37	Set heading slot P1 to zero (6 thru 25)
38	Type contents of heading slot P1 on teletype
40	Integrate spectrum between marks
41	Find centroid between marks
42	Output answer on teletype
43	Store answer in heading slot P1 (restricted to slots 5 thru 26)
44	Read displayed time on sequence timer into heading slot 0
45	Type out time of day
46	Set Julian Day calendar
47	Carriage return and line feed
20	Set program pointer for editing
21	List program from P1 thru P2 on teletype
22	Clear entire program buffer
24	Stop program
25	Go to P1 unconditionally
26	Conditional branch
23	Start program at step P1
27	Restart program after pause

TI 960 DATA COLLECTION PROGRAM

```
 0    15
 1    10
 2    45
 3    12
 4    45
 5    11
 6    47
 7    38:3
 8    44
 9    47
10    38:0
11    47
12    38:2
13    47
14    38:5
15    35:5:2:20
16    47
17    38:20
18    41:1012:1037
19    47
20    42
21    28:47:986:1011
22    43:7
23    28:47:1012:1037
24    43:8
25    28:47:1038:1063
26    43:9
27    34:7:9:10
28    33:10:2:11
29    35:8:11:12
30    47
31    38:12
32    33:0:60:13
33    47
34    38:13
35    51:12:13:14
36    47
37    38:14
38    33:20:2:21
39    34:21:2:22
40    33:22:60:23
41    47
42    38:23
43    52
44    2
45    47
46    24
47    40:3544:3534
48    47
49    42
50    29
```

TI 960 SAMPLE DATA OUTPUT

```
B1
SHELF NO.  ?   5

  TIME  13:53:42    DAY  263    TIME  13:54:46     DAY  263
           10  (spectrum number)
           60  (live time of counting interval)
       50,025  (time of day at start of count in seconds)
       50,086  (time of day at end of count in seconds)
           61  (true time of counting interval)
    1,013.24  (channel number of the peak centroid)
           43  (integral of counts in the region on low-energy side)
        1,877  (integral of counts in the peak)
           15  (integral of counts in the region on high-energy side)
        1,848  (net integral of counts in the peak)
            1  (live time of the counting interval in minutes)
        1,848  (counting rate in the peak in counts/minute)
          834  (time of day at midpoint of counting interval in minutes)
  TAPE WRIT   0 to 3,999        TIME  13:55:22     DAY  263

S1
SHELF NO.  ?   5

  TIME  13:55:42    DAY  263    TIME  13:56:47     DAY  263
           11
           60
       50,146
       50,207
           61
    1,013.25
          234
       11,549
           23
       11,421
            1
       11,421
          836
  TAPE WRIT   0 to 3,999        TIME  13:57:24     DAY  263

B1
SHELF NO.  ?   5

  TIME  13:55:42    DAY  263    TIME  13:58:44     DAY  263
           12
           60
       50,264
       50,324
           60
    1,013.31
           56
        1,536
           18
        1,499
            1
        1,499
          838
  TAPE WRIT   0 to 3,999        TIME  13:59:20     DAY  263
```

APPENDIX B

ABSTRACTS OF PAPERS PRESENTED AT MEETINGS OF THE AMERICAN CHEMICAL SOCIETY

Presented at the 176th meeting of the American Chemical Society,
Miami Beach, Florida, September 10-15, 1978.

NONDESTRUCTIVE DETERMINATION OF NITROGEN IN ATMOSPHERIC AEROSOLS BY CHARGED-PARTICLE-INDUCED NUCLEAR REACTIONS*

Mark Clemenson, Tihomir Novakov, and Samuel S. Markowitz
Department of Chemistry and Lawrence Berkeley Laboratory
University of California, Berkeley, CA 94720

Low-Z elements, such as carbon, nitrogen, oxygen and sulfur, are important constitutents in atmospheric aerosols; such particulate matter is contributing strongly to air pollution. There is, however, no generally satisfactory method of analysis — that is nondestructive and fairly rapid — to determine quantitatively low-Z elements. X-ray fluorescence, an important tool for the determination of heavy-element concentrations, is of limited practical use for low-Z elements because of low fluorescence yields and large x-ray absorptive effects. Neutron activation is not generally suitable because of low cross sections and the lack of a readily-detectable induced radioactivity. We have developed a new method for nondestructive nitrogen analysis in aerosols — sensitive and directly applied to the original samples — that uses the nuclear reaction $N^{14}(p,\alpha)C^{11}$ with low-energy protons from the LBL 88-inch cyclotron. The radioactive C^{11}, a 20.4-min positron emitter, is measured via its 0.511-MeV annihilation radiation with a Ge(Li) γ-ray spectrometer. A brief, 1-min, bombardment at 1 μA beam intensity is sufficient. Interfering elements are minimal. The results have been checked by independent methods and are quite satisfactory.

*Supported by the U.S. NSF and DOE.

Presented at the 178th meeting of the American Chemical Society, Washington, D.C., September 9-14, 1979.

THE $C^{12}(d,n)N^{13}$ NUCLEAR REACTION FOR DETERMINATION OF CARBON IN ATMOSPHERIC AEROSOLS*

Mark Clemenson, Samuel S. Markowitz, and Tihomir Novakov
Department of Chemistry and Lawrence Berkeley Laboratory
University of California, Berkeley, CA 94720

Carbon-containing particulate matter is important to our understanding of the chemistry of substances produced in the environment. Particulates, as atmospheric aerosols contain many low-Z elements that are difficult to determine with a nondestructive, sensitive method. X-ray fluorescence, an important tool for the determination of heavy-element concentrations, is of limited practical use for low-Z elements because of low fluorescence yields and large x-ray absorptive effects. Neutron activation is not generally suitable because of low cross sections and the lack of a readily-detectable induced radioactivity. Here we present a rapid, nondestructive nuclear activation method that induces the short-lived positron emitter, 10.0-min N^{13}, from low-energy deuteron reactions. The LBL 88-inch cyclotron is used to supply reliable beam intensities of ~1 μA for 1-minute bombardments. The N^{13} is measured via the decay of its 0.511-MeV annihilation radiation with a Ge(Li) γ-ray spectrometer that is calibrated with standards supplied by the National Bureau of Standards. Our method is virtually interference-free. Excellent results have been obtained by comparison of our (d,n) analyses with those obtained by two independent carbon-combustion methods.

*Supported by the U.S. DOE and NSF.

REFERENCES

1. L.A.Chambers, in "Air Pollution," Third Edition, A.C.Stern, editor, 1, 13 (1976).
2. A.Altshuller and J.Bufalini, Environ. Sci. Tech. 5, 39 (1971).
3. K.T.Whitby, R.J.Charlson, W.E.Wilson, R.K.Stevens, and R.E.Lee,Jr., Science 183, 1098 (1974).
4. K.T.Whitby, in "Proceedings of the Conference on Carbonaceous Particles in the Atmosphere," T.Novakov, editor, Lawrence Berkeley Laboratory Report LBL-9037 (1979), p.201.
5. R.E.Lee,Jr. and J.Hein, Anal. Chem. 46, 931 (1974).
6. R.Belcher, G.Ingram, and J.R.Majer, Talanta 16, 881 (1969).
7. Galbraith Labs, Inc., P.O.Box 4187 Lonsdale, Knoxville, TN 37921.
8. Kevex Corporation, 898 Mahler Road, Burlingame, CA 94010.
9. G.Friedlander, J.W.Kennedy, and J.M.Miller, Nuclear and Radiochemistry, Second Edition (John Wiley & Sons, Inc., New York, 1964).
10. IRT Corporation, 7650 Convoy Court, San Diego, CA 92138.
11. E.S.Macias, C.D.Radcliffe, C.W.Lewis, and C.R.Sawicki, Anal. Chem. 50, 1120 (1978).
12. S.S.Markowitz and J.D.Mahony, Anal. Chem. 34, 329 (1962).
13. F.Joliet and I.Curie, Compt. Rend. 198, 254 (1934).
14. G.T.Seaborg and J.Livingood, J. Am. Chem. Soc. 60, 1784 (1938).
15. H.J.M.Bowen and D.Gibbons, Radioactivation Analysis (Oxford University Press, London, 1963).
16. W.S.Lyon and H.H.Ross, Anal. Chem. 50, 804 (1978).
17. C.F.Williamson, J.P.Boujot, and J.Picard, Centre d'Etudes Nucléaires de Saclay, France, Report CEA-R 3042 (1966).

18. L.C.Northcliffe and R.F.Schilling, Nuclear Data Tables 7, 233 (1970).

19. E.Browne, J.M.Dairiki, R.E.Doebler, A.A.Shihab-Eldin, L.J.Jardine, J.K.Tuli, and A.B.Buyrn, Table of Isotopes, Seventh Edition, C.M.Lederer and V.S.Shirley, editors, (John Wiley & Sons, Inc., New York, 1978).

20. E.O.Lawrence and M.S.Livingston, Phys. Rev. 37, 1707 (1931).

21. L.H.Thomas, Phys. Rev. 54, 580 (1938).

22. E.L.Kelley, Nucl. Instr. Methods 18-19, 33 (1962).

23. Tracor Northern, 2551 West Beltline Highway, Middleton, WI 53562.

24. Texas Instruments, Dallas, TX 75222. This unit is "out of production."

25. G.B.Cook and J.F.Duncan, Modern Radiochemical Practice (Clarendon Press, Oxford, 1952).

26. B.W.Hoffman and S.B.Van Camerik, Anal. Chem. 39, 1198 (1967).

27. J.B.Cumming, in "Applications of Computers to Nuclear and Radiochemistry," G.D.O'Kelly, editor, National Academy of Science/ National Research Council, Nucl. Sci. Series NAS-NS 3107, 25 (1963).

28. J.A.Cooper, Battelle Northwest Laboratories Report BNWL-SA-4690.

29. O.D.Brill', Soviet. Jour. of Nucl. Phys. 1, 37 (1965).

30. R.L.Hahn and E.Ricci, Nucl. Phys. A101, 353 (1967).

31. V.R.Casella, D.R.Christmas, T.Ido, and A.P.Wolf, Radiochim. Acta 25, 17 (1978).

32. M.Epherre and C.Seide, Phys. Rev. C 3, 2167 (1971).

33. O.D.Brill' and L.V.Sumin, Atomnaya Énergiya 7, 377 (1959).

34. D.M.Lee, C.V.Stauffacher, and S.S.Markowitz, Anal. Chem. 42, 994 (1970).

35. R.L.Hahn and E.Ricci, Phys. Rev. 146, 650 (1966).

36. J.D.Mahony, Lawrence Radiation Laboratory Report UCRL-11780, Ph.D. Thesis (1965).

37. N.N.Krasnov, Soviet. At. Ener. 28, 333 (1970).

38. A.B.Whitehead and J.S.Foster, Can. J. Phys. 36, 1276 (1958).

39. L.A.Gundel, S.G.Chang, M.S.Clemenson, S.S.Markowitz, and T.Novakov, in "Nitrogenous Air Pollutants," D.Grosjean, editor (Ann Arbor Science Publishers, Inc., Ann Arbor, 1979).